

Characterization of a novel family of nucleobase transporters

Dissertation

zur Erlangung des Grades eines Doktors
der Naturwissenschaften
der Fakultät für Biologie
der Eberhard-Karls Universität Tübingen

vorgelegt von
Anja Schmidt
aus Korbach

2004

Tag der mündlichen Prüfung: 27. August 2004

Dekan: Prof. Dr. H.-U. Schnitzler

1. Berichterstatter: Prof. Dr. W. B. Frommer
2. Berichterstatter: Prof. Dr. H. U. Seitz

Table of Contents

TABLE OF CONTENTS	1
(I) ZUSAMMENFASSUNG	5
(II) SUMMARY	6
ABBREVIATIONS	7
1. INTRODUCTION	8
1.1. Role of nucleobases in living cells	8
1.1.1. Nomenclature of nucleobases, nucleosides and nucleotides	8
1.1.2. Nucleotide <i>de novo</i> synthesis	8
1.1.3. Fate of free nucleobases and nucleosides in cells	9
1.1.4. Interplay of <i>de novo</i> synthesis, salvaging and degradation	12
1.1.5. Role of transport in salvaging	13
1.2. Transporter families for nucleobases and nucleosides	13
1.2.1. The family of UPS transporters	14
1.3. Mechanism and regulation of membrane transport	14
1.3.1. Mechanism of transport	14
1.3.2. Walker motifs	15
1.3.3. Regulation of transport	16
1.4. Real time visualization of metabolite concentrations	16
1.4.1. FRET	17
1.4.2. Metabolite Nanosensors	17
1.4.3. The <i>Escherichia coli</i> Purine Repressor PurR	18
1.5. Aim of this work	18
2. MATERIAL AND METHODS	20
2.1. Material	20
2.1.1. Enzymes	20
2.1.2. Oligonucleotides	20
2.1.3. Plants	20
2.1.4. Bacterial and Yeast Strains	20
2.1.4.1. <i>Escherichia coli</i> (<i>E. coli</i>)	20
2.1.4.2. <i>Agrobacterium tumefaciens</i>	20
2.1.4.3. <i>Saccharomyces cerevisiae</i>	21
2.1.5. Vectors	21
2.1.6. Media	21
2.1.6.1. Media for growth of bacteria	21
2.1.6.2. Media for growth of yeast	22
2.1.6.3. Plant cell culture medium	23
2.1.6.4. Solutions for preparation transformation of protoplasts	24

2.1.6.5. Media for growth of <i>Arabidopsis thaliana</i> plants	24
2.1.6.6. Seed sterilization	25
2.1.6.7. For <i>Arabidopsis</i> transformation	25
2.1.7. Buffers and solutions.....	26
2.1.7.1. Split ubiquitin assays.....	26
2.1.7.2. GUS-assay	26
2.1.7.3. Oocyte work and electrophysiology.....	26
2.1.7.4. RNA-extraction	27
2.2. Methods.....	27
2.2.1. Standard methods	27
2.2.2. Transformation methods for bacteria and yeast	27
2.2.2.1. <i>Escherichia coli</i>	27
2.2.2.2. <i>Agrobacterium tumefaciens</i>	27
2.2.2.3. <i>Saccharomyces cerevisiae</i>	28
2.2.3. DNA-work.....	28
2.2.3.1. Cloning of <i>AtUPS</i> cDNAs.....	28
2.2.3.2. Oocyte expression constructs	28
2.2.3.3. Yeast expression constructs	29
2.2.3.4. GFP-fusion constructs	29
2.2.3.5. Promoter-GUS constructs	29
2.2.3.6. <i>UPS1</i> PTGS construct	30
2.2.3.7. <i>UPS5s</i> overexpression construct	30
2.2.3.8. Sensor cloning	30
2.2.4. Yeast methods	30
2.2.4.1. Complementation and uptake assays with yeast	30
2.2.4.2. Split ubiquitin assays (Obrdlík <i>et al.</i> , 2004).....	31
2.2.5. Expression and electrophysiology in <i>Xenopus laevis</i> oocytes	32
2.2.5.1. Expression in <i>Xenopus laevis</i> oocytes.....	32
2.2.5.2. Electrophysiology.....	32
2.2.6. Cell cultures.....	33
2.2.7. Preparation of protoplasts and expression of GFP constructs.....	33
2.2.8. Plant growth and transgenic lines.....	33
2.2.8.1. Plant growth	33
2.2.8.2. Plant transformation and recovery of transgenic lines	34
2.2.8.3. T-DNA insertion Lines.....	34
2.2.9. Promoter GUS assays.....	35
2.2.10. RT-PCR analysis	35
2.2.11. Protein expression and purification.....	36
3. RESULTS.....	37
3.1. Investigation of the <i>Arabidopsis thaliana</i> UPS family	37
3.1.1. The <i>AtUPS</i> family	37
3.1.2. Cloning of members of the <i>AtUPS</i> family	39
3.1.3. <i>AtUPS1</i> , 2 and 5 mediate transport of purine degradation products and pyrimidines.....	39
3.1.3.1. <i>AtUPS1</i> , <i>AtUPS2</i> and <i>AtUPS5</i> mediate uptake of allantoin	39
3.1.3.2. <i>AtUPS1</i> , <i>AtUPS2</i> and <i>AtUPS5</i> also act as uracil transporters.....	40
3.1.3.3. <i>AtUPS1</i> and <i>AtUPS2</i> were functionally expressed in <i>Xenopus laevis</i> oocytes... ..	41
3.1.3.3.1. <i>AtUPS1</i> and <i>AtUPS2</i> mediate transport of a range of substrates	41
3.1.3.3.2. Affinities of <i>AtUPS1</i> and <i>AtUPS2</i> are higher to uracil than to allantoin	44

3.1.4. Transport Mechanism and Regulation	45
3.1.4.1. The currents mediated by AtUPS1 and AtUPS2 are proton dependent.....	45
3.1.4.2. Mutations in ATP/GTP-binding motifs of <i>AtUPS1</i> and similar sequences of <i>AtUPS2</i> affect transport.....	46
3.1.4.3. Is AtUPS5s involved in regulation of transport?	48
3.1.4.4. Coexpression in yeast and <i>Xenopus</i> oocytes	49
3.1.5. Members of the <i>AtUPS</i> family are differentially expressed and regulated in plants .	51
3.1.5.1. Mature plants.....	51
3.1.5.2. Germination and early seedling development.....	54
3.1.5.3. Expression of <i>AtUPS</i> is modulated by nutritional and stress conditions	56
3.1.6. Analysis of <i>AtUPS1</i> PTGS lines and <i>AtUPS2</i> or <i>AtUPS5</i> T-DNA insertion lines	60
3.2. Towards establishment of a nucleobase sensor	63
3.2.1. Constructs with different backbones	63
3.2.2. Repressor mutants affected protein expression and maturation.....	65
3.2.3. Nucleobases can serve as quenchers for fluorescence	65
3.2.4. Changes in steady-state FRET efficiency were observed for a mutant repressor	66
4. DISCUSSION	68
4.1. Transport of uracil by <i>Arabidopsis UPS</i> transporters	68
4.2. <i>PvUPS</i> and <i>AtUPS</i> – two plant families, two different roles of <i>UPS</i>-transporters? ..	68
4.3. Regulation at protein level.....	69
4.3.1. Does the Walker A motif play a role in nucleotide sensing?	69
4.3.2. Is AtUPS5s involved in regulation of AtUPS5?	69
4.4. Correlations between <i>AtUPS</i> expression and uracil salvaging.....	70
4.5. Stress conditions and effects of differences of the C:N ratio.....	71
4.6. Effect of 5-FU on plants of <i>ups2</i>, <i>ups5</i> and <i>UPS1</i> PTGS lines.....	71
4.7. Role of UPS transporters in <i>Arabidopsis</i> development	72
4.8. Nucleobase nanosensors.....	72
4.9. Conclusions and perspectives.....	73
5. REFERENCES	74
6. APPENDICES	80
6.1. Sequences of primers	80
6.2. <i>UPS</i> expression in plants of <i>UPS1</i> PTGS lines	81
6.3. Maps of constructs	83
6.3.1. Constructs for expression in yeast.....	83
6.3.2. GFP-expression constructs	83
6.3.3. Promoter-GUS constructs	83

6.3.4. UPS5s over-expression construct.....	84
6.3.5. FLIP _{PurR}	84
7. ACKNOWLEDGEMENTS	85
LEBENS LAUF	86

(i) Zusammenfassung

Nucleotide sind essentielle Metaboliten aller Zellen. Insbesondere, wenn ihre Neusynthese nicht ausreicht, um den zellulären Bedarf zu decken, spielt die Wiederverwertung vorgefertigter Nucleobasen eine wichtige Rolle. Dies ist häufig der Fall aufgrund erhöhter Zellteilungsaktivität, z.B. während der frühen Keimlingsentwicklung. Obwohl die Aufnahme von Pyrimidinen in Zellen beschrieben worden ist, sind bisher keine Uracil- oder Thymintransporter höherer Eukaryoten charakterisiert worden. Vor kurzem sind *AtUPS1* (aus *Arabidopsis thaliana*, Ackerschmalwand) und *PvUPS1* (aus *Phaseolus vulgaris*, Gartenbohne) als Transporter für Allantoin identifiziert worden. Im Gegensatz zu vielen Bohnenarten transportiert *Arabidopsis* organischen Stickstoff jedoch überwiegend als Aminosäuren. Da in *Brassicaceae* bisher kein Transport von Allantoin beschrieben wurde, ist denkbar, dass hier eine strukturell ähnliche Verbindung das eigentliche physiologische Substrat sein könnte.

Insgesamt kodiert das *Arabidopsis* Genom für fünf UPS Transporter. Um die Funktion der *AtUPS* Familie besser zu verstehen, wurden in der vorliegenden Arbeit verschiedene Mitglieder charakterisiert durch (i) detaillierte Untersuchung der Substratspezifitäten in *Xenopus* Oocyten (*AtUPS1*, 2), (ii) Analyse des Transportmechanismus und der Regulation verschiedener UPS Proteine (*AtUPS1*, 2, 5), (iii) Analyse der Expression in Pflanzen durch Promoter-GUS Studien und RT-PCR (*AtUPS1-5*) und (iv) Untersuchung transgener Pflanzen mit fehlender oder verminderter Expression einzelner *UPS* durch T-DNA Insertionen oder PTGS (post-transcriptional gene silencing) (*AtUPS1*, 2, 5).

AtUPS1 und 2 transportierten eine Vielzahl strukturell ähnlicher Purin-Abbauprodukte und auch Pyrimidine. Sie hatten außerdem beide eine hohe Affinität zu Uracil (~ 6µM). Zudem hatten *AtUPS1* und *AtUPS2* den gleichen Transportmechanismus: sie scheinen ungeladene Substrate durch H⁺-Cotransport zu transportieren. Im Übrigen ist eine Nucleotid-Bindedomäne (Walker A Motiv), die eine regulatorische Funktion ausüben könnte, in allen *AtUPS*-Sequenzen außer *AtUPS2* vorhergesagt. Zwei Splicing-Varianten von *AtUPS5* wurden kloniert und analysiert. Während *AtUPS5* auch Allantoin, Uracil und andere Heterocyklen transportiert, könnte *AtUPS5s*, die kürzere Splicing-Variante von *AtUPS5*, durch Interaktion mit *AtUPS5* an einer Regulation des Transports beteiligt sein. Die Transportrate von *AtUPS5* wurde durch eine Co-Expression mit *AtUPS5s* in Hefe deutlich verringert wurde.

Das Expressionsmuster verschiedener *AtUPS* Transporter könnte darüber hinaus auf Aufgaben im Nucleobasen-Recycling hinweisen, wie z.B. die hohe Expressionsraten von *AtUPS1* während früher Stadien der Keimlingsentwicklung. *AtUPS4* könnte an der Versorgung von Pollen mit Uracil beteiligt sein, während *AtUPS2* und *AtUPS5* sowohl eine Rolle im Langstrecken-Transport von Nucleobasen als auch im Transport auf zellulärer Ebene spielen könnten. Auch unter Stressbedingungen, die Nucleotiden-Mangel auslösen können (Stickstoff-Mangel, Salz Stress) war die Expression verschiedener UPS erhöht. Darüber hinaus wurde gefunden, dass T-DNA Insertionslinien von *UPS2* und *UPS5*, sowie Linien mit erniedrigtem *UPS1* mRNA Level (PTGS-Linien) toleranter gegenüber 5-Fluorouracil (5-FU) sind als der Wildtyp. Dies impliziert, dass *UPS* in *Arabidopsis* wichtige Transporter für Uracil und eventuell andere Nucleobasen sein könnten, während sich Bohnen die geringere Selektivität gegenüber Substraten für den Allantointransport zu nutze gemacht haben.

Um jedoch den Transport von Nucleobasen und Derivaten in Pflanzen detailliert zu verstehen, ist eine Bestimmung ihrer dynamischen zellulären und subzellulären Konzentrationen notwendig. Als Ausgangspunkt zur weiteren Entwicklung und Optimierung von Nucleobases Sensoren wurde daher ein auf FRET-basierender Hypoxanthin-Sensor entwickelt und *in vitro* getestet.

(ii) Summary

Salvaging of nucleobases from storage tissues plays an important role in providing nucleobases to cells which are unable to synthesize sufficient amounts for their needs, e.g. during early phases of seedling development, when cells divide rapidly. Cellular uptake systems for pyrimidines have been described so far, but in higher eukaryotes, transporters of thymine and uracil have not been characterized. *AtUPS1* and *PvUPS1* were recently identified as transporters of allantoin in *Arabidopsis* and French bean, respectively. However, in contrast to tropical legumes, *Arabidopsis* mainly uses amino acids for long distance transport. Allantoin transport has not been described in *Brassicaceae*. Thus, the physiological substrates of UPS transporters in *Arabidopsis* may be compounds structurally related to allantoin.

The *Arabidopsis* genome encodes five UPS transporters. For a better understanding of the role of members of the *AtUPS* family, different members were characterized in this work by (i) detailed investigation of substrate specificities when expressed in *Xenopus* oocytes (*AtUPS1*, 2), (ii) analysis of transport mechanism and regulation (*AtUPS1*, 2, 5), (iii) analysis of expression pattern in plants by promoter-GUS studies and RT-PCR, and (iv) investigation of transgenic plants deficient or lower in expression of *AtUPS* members due to T-DNA insertions or PTGS (post transcriptional gene silencing) (*AtUPS1*, 2, 5).

AtUPS1 and *AtUPS2* have broad substrate specificities covering cyclic purine degradation products as well as pyrimidines. Moreover, they both mediated high-affinity transport of uracil (~6 μM). *AtUPS1* and *AtUPS2* seemed to transport uncharged substrates by H^+ -cotransport. With the exception of *AtUPS2*, a nucleotide-binding domain (Walker A motif) is predicted in the UPS sequences. It might have a role in the regulation of transport mediated by *AtUPS* proteins. In addition, two splicing variants of *AtUPS5* were cloned and analyzed (*AtUPS5* and a shorter variant, *AtUPS5s*). *AtUPS5* also mediated the transport of allantoin, uracil and other heterocycles. *AtUPS5s* might be involved in the regulation of transport mediated by *AtUPS5* by interaction or complex formation with *UPS5*, since coexpression of both proteins in yeast decreased the transport efficiency of *AtUPS5* significantly.

Moreover, the expression patterns of members of the *AtUPS* family suggest functions in nucleobase salvaging, for example the high expression of *AtUPS1* during germination and the early stages of seedling development. *AtUPS4* might play a role in uracil supply to pollen. *AtUPS2* and *AtUPS5* might serve the long-range transport of nucleobases and possibly the transport involved in cellular turnover. In addition, expression of members of the *AtUPS* family was elevated in plants grown under conditions that can lead to nucleotide deficiency (nitrogen deficiency, salt stress). *Arabidopsis ups2* and *ups5* T-DNA insertion mutants and *ups1* lines, in which transcript levels were reduced by PTGS, were more tolerant to (5-fluorouracil) 5-FU, compared to the wild type. The results suggest that in *Arabidopsis* UPS transporters are the main transporters of uracil and potentially other nucleobases, whereas during evolution legumes may have taken advantage of the low selectivity of UPS proteins for the long distance transport of allantoin.

Nevertheless, for a detailed understanding of the transport of nucleobases and derivatives in plants, knowledge about their cellular and subcellular concentrations under dynamic conditions of living plant cells is necessary. Therefore, as a starting point for the imaging of nucleobases in plant cells, a FRET-based sensor for the purine hypoxanthine was developed and tested *in vitro*.

Abbreviations

ABC	ATP-binding cassette
CDB	Corepressor binding domain
CFP	Cyan Fluorescent Protein
CNT	Concentrative Nucleoside Transporter
ECFP	Enhanced cyan fluorescent protein
<i>E. coli</i>	<i>Escherichia coli</i>
EYFP	Enhanced Yellow Fluorescent Protein
ENT	Equilibrative Nucleoside Transporter
FLIP	Fluorescent Indicator Proteins
FRET	Fluorescence Resonance Energy Transfer
GFP	Green Fluorescent Protein
GUS	β -glucuronidase
5-FU	5-fluorouracil
NAT	Nucleobase Ascorbate Transporter
NDB	Nucleotide Binding domain
NDP	nucleoside diphosphates
NMP	nucleoside monophosphates
NTP	nucleoside triphosphates
OMP	orotidylate
PBP	Periplasmic binding Protein
PMA	Plasma Membrane ATPase
PRPP	5-phosphoribosyl-1-pyrophosphate
PRT	Purine Related Transporter
PTGS	post translational gene silencing
PUP	Purine Permease
PurR	Purine Repressor
Pyase	nucleoside phosphorylase
RBP	Ribose Binding Protein
Rtases	phosphoribosyltransferases
UDPglc	uridine diphosphate glucose
UPS	Ureide Permeases
YFP	Yellow Fluorescent Protein

1. Introduction

1.1. Role of nucleobases in living cells

Nucleotides play essential roles in all living organisms. They are building blocks for RNA and DNA synthesis and precursors of essential coenzymes (NAD⁺, FAD, CoA), hormones (cytokinins) and secondary metabolites in plants (e.g. caffeine), involved in the important regulation of development and defense. ATP and GTP are the main forms of chemically bound energy. The nucleotide pool of plants consists mainly of adenine nucleotides with ~80-200 nmol/g fresh weight. The second most important pool is represented by uracil nucleotides (Stasolla *et al.*, 2003). Nucleoside diphosphate sugars, like uridine diphosphate glucose (UDPglc), are a major fraction of the total nucleotide pool. UDP-sugars serving as activated intermediates in the synthesis of sucrose and cell wall polymers predominate (Wagner and Backer, 1992), whereas ADP-glucose acts as glycosyl donor in starch synthesis (Preiss, 1988; Wagner and Backer, 1992).

1.1.1. Nomenclature of nucleobases, nucleosides and nucleotides

Nucleobases are *N*-heterocycles and derivatives of either purine (e.g. A (adenine), G (guanine), or pyrimidine (e.g. U (uracil), T (thymine), C (cytosine)) (Fig. 1).

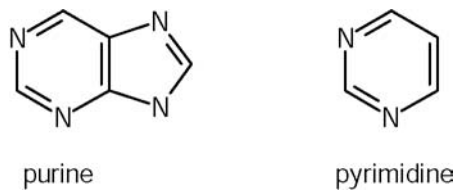


Fig. 1: Structure of purine and pyrimidine bases

Nucleosides are constituted of a nucleobase bound to a pentose sugar moiety, either ribose or deoxyribose. Nucleotides, in comparison, are phosphate esters of nucleosides, like nucleoside monophosphates (NMP), nucleoside diphosphates (NDP) and nucleoside triphosphates (NTP), having additional one, two or three phosphate groups bound to the pentose moiety respectively.

1.1.2. Nucleotide *de novo* synthesis

Metabolic pathways in plants are similar to the pathways analyzed in bacteria or animals. Nucleotides are the products of the *de novo* synthesis pathway, while nucleosides and nucleobases come from nucleotide degradation. Nucleotide *de novo* synthesis pathways have high energy requirements. In addition, availability of nitrogen, carbon and phosphate sources is essential for *de novo* synthesis of purine and pyrimidine nucleotides. Amino acids, derivatives of tetrahydrofolate, NH₄⁺ and CO₂ are the main metabolic precursors. The ribose-phosphate moiety of both purine and pyrimidine nucleotides comes from 5-phosphoribosyl-1-pyrophosphate (PRPP), which is synthesized from ATP and ribose-5-phosphate. The pyrimidine nucleotide *de novo* synthesis begins with a series of four reactions yielding to orotate, which is subsequently converted to UMP via orotidylate (OMP) (Fig. 2). UMP in turn is modified to UTP and CTP.

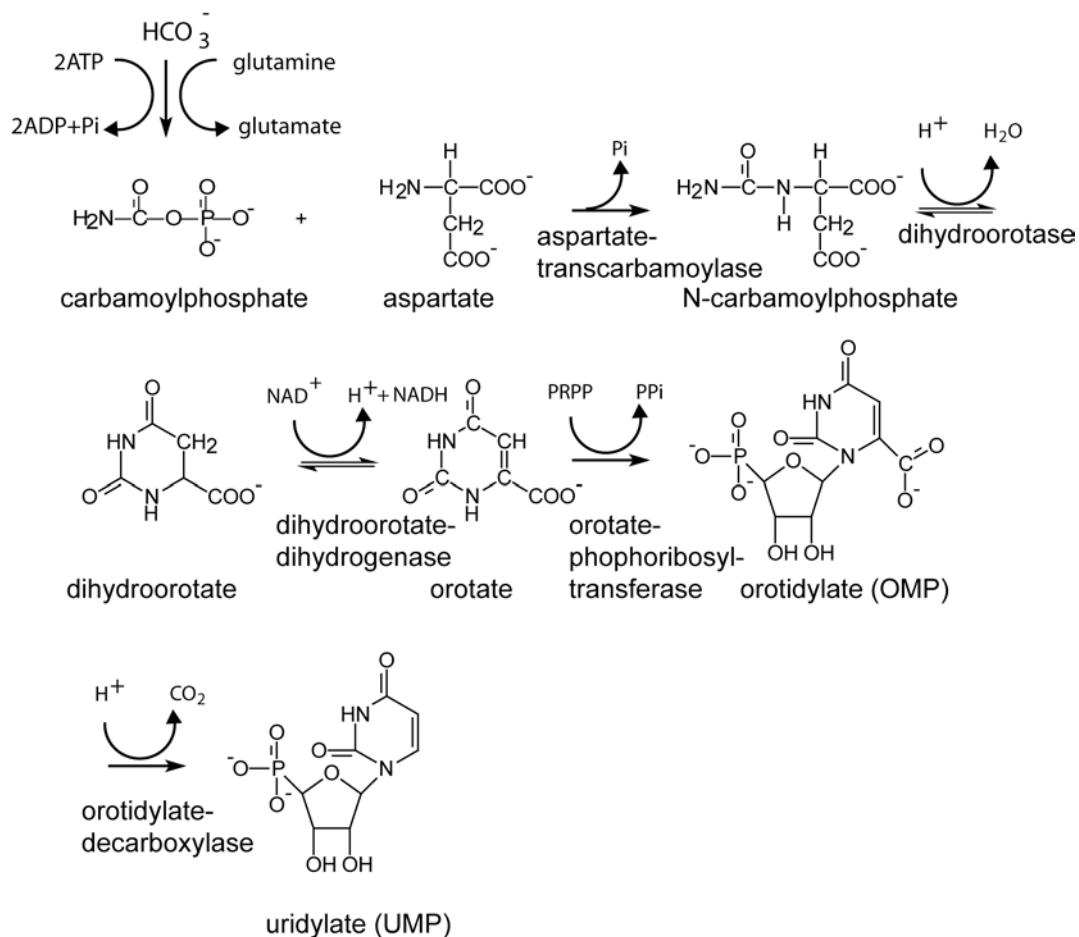


Fig. 2: Pyrimidine de novo synthesis.

Aspartate-transcarbamoylase catalyzes the synthesis of N-carbamoylphosphate from carbamoylphosphate and aspartate. In the next reaction, dihydroorotate is formed by cyclization of N-carbamoylphosphate. Formation of orotate by dehydration of dihydroorotate is catalyzed by dihydroorotate-dehydrogenase. In the next step, the ribose-phosphate moiety is added. Subsequently, uridine monophosphate (UMP) is obtained by decarboxylation.

PRPP and glutamine are substrates in the first step of purine *de novo* synthesis. IMP is synthesized in a series of 10 successive reactions, and subsequently used for the synthesis of AMP and GMP. The purine nucleotide synthesis is feedback controlled by the end-products (AMP, GMP and IMP in the case of purine nucleotide synthesis), while levels of UMP and UDP are involved in the regulation of pyrimidine nucleotide synthesis (Wagner and Backer, 1992; Stasolla *et al.*, 2003). Enzymes for UMP *de novo* synthesis are localized in different subcellular compartments including chloroplasts and the mitochondrial intermembrane space (dihydroorotate dehydrogenase) (Wagner and Backer, 1992; Kafer and Thornburg, 1999). So far, very little is known about the subcellular localization of the enzymes involved in purine nucleotide synthesis (Atkins, *et al.*, 1982; Boland and Schubert, 1983).

1.1.3. Fate of free nucleobases and nucleosides in cells

In contrast to bacteria and animal cells, considerable amounts of free bases and nucleosides seem to be present in plant tissues (Sawert *et al.*, 1987; Sawert *et al.*, 1988; Wagner and Backer, 1992). They mainly come from RNA breakdown in the vacuole and can be further degraded (Wagner and Backer, 1992). Among the pyrimidine bases, uracil and thymine are degraded via reductive pathways to β -alanine or β -aminoisobutyrate while cytosine is not

metabolized (Stasolla *et al.*, 2003). Instead of degradation of the cytosine base, the nucleoside cytidine is converted to uridine, which is subsequently metabolized to uracil. Purines are degraded via an oxidative pathway. Intermediates of the purine breakdown are, for example, xanthine, uric acid, and the ureides allantoin and allantoic acid (Fig. 3). Allantoic acid can be further degraded in NH_3 , CO_2 and glyoxylate following two alternative pathways (Winkler *et al.*, 2003; Vadez and Sinclair, 2000; Stasolla *et al.*, 2003).

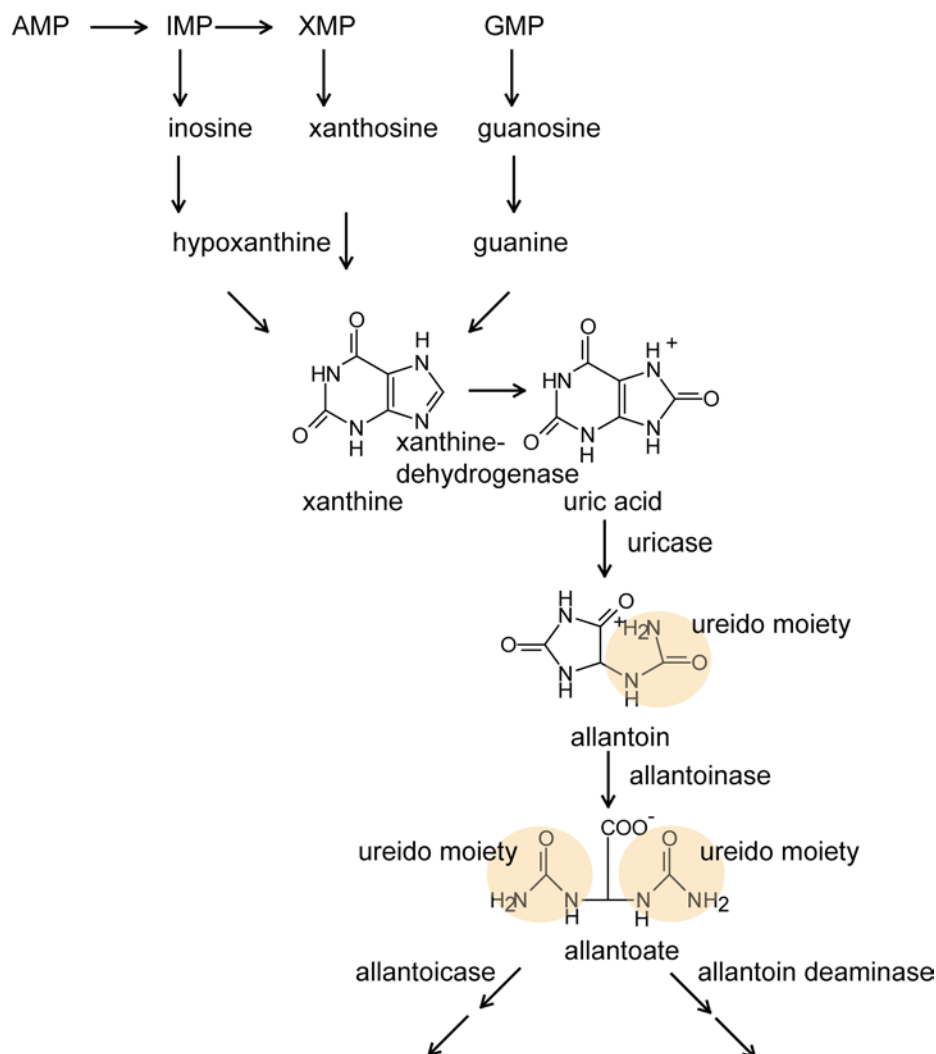


Fig. 3: Purine degradation pathway, after (Ashihara and Nobusawa, 1981)

Purines are degraded via an oxidative pathway involving xanthine, uric acid, and the ureides allantoin and allantoate. Allantoate can be further degraded by two different pathways, involving either allantoicase or allantoin-deaminase.

Alternatively to their degradation, nucleobases and nucleosides can be reused, depending on the cellular need. In the salvage pathway, preformed nucleosides or nucleobases are recycled to nucleotides (Fig. 4). A major advantage of the salvage pathway for nucleotide synthesis is that less energy is required than for the *de novo* synthesis.

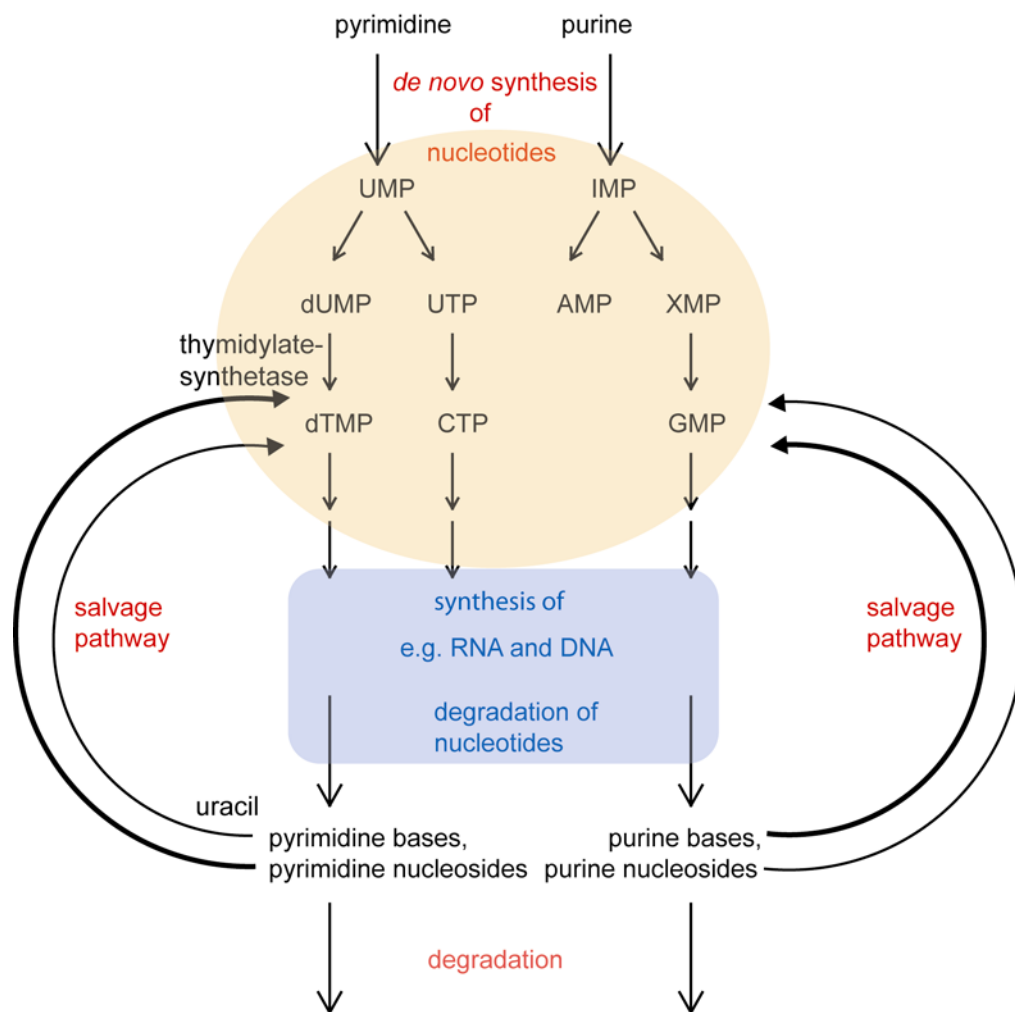


Fig. 4: Scheme of nucleotide de novo synthesis, salvaging and degradation.

Purine and pyrimidine nucleotides are synthesized *de novo* by two different pathways. They are used as building blocks for DNA and RNA and a multitude of other metabolites. Free nucleobases and nucleosides come from the degradation of nucleotides, mainly from RNA degradation in the vacuole. They can subsequently be degraded or salvaged to nucleotides. While purine bases are salvaged more efficiently than purine nucleosides, pyrimidine nucleosides are salvaged more efficiently than pyrimidine bases.

Nucleobases can be salvaged by two different types of enzymes: phosphoribosyltransferases (Rtases) and nucleoside phosphorylases (Pyases). Rtases use PRPP for nucleotide synthesis from nucleobases, while Pyases catalyze the conversion from nucleobases to nucleosides involving ribose-1-phosphate (Wagner and Backer, 1992) (Fig. 5). In plants, uracil seems to be the only pyrimidine base used for salvaging: cytosine can not be salvaged due to a lack of cytosine deaminase or cytosine Rtase activity (Wagner and Backer, 1992; Stougaard, 1994; Katahira and Ashihara, 2002). No evidence for the salvaging of thymine has been found (Wagner and Backer, 1992).

Two different types of Rtases salvage free purine bases, with specificities for adenine or for hypoxanthine/guanine. The importance of adenine salvaging is demonstrated for plants, since an *Arabidopsis* mutant deficient in adenine Rtase shows retarded growth and male sterility (Moffatt and Somerville, 1988). Different nucleosides like desoxy thymidine, uridine, cytidine or adenosine can be salvaged directly by either kinases or phosphotransferases (Ptases).

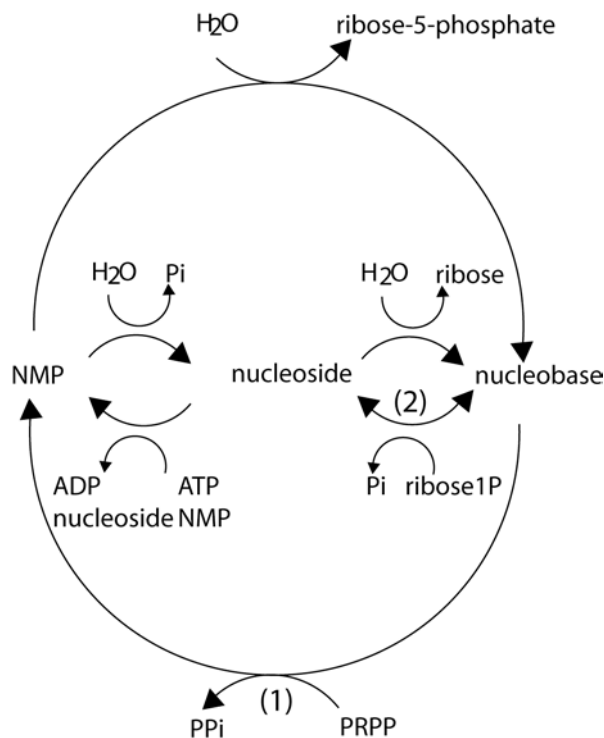


Fig. 5: Main enzymatic steps in pathways of nucleobase and nucleoside salvage after (Wagner and Backer, 1992).

Nucleobases can be salvaged by two different types of enzymes. Rtases (1) catalyze the formation of nucleoside monophosphates, using PRPP, while Pyases use ribose-1-phosphate for the formation of nucleosidases (2).

Due to the enzymatic activities, there is one evident difference between the salvaging of purines and the salvaging of pyrimidines: While purine bases are salvaged with higher efficiency than purine nucleosides, in the case of pyrimidines the opposite seems to be true; pyrimidine nucleosides are salvaged with higher efficiency than uracil (Wagner and Backer, 1992) (Fig. 4).

1.1.4. Interplay of *de novo* synthesis, salvaging and degradation

Tight regulation between the metabolic pathways of synthesis, salvage and degradation is required. Cells with an elevated demand for nucleotides often rely on salvaging pathways, especially when the activities of enzymes for *de novo* synthesis are low or absent, e.g. during germination when cells divide rapidly. While salvaging of nucleobases and nucleosides predominates at the inception of germination, its importance declines when germination proceeds and *de novo* synthesis takes over (Stasolla *et al.*, 2002; Stasolla *et al.*, 2003). Decreased salvaging activities are accompanied by the degradation of preformed bases, leading to ureide formation (Guranowski and Barankiewicz, 1979; Ashihara and Nobusawa, 1981; Stasolla *et al.*, 2003). In addition, salvaging activity in cultured cells during the lag phase of growth contributes to an elevation of total nucleotide levels in preparation for cell division (Stasolla *et al.*, 2003). Since nucleotide *de novo* synthesis depends on the availability of carbon, nitrogen and phosphate sources, nutritional starvation can also result in increased salvaging activity. During senescence, increased rates of nucleic acids degradation lead to elevated amounts of free nucleobases and nucleosides. These can be degraded or reused by neighboring cells or tissues. High activity in uracil salvaging seem to play a role in reuse of preformed pyrimidine bases during early senescent stages of leaves, as reported for tobacco (Ashihara, 1981). In addition, the cellular compartments like the cytoplasm might depend on the salvaging of nucleobases and nucleosides, since enzymes for *de novo* uracil nucleotide synthesis are localized in chloroplasts and mitochondria, while salvaging enzymes are mainly observed in cytoplasm (Wagner and Backer, 1992).

1.1.5. Role of transport in salvaging

Due to the fact that nucleotide breakdown rarely occurs directly at sites of high demand, the transport of nucleobases and nucleosides from adjacent or storage tissues is often required for the supply of cells or cellular compartments. These transport processes do not exclusively occur in plants but play a role in a broad range of different organisms. Protozoan parasites, for example, rely on import and salvaging, because they are not capable of purine nucleotide *de novo* synthesis. In microorganisms, transport is used for supply of nucleobases as well as nitrogen. Transport systems have also been described in a variety of mammalian cell types (de Koning and Diallinas, 2000). In plants, several studies on nucleobase metabolism, based on precursor feeding experiments, demonstrate import processes of nucleobases and nucleosides in tissues (Ashihara and Nobusawa, 1981; Wagner and Backer, 1992; Ashihara *et al.*, 1997; Kafer and Thornburg, 1999; Stasolla *et al.*, 2002; Stasolla *et al.*, 2003). Moreover, the uptake of nucleobases or nucleosides from storage tissues has been demonstrated for germinating castor beans (Kombrink and Beevers, 1983). Different transport systems mediate active import from endosperm into cotyledons. Nucleosides are transported at higher rates than free nucleobases. Among the free bases, adenine is imported into cotyledons with highest efficiency while uracil, cytosine, guanine, and hypoxanthine are transported at lower rates. Uracil was shown to be transported by a high affinity transport system (K_m of 41 μ M), although the molecular identity of this transport system remains unknown (Kombrink and Beevers, 1983). The uptake of the nucleosides adenosine, guanosine, cytidine and uridine against the concentration gradient in petunia pollen (Kamboj and Jackson, 1984; Kamboj and Jackson, 1985; Kamboj and Jackson, 1987) and the supply of nucleosides from carpel after germination of the pollen (van der Donk, 1974; Jackson and Linskens, 1978; Jackson and Linskens, 1980) probably contribute to the enlargement of the nucleotide pool for pollen tube growth.

1.2. Transporter families for nucleobases and nucleosides

To date, a number of families of membrane transporters for nucleobases and nucleosides have been described, including Nucleobase Ascorbate Transporters (*NAT*), which are present in eubacteria, archaeobacteria, fungi, plants, insects, nematodes and mammals (e.g. humans), the microbial Purine-Related Transporter family (*PRT*) identified only in fungi, bacteria and archaeobacteria, and the plant family of Purine-Permeases (*PUP*) (de Koning and Diallinas, 2000). Members of the *NAT* family are bacterial purine or pyrimidine transporters, like UraA and PyrP, mediating uracil transport in *Escherichia coli* (Andersen *et al.*, 1995; de Koning and Diallinas, 2000) and *Bacillus* species (Ghim and Neuhard, 1994), respectively. UapA and UapC, purine transporters from *Aspergillus* (Gorfinkiel *et al.*, 1993, Diallinas *et al.*, 1995), and mammalian ascorbate transporters all belong to the *NAT* family (Tsukaguchi *et al.*, 1999). *FUR4* and *DAL4*, the yeast transporters of uracil and allantoin respectively (Yoo *et al.*, 1992), belong to the *PRT* family. In addition, two families of nucleoside transporters are known mainly based on investigations in mammals (Kong *et al.*, 2004): the Equilibrative Nucleoside Transporters (*ENT*) and Concentrative Nucleoside Transporters (*CNT*).

In plants, knowledge about nucleobase and nucleoside transport is scarce. Nucleoside transporters of *Arabidopsis* (*AtENT*) have already been described (Möhlmann *et al.*, 2001; Li *et al.*, 2003; Wormit *et al.*, 2004). Moreover, some transporters for nucleobases and derivatives are described. A member of the *NAT* family from tomato, *LPE1*, mediates transport of the purine degradation products xanthine and uric acid (*LPE1*) (Argyrou *et al.*, 2001). Moreover, transporters for mainly purine bases and derivatives have been characterized from *Arabidopsis*: *AtPUPs* mediate the uptake of adenine, cytokinins, caffeine and cytosine (Gillissen *et al.*, 2000; Bürkle *et al.*, 2003).

Although putative uracil transporters have been identified in the *Arabidopsis* genome, like the gene At5g03555, a putative member of the *PRT* family, or members of the *NAT* family (Ward, 2001), their functionality has not been described. However, until now, no transporter of the pyrimidines uracil and thymine has been characterized at the molecular level in plants or other higher eukaryotes.

1.2.1. The family of UPS transporters

Allantoin and allantoic acid are intermediates of the purine degradation pathway. They belong to the group of ureides, due to a ureido-moiety in their structure (Fig. 2). *AtUPS1* (At2g03590) from *Arabidopsis* has recently been identified, and has been shown to mediate allantoin transport in a yeast complementation assay. The yeast *dal4 dal5* double mutant strain that is deficient in transporters of allantoin and allantoic acid, was transformed with a cDNA library of *Arabidopsis* (Desimone *et al.*, 2002). Growth of yeast colonies on medium with allantoin as sole nitrogen source was analyzed leading to the identification of *AtUPS1*, a member of a novel family of transmembrane proteins named Ureide Permeases (*UPS*) (Desimone *et al.*, 2002). Four additional putative proteins in *Arabidopsis*, *AtUPS2* (At2g03530), *AtUPS3* (At2g03600), *AtUPS4* (At2g03520) and *AtUPS5* (At1g26440) displaying sequence identities with *AtUPS1* ranking between 63 % and 82 % on amino acid level were identified by database searches, as well as one related cDNA from the legume *Vigna unguiculata* (*VuA3/X90487*) (Desimone *et al.*, 2002; Pélissier *et al.*, 2004). Moreover, a related gene from French bean (*Phaseolus vulgaris*) was cloned using degenerated primers based on the *AtUPS1* sequence (Pélissier *et al.*, 2004). Thus the *UPS* family is represented in legumes and *Arabidopsis*, and probably other plant species, as indicated by ESTs (Desimone *et al.*, 2002).

Ureides are used as transport and storage compounds for organic nitrogen in tropical and subtropical legumes and *Boraginaceae*, respectively (Schubert and Boland, 1990; Castro *et al.*, 2001; Pélissier *et al.*, 2004). Nitrogen fixed in the root nodules of legumes is mainly metabolized to ureides and then distributed within the plant. These compounds represent up to 90 % of the total nitrogen in the xylem of nitrogen fixing tropical legumes, and concentrations of ~10 mM have been found in soybean xylem (Rainbird *et al.*, 1984). The importance of ureide transport in nodulated legumes suggests, that allantoin might be the physiological substrate of *PvUPS1*. In agreement with a role in long distance allantoin transport in French bean, *PvUPS1* is expressed in the endodermis and vasculature of nodules (Pélissier *et al.*, 2004). In contrast, no evidence of the importance of allantoin for long distance transport in *Arabidopsis* or other *Brassicaceae* has been found. *Arabidopsis* uses mainly amino acids for the transport of organic nitrogen in xylem or phloem. Analysis of transport features of *AtUPS1* and *PvUPS1* indicated that members of the *UPS* family also recognize other oxo-*N*-heterocycles structurally related to allantoin, in addition to allantoin itself. Thus it is conceivable that in *Arabidopsis* *UPS* transporters might have another physiological substrate, like the structurally related free pyrimidine bases.

1.3. Mechanism and regulation of membrane transport

1.3.1. Mechanism of transport

Membranes are barriers for solutes, since the diffusion of most compounds through the lipid bilayer is very slow. Transmembrane proteins are thus necessary to allow the efficient exchange of molecules across membranes, therefore creating potential selectivity for diffusion or transport. Since the number of transporters in a membrane is limited, transport processes are saturable. Transport rates are dependent on the concentrations of the substrates, for example nucleobases, and can be described by a Michaelis-Menten formula, defining the K_m value as the concentration at which half of the transporter proteins are saturated with substrate.

In principle, transport can be mediated by either channels or carriers. Channels, e.g. those transporting ions, form pores displaying size or charge selectivity. They facilitate diffusion along electrical or concentration gradients. Carriers specifically bind substrates and undergo conformational changes involved in the transport and release of the substrate. The mediated transport can either be passive along concentration or electrical gradients, or active against concentration gradients. Active transport against concentration gradients can be coupled to a metabolic energy source, e.g. ATP-hydrolysis as in the case of H⁺-ATPases (primary active transport), or are energized by co-transport of solutes, e.g. H⁺ or Na⁺, using gradients established across membranes (secondary active transport). In this case co-transport can be mediated in the same direction (symport) as the substrate or in the opposite direction (antiport).

AtUPS1 and PvUPS1 transport allantoin by H⁺-cotransport. Rates of ¹⁴C-allantoin uptake by *AtUPS1* or *PvUPS1* expressed in the yeast *dal4 dal5* mutant depend on the pH, with maxima in the range between 4 and 5. Moreover, uptake rates are sensitive to the presence of protonophores (Desimone *et al.*, 2002; Pélissier *et al.*, 2004). For *AtUPS1*, the dependence of uptake rates on pH is confirmed upon expression in *Xenopus* oocytes (Desimone *et al.*, 2002).

1.3.2. Walker motifs

The Walker A consensus sequence (P-loop) [AG]-x(4)-G-K-[ST]¹ is found in UPS sequences. This motive is a feature of ATP/GTP binding proteins, for example the family of ATP-binding cassette (ABC)-transporters. In ABC transporters, the Walker A motif is a part of a so called nucleotide binding domain. Distinct amino acid residues of the Walker A motif play a role in binding the phosphate moiety of ATP/GTP (Lutkenhaus and Sundaramoorthy, 2003). In ABC transporters, ATP or GTP hydrolysis typically energizes the primary active transport of solutes across membranes (Stefkova *et al.*, 2004). AtUPS1 and PvUPS1, in contrast, act by a secondary active transport mechanism. Thus, it is surprising that a Walker A consensus sequence is present in all AtUPS sequences except AtUPS2 (<http://ca.expasy.org/cgi-bin/nicedoc.pl?PDOC00017>; Walker *et al.*, 1982; Saraste and Wittinghofer, 1990; Desimone *et al.*, 2002) and the UPS sequences of legumes. AtUPS2 has an arginine residue instead of threonine or serine at the end of the consensus motif (Fig. 6).

Consensus	GXXXXGKS
	(A) T
AtPGP1	INGGEKVGIVGRTGAGKSSLTGLFRIN
hMDR1a	VQSGQTVALVGNVSGKSTTVQLMQRLY
hMRP1b	INGGEKVGIVGRTGAGKSSLTGLFRIN
hCFTR1	IERGQLLAVAGSTGAGKTSLLMMIMGEL
STE6	FSAGQFTFIVGKSGSGKSTLSNLLRFY
AtUPS1	AFLIELEKQRAIKVFGKSTIIGLVITFF
AtUPS2	RFLIELENTRAIKVFGKRKIIGLAITFF
AtUPS3	DFLIEVEKQRAIKVFGKSTIIGLAITFF
AtUPS4	GVYVELENKRAIKVFGKSIMIGLFITLF
AtUPS5	AFLIALENKRAIKVLGKSMVVGLGITFF
VuA3	VFLLELEERRAIKVFGKSTLIGLALTFS
PvUPS1	VFLIELEERRAIKVFGKSTLIGLSLTFS

Fig. 6 : Walker A consensus sequences.

Walker A consensus motif of AtUPS proteins, PvUPS1, VuA3, a similar protein from *Vigna unguiculata*, and different ABC transporters from *Arabidopsis* (AtPGP1 (Dudler and Hertig, 1992; Geisler *et al.*, 2003)), human (hMDR1a and hMDR1b (Christensen and LeBlanc, 1996)), or yeast (STE6 (Michaelis, 1993)).

¹ x stands for non conserved amino acids, amino acids in brackets can replace each other

Since it is unlikely that transport mediated by UPS proteins can be energized by two different mechanisms, the Walker A consensus sequence might have different functions in UPS. ATP/GTP binding could be involved in the regulation of dimerisation or oligomerisation of transporters, as shown for mammalian mitochondrial ABC transporters (half size transporters) (Galluhn and Langer, 2004; Graf *et al.*, 2004).

1.3.3. Regulation of transport

There are multiple ways of controlling transport activity, e.g. by regulating gene expression. Moreover, protein stability and activity can be modified, e.g. by protein-protein interactions or posttranslational modifications (like phosphorylation). Also, ubiquitinylation is involved in targeting proteins for degradation, as shown for the yeast uracil transporter FUR4 (Séron *et al.*, 1999).

There is increasing evidence for the homo- or heteromerization of transporters. Complex formation is presumably involved in the regulation of the transport efficiency (Dupre and Haguenaer-Tsapais, 2003; Hearn *et al.*, 2003; Ludewig and Frommer, 2003). The mammalian glucose transporter (GLUT1), the human dopamine transporter (DAT) (Torres *et al.*, 2003), and a human serotonin transporter (Kilic and Rudnick, 2000; Schmid *et al.*, 2001), were recently shown to form complexes in a cooperative fashion (Hebert and Carruthers, 1992). Dimerisation also has an impact on the function of the bacterial lactose transporter lacS (Veenhoff *et al.*, 2001). In plants, modulation of transport efficiency by homo- and hetero-oligomerization was shown for sucrose transporters (Reinders *et al.*, 2002a; Reinders *et al.*, 2002b; Schulze *et al.*, 2003), and the ammonium transporter, LeAMT1;1 (Ludewig *et al.*, 2003), or polar auxin transport mediated by the ABC-transporters AtPGP1 and AtPGP19 (Geisler *et al.*, 2003).

Since tight regulation of nucleotide metabolism, including salvage pathways and degradation and transport processes of metabolites is needed, it is conceivable that complex formation of transporters might play a role in regulation. This has so far not been described for plant transporters for nucleobases or nucleosides or UPS transporters.

1.4. Real time visualization of metabolite concentrations

For transporters involved in nucleotide metabolism, e.g. synthesis, degradation or salvaging, dynamic regulation is needed to suit transiently changing conditions. For a detailed understanding of transport processes, knowledge about cellular and subcellular levels of metabolites is required. Though investigations of nucleobase metabolites in different tissues from several species have been performed (Wagner and Backer, 1992), they do not include all subcellular compartments or changes due to dynamic physiological conditions, e.g. cell cycle or nutrition. Thus, a non-destructive method allowing real-time determination of nucleobases on subcellular level under physiological conditions would be needed.

Significant progress in imaging of cellular variations of ion and metabolite levels has been made possible by the development of a variety of chemical dyes. However, the application of dyes to living organisms can be invasive since they have to be loaded into cells. Genetically encoded sensors are therefore more advantageous. Such sensors suitable for imaging at the cellular level have recently been developed using Fluorescence Resonance Energy Transfer (FRET) and variants of the green fluorescent protein (GFP), which has been cloned from the jellyfish *Aequorea victoria*. The major advantage of this methodology is that real-time measurements are possible in a non-destructive manner.

1.4.1. FRET

Fluorescence Resonance Energy Transfer (FRET) is based on the transfer of excited state energy from a fluorescent donor to an acceptor molecule, without emission and reabsorption of a photon. It results from long-range dipole-dipole interactions. The efficiency of energy transfer is highly dependent on the distance between fluorophores². The Förster distance (R_0) is the distance at which FRET efficiency is 50 % (Förster, 1948). R_0 of a specific pair of donor and acceptor molecules is dependent on a variety of parameters: the quantum yield of the donor, the extent of spectral overlap between donor emission and acceptor absorption, the relative orientation of donor and acceptor dipoles, and the refractive index of the medium. It is typically ~20-60 Å for donor/acceptor molecule pairs and thus in the range of diameters of many proteins. Therefore FRET is theoretically applicable to the determination of distances in biological systems. Provided suitable FRET conditions are given, decreasing the distance between donor and acceptor molecules will thus result in decreased emission of the donor fluorophore and enhanced emission of the acceptor fluorophore.

1.4.2. Metabolite Nanosensors

The first sensors recording changes in solute concentrations using reversible conformational changes of protein structures and FRET have recently been developed. The so called “cameleon” chimeric proteins use calmodulin and the calmodulin binding protein M13 as reporter domains for Ca^{2+} binding and fluorescent proteins (GFP variants) as FRET partners (Miyawaki *et al.*, 1997; Miyawaki *et al.*, 1999). Ca^{2+} binding to calmodulin triggers binding of calmodulin to the M13 domain inducing a severe structural change. These changes alter the distance between the fluorescent proteins fused to calmodulin, for example CFP and YFP, resulting in modified FRET efficiency.

In addition to sensors for ions, sensors for the detection of primary metabolites (e.g. maltose, ribose, glucose) have recently been developed, using periplasmic binding proteins (PBPs) as reporter domains (Fehr *et al.*, 2002; Fehr *et al.*, 2003; Lager *et al.*, 2003; Ye and Schultz, 2003). Periplasmic binding proteins (PBP) comprise of a variety of proteins located in the periplasm between the inner and outer membrane of Gram-negative bacteria. They are involved in chemotaxis and transport processes by binding of different compounds including sugars, amino acids, oligopeptides, vitamins, and cations, and delivery to the corresponding transporter or receptor. They are all structurally related, each consisting of two globular domains and a flexible region. The most striking feature of PBPs is a conformational change involved in substrate binding, enclosing the ligand in a twist-hinge motion resembling a Venus flytrap (Felder *et al.*, 1999). Taking advantage of the conformational changes of PBPs upon substrate binding and of the spectral features of GFP variants, FLIPs (Fluorescent Indicator Proteins) have been developed by fusing maltose, ribose or glucose binding proteins between ECFP and EYFP (Fehr *et al.*, 2002; Fehr *et al.*, 2003; Lager *et al.*, 2003). Changes in the distance between CFP and YFP due to the closing or opening of the PBPs upon substrate binding and release thus leads to differences in steady state FRET efficiency.

Despite low sequence similarities, similar structures and conformational changes can be found for the GalII/LacI type of repressors, for example the *Escherichia coli* lactose repressor LacI and the purine repressor PurR (Felder *et al.*, 1999).

² inverse proportional to the sixth power of the distance

1.4.3. The *Escherichia coli* Purine Repressor PurR

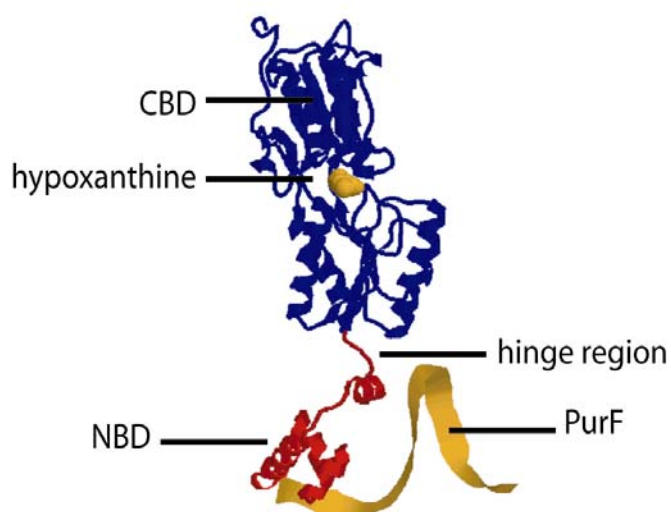


Fig. 7: Structure of the Purine Repressor (PurR) from *Escherichia coli* (PDB 1PNR).

Bound DNA (*PurF*) and the corepressor hypoxanthine are shown in orange. PurR consists in a nucleotide binding domain (NBD, red, residues 1-60) and a corepressor binding domain (CBD, blue, residues 61-341).

The *Escherichia coli* Purine Repressor (PurR) is a member of the GalI/LacI family of transcription repressors, regulating a set of genes controlling nucleotide synthesis (Choi and Zalkin, 1994). PurR (Fig. 7) is a 38 kDa protein consisting in a N-terminal nucleotide binding domain (NBD) (residues 1-60) and a C-terminal corepressor-binding domain (CBD) (residues 61-341)³, the latter being structurally similar to PBPs (Choi and Zalkin, 1994; Huffman *et al.*, 2002).

The family of LacI/GalR repressors might have evolved from ancestral PBPs by acquiring the N-terminal nucleotide binding domain (Fukami-Koboyashi *et al.*, 2003). In contrast to the monomeric PBPs, PurR is functional as a dimer. Hypoxanthine and guanine act as corepressors for PurR (Choi and Zalkin, 1994; Lu *et al.*, 1998a; Lu *et al.*, 1998b; Huffman *et al.*, 2002). Corepressor binding induces a conformational change and closure of the CBD entrapping the substrate. Structural rearrangements position the NBD so that in presence of operator DNA (*PurF*, a 16 bp sequence) a flexible hinge comprising residues 48-56 can undergo a coil to helix transition allowing DNA binding (Huffman *et al.*, 2002).

The Ribose Binding Protein has already been successfully used for nanosensor development (Lager *et al.*, 2003). The CBD of PurR and the Ribose Binding Protein (RBP) in the closed conformations are highly structurally related, though PurR is slightly more open. This suggests that PurR might be a valuable tool for development of a nucleobase sensor. Though PurR mainly binds hypoxanthine and guanine, other substrate specificities could be achieved by structure based mutational design or random mutagenesis approaches (Fehr *et al.*, 2003; Lager *et al.*, 2003; Looger *et al.*, 2003).

1.5. Aim of this work

Nucleotides and derivatives are one of the most important groups of metabolites in organisms. They are essential for the growth and development of plants. Understanding the interplay of all the pathways involved in nucleotide metabolism is still limited by the fact that knowledge about concentrations of involved compounds in cells or tissues is scarce and hardly anything is known about fluxes between different compartments. In addition, knowledge about

³ For crystal structures see <http://www.rcsb.org/pdb/cgi/resultBrowser.cgi>.

transmembrane proteins mediating the transport of nucleobases and their derivatives involved in metabolic pathways, like salvaging, is fragmentary.

The aim of this thesis was to contribute to a better understanding of the dynamics of nucleobases and derivatives in plants. Two different approaches were set up:

(i) *AtUPS1* was recently identified as a transporter of allantoin and other, structurally related heterocyclic compounds in *Arabidopsis*. Since no evidence of the importance of allantoin transport in *Arabidopsis* is given, the physiological importance remained obscure. In this study, the closest homologues of *AtUPS1* were cloned. The substrate specificity of selected family members was determined by expression in heterologous systems and determination of uptake kinetics. The mechanism and regulation of transport were investigated. To obtain insight into the physiological function of UPS transporters, the regulation of expression and spatial expression patterns were analysed. In addition, public collections were screened for insertional mutants to obtain information about the *in vivo* function of UPS by analysis of the phenotypes of loss-of-function mutants. All together, the combination of different approaches will help towards an understanding of the contribution of *AtUPS* proteins to transport processes of nucleobases, derivatives and degradation products in plants.

(ii) The *Escherichia coli* Purine Repressor PurR was used as basis for the development of a nucleobase sensor similar to the described maltose and ribose nanosensors. The generation of a functional metabolite sensor based on PurR would be of great value as starting point for *in vivo* imaging of nucleobases and derivatives.

2. Material and Methods

2.1. Material

2.1.1. Enzymes

Restriction enzymes were purchased from Fermentas GmbH (St. Leon-Rot, Germany) or New England Biolabs (Frankfurt, Germany).

2.1.2. Oligonucleotides

Oligonucleotides were purchased from Sigma ARK (Darmstadt, Germany), TIB MOLBIOL (Berlin, Germany), Invitrogen (Karlsruhe, Germany) and the PAN-Facility (Stanford, USA); sequences of oligonucleotides are listed in the Appendices (Table 1).

2.1.3. Plants

Arabidopsis thaliana Col-0 was used throughout this study. T-DNA insertion lines were obtained from the Arabidopsis Biological Resource Center (ABRC, Ohio, USA) (Alonso *et al.*, 2003).

2.1.4. Bacterial and Yeast Strains

2.1.4.1. *Escherichia coli* (*E. coli*)

Procedures for manipulating *E. coli* have previously been described (Sambrook *et al.*, 1989).

K12 (Blattner *et al.*, 1997)
F', lambda, e14, rac

DH5α (Invitrogen GmbH, Karlsruhe, Germany)
F' phi80dlacZ delta M15 delta (*lacZYA-argF*)U169 *deoR recA1 endA1 hsdR17* (r_k^- , m_k^+)
gal' phoA supE44 lambda-thi-1 gyrA96 relA1

XL1Blue (Stratagene, La Jolla, USA)
recA1 endA1 gyrA96 thi-1 hsdR17 supE44 relA1 lac[F'proAB *lacI*^qΔM15, Tn10 (Tet^r)]

Top10F' (Invitrogen GmbH, Karlsruhe, Germany)
F' {*lacI*^q Tn10 (Tet^R)} *mcrAΔ(mrr-hsd RMS - mcrBC) Φ 80lacZΔM15ΔlacZX74 recA1 araD139Δ(ara-leu)7697galUgalK rpsLendA1nupG*

BL21Gold (DE3) (Stratagene, La Jolla, USA)
E. coli B F' *ompT hsdS*($r_B^- m_B^-$) *scm*⁺ Tet^r *gal λ* (DE3) *endA Hte*

2.1.4.2. *Agrobacterium tumefaciens*

Agrobacterium tumefaciens GV3101 (pMP90) (Koncz and Schell, 1986)

2.1.4.3. <i>Saccharomyces cerevisiae</i>	
23344c	Mat α <i>ura3-52</i> (Soussi-Boudekou <i>et al.</i> , 1997)
THY.AP5	<i>MATΔ URA3 leu2 trp1 his3 loxP::ade2</i> (Obrdlik <i>et al.</i> , 2004)
THY.AP4	<i>MATα ura3 leu2 lexA::lacZ::trp1 lexA::HIS3 lexA::ADE2</i> (Obrdlik <i>et al.</i> , 2004)
<i>dal4 dal5</i>	derived from 23344c by disruption of <i>dal4</i> and <i>dal5</i> (Desimone <i>et al.</i> , 2002)
Y05963 (<i>dal4</i>)	Mat <i>a</i> ; <i>his3Δ1</i> ; <i>leu2Δ0</i> ; <i>met15Δ0</i> ; <i>ura3Δ0</i> ; YIR028w::kanMX4 (Euroscarf, Frankfurt, Germany)
<i>fur4</i>	derived from CEN.PK 2-1C (<i>MATα</i> , <i>ura3-52</i> ; <i>trp1-289</i> ; <i>leu2-3-112</i> ; <i>his3Δ1</i> ; MAL2-8 ^C : <i>Suc2</i> (Euroscarf, Frankfurt, Germany) by using a loxP-KanMX-loxP disruption cassette

2.1.5. Vectors

pCR4TopoBlunt	Invitrogen GmbH, Karlsruhe, Germany
pGEM [®] Teasy	Promega, Mannheim, Germany
pRSETB	Invitrogen
pDR195	provided by Doris Rentsch (Rentsch <i>et al.</i> , 1995)
pMD200	derived from pDR195 as described, provided by Marcelo Desimone
pDR199	derived from pDR195, provided by Gabriel Schaaf (Schaaf, 2004)
pACT2	(BD Biosciences, Mississauga, Canada)
pNXgate3HA	provided by Petr Obrdlik (Obrdlik <i>et al.</i> , 2004)
pXNgate3HA	provided by Petr Obrdlik (Obrdlik <i>et al.</i> , 2004)
pMetYCGate	provided by Petr Obrdlik (Obrdlik <i>et al.</i> , 2004)
pNubWT-2	provided by Petr Obrdlik (Obrdlik <i>et al.</i> , 2004)
pFL61	(Minet <i>et al.</i> , 1992)
pOO2	provided by Uwe Ludewig (Ludewig <i>et al.</i> , 2002)
CF203	derived from pPZP212 (Hajdukiewicz <i>et al.</i> , 1994), provided by Dr. Christian Fankhauser, University of Geneva
pCB302.3	(Xiang <i>et al.</i> , 1999)
pCB308	(Xiang <i>et al.</i> , 1999)

2.1.6. Media

2.1.6.1. Media for growth of bacteria

Escherichia coli was grown at 37 °C on Luria Broth (LB) medium (Sambrook *et al.*, 1989), unless that otherwise stated. *Agrobacterium tumefaciens* was grown at 28 °C on Broth medium.

LB

For solid media 1.5 % agarose (Oxoid, Hampshire, UK) was added.

5 g/L	yeast extract	(Difco [™])
10 g/L	tryptone	(Bacto [™] , Becton Dickinson GmbH Heidelberg, Germany)
10 g/L	NaCl	(Merck, Darmstadt, Germany)

Broth

For solid media 1.5 % agarose (Oxoid) was added.

5 g/L	yeast extract	(Difco™)
10 g/L	tryptone	(Bacto™)
10 g/L	NaCl	(Merck)
1 g/L	glucose	(Merck)

2.1.6.2. Media for growth of yeast

Saccharomyces cerevisiae were grown at 28 °C on either full medium Yeast extract Peptone Dextrose (YPD), Synthetic Complete (SC) medium, or Synthetic Defined (SD) medium (Adams *et al.*, 1997). For solid medium, 2 % agarose (Oxoid) was added.

YPD

10 g/L	yeast extract	(Difco™)
20 g/L	peptone	(Bacto™)
5 g/L	(NH ₄) ₂ SO ₄	(Carl-Roth GmbH & Co, Karlsruhe, Germany)
20 g/L	glucose	(Merck)

SC

1.7 g/L	yeast nitrogen base, without amino acids, without ammonium	(Becton Dickinson GmbH)
20 g/L	glucose	(Merck)
5 g/L	(NH ₄) ₂ SO ₄	(Carl-Roth GmbH)
1.5 g/L	Dropout Mix	(AHTUM)

pH 6-6.3 with NaOH

SC/AHL

SC supplemented with

10 mL/L	adenine sulfate stock solution
2 mL/L	histidine stock solution
2 mL/L	leucine stock solution

SC/AHTU

10 mL/L	adenine sulfate stock solution
2 mL/L	histidine stock solution
2 mL/L	tryptophan stock solution
10 mL/L	uracil stock solution

Amino acid stock solutions

Amino acids were purchased from Sigma-Aldrich (München, Germany).

2 g/L	adenine hemisulfate
2 g/L	uracil
10 g/L	tryptophan
10 g/L	leucine
10 g/L	histidine
10 g/L	methionine

Dropout Mix (AHTUM) (Adams *et al.*, 1997)

Chemicals were purchased from Sigma-Aldrich, unless that otherwise stated.

2.0 g alanine
2.0 g arginine
2.0 g asparagine
2.0 g aspartate
2.0 g cysteine (Fluka, München, Germany)
2.0 g glutamine (Merck)
2.0 g glutamate
2.0 g glycine
2.0 g inositol
2.0 g isoleucine
2.0 g lysine
0.2 g para-aminobenzoic acid
2.0 g phenylalanine
2.0 g proline
2.0 g serine
2.0 g threonine
2.0 g tyrosine
2.0 g valine

SD

1.7 g/L yeast nitrogen base, without amino acids, without ammonium
(Becton Dickinson)
20 g/L glucose (Merck)
5 g/L (NH₄)₂SO₄ (Carl-Roth GmbH)
pH 6-6.3 with NaOH

2.1.6.3. Plant cell culture medium

BY-2 Medium

4.30 g/L MS salts (Gibco™, Invitrogen, Karlsruhe, Germany)
100 mg/L myo-Inositol (Sigma-Aldrich)
1 mg/L thiamine (Sigma-Aldrich)
0.2 mg/L 2,4-dichlorophenoxyacetic acid
(2,4 D; Duchefa, Haarlem, Netherlands)
255 mg/L KH₂PO₄ (Merck)
30 g/L sucrose (Sigma-Aldrich)
pH 5.0 with KOH

2.4-D

40 mg dichlorophenoxyacetic acid (Duchefa)
4 mL EtOH
in a total volume of 40 mL H₂O.

2.1.6.4. Solutions for preparation transformation of protoplasts

Cell wall digestion solution

1.00 % (w/v)	cellulase	(Paesel + Lorelei GmbH & Co., Frankfurt, Germany)
0.25 % (w/v)	Macerozym R-10	(Duchefa)
8 mM	CaCl ₂ x2 H ₂ O	(Merck)
400 mM	mannitol	(Merck)
pH 5.5		

Cell wall digestion solution without enzymes

8 mM	CaCl ₂ x2 H ₂ O	(Merck)
400 mM	mannitol	(Merck)
pH 5.5		

W5 solution

154 mM	NaCl	(Merck)
125 mM	CaCl ₂ x2 H ₂ O	(Merck)
5 mM	KCl	(Merck)
5 mM	glucose	(Merck)
pH 5.8-6		

MMM solution

15 mM	MgCl ₂ x6 H ₂ O	(Merck)
0.1 % (w/v)	MES	(Sigma-Aldrich)
5 mM	KCl	(Merck)
5 mM	glucose	(Merck)
pH 5.8		

PEG solution

40 % (w/v)	PEG 4000 (Polyethylenglycol)	(Fluka)
400 mM	mannitol	(Merck)
100 mM	Ca(NO ₃) ₂ x4 H ₂ O	(Merck)
pH 8-9		

2.1.6.5. Media for growth of *Arabidopsis thaliana* plants

1 % of sucrose was added, unless that otherwise stated. For solid medium, 0.7% of agar (Gibco™) was added.

MS medium

4.3 g/L	MS salts	(Gibco™)
10 mM	MES	(Sigma-Aldrich)
pH 5.7 with KOH		

MS medium modified

Ingredients were purchased from Merck, unless that otherwise stated.

25 mL/L	Macro solution 1
25 mL/L	Macro solution 2
25 mL/L	Macro solution 3
2.5 mL/L	Micro solution
2.5 mL/L	Chelator solution
10 mM	MES (Sigma-Aldrich)
pH 5.7 with KOH	

Macro solution 1

8.8 g/L	CaCl ₂
---------	-------------------

Macro solution 2

7.4 g/L	MgSO ₄
---------	-------------------

Macro solution 3

3.4 g/L	KH ₂ PO ₄
---------	---------------------------------

Micro solution

1.24 g/L	H ₃ BO ₃
3.38 g/L	MnSO ₄ xH ₂ O
1.72 g/L	ZnSO ₄ x7H ₂ O
0.166 g/L	KI
0.05 g/L	Na ₂ MoO ₄ x2H ₂ O
0.005 g/L	CuSO ₄ x5H ₂ O
0.005 g/L	CoCl ₂ x6H ₂ O (Sigma-Aldrich)

Chelator

7.46 g/L	Na ₂ EDTAx2H ₂ O
5.57 g/L	FeSO ₄ x7H ₂ O

2.1.6.6. Seed sterilization

Sterilization solution

900 µL	sterile water
1.5 µL	10 % sterile filtered Triton X-100 (Serva, Heidelberg, Germany)
100 µL	12 % sodium hypochloride (Carl-Roth GmbH)

2.1.6.7. For *Arabidopsis* transformation

Infiltration Medium

2.15 g/L	MS salts (Gibco™)
0.044 µM	benzylaminopurine (Sigma-Aldrich; stock in DMSO)
0.02 %	Silwet L-77 (Lehle Seeds, Round Rock, USA)
pH 5.7 with KOH	

2.1.7. Buffers and solutions

2.1.7.1. Split ubiquitin assays

Z-buffer

Chemicals were purchased from Merck (Darmstadt, Germany).

10.680 g/L $\text{Na}_2\text{HPO}_4 \cdot 2\text{H}_2\text{O}$

5.500 g/L $\text{NaH}_2\text{PO}_4 \cdot \text{H}_2\text{O}$

0.750 g/L KCl

0.246 g/L $\text{MgSO}_4 \cdot 7\text{H}_2\text{O}$

to pH 7 with NaOH

X-Gal solution

80 mg/mL X-Gal (5-bromo-4-chloro-3-indolyl- β -D-galactoside; St. Leon Roth, Germany) in DMF (dimethylformamide).

10 % SDS (Carl-Roth GmbH)

2.1.7.2. GUS-assay

GUS-staining solution 1

1 mM	X-Gluc (5-bromo-4-chloro-3-indolyl-beta-D-glucuronic acid), (Duchefa, Netherlands), (stock 100 mM in dimethylformamide)
100 mM	sodium phosphate buffer pH 7.2
10 mM	EDTA (Merck)
0.2 % (v/v)	Triton X 100 (Serva)
3 mM	potassium ferrocyanide (Merck)
0.5 mM	potassium ferricyanide (Fluka)

GUS-staining solution 2

48.5 mM	sodium phosphate buffer pH 7.2
0.49 mM	potassium ferrocyanide (Merck)
0.49 mM	potassium ferricyanide (Fluka)
0.97 mM	X-Gluc (stock 100 mM in dimethylformamide)

Periodic acid schiff reagent

5 g p-rosanilin (Sigma-Aldrich, München, Germany) in 900 mL H_2O hot water ($\sim 90^\circ\text{C}$)

The solution was stirred for 1 min, filtered and cooled to $\sim 50^\circ\text{C}$. 50 mL 1N HCl and 5 g $\text{Na}_2\text{S}_2\text{O}_4$ (Fluka) were added.

2.1.7.3. Oocyte work and electrophysiology

Chemicals were purchased from Merck, unless that otherwise stated.

Solution 1

82.5 mM NaCl

2 mM KCl

1 mM MgCl_2

5 mM HEPES at pH 7.4 (Biomol, Heidelberg, Germany)

“Wash solution” standard perfusion solution

100 mM	choline-chloride	(Sigma-Aldrich)
2 mM	CaCl ₂	(Merck)
2 mM	MgCl ₂	(Merck)
5 mM	MES-Tris at pH 5.5	

ND96 solution

Chemicals were purchased from Merck.

96 mM	NaCl
2 mM	KCl
1 mM	MgCl ₂
1.8 mM	CaCl ₂
5 mM	HEPES at pH 7.4

2.1.7.4. RNA-extraction

CTAB-buffer

Chemicals were purchased from (Sigma-Aldrich) unless that otherwise stated.

2 % (w/v)	CTAB (N-Cetyl-N, N, N, -trimethylammoniumbromide)	
2 % (w/v)	PVP (Polyvinylpyrrolidone K28-32)	
100 mM	Tris-HCl pH 8	(Carl-Roth GmbH)
25 mM	EDTA pH 8	(Merck)
2 M	NaCl	(Merck)
0.5g/L	spermidine	
2 % (v/v)	β-mercaptoethanol	were added before use.

2.2. Methods

2.2.1. Standard methods

Standard methods such as restriction digestion, plasmid preparation, gel electrophoretic DNA separation, DNA isolation from agarose gels, PCR amplification and cloning steps, etc. were performed as described (Sambrook *et al.*, 1989). Sequencing of DNA was done by the chain terminating method (Sanger *et al.*, 1977) using a Big Dye Terminator Cycle Sequencing Ready Reaction Kit (Perkin Elmer, Warrington, UK), by Sequetech Corporation (Mountain View, USA) or by GATC Company (Konstanz, Germany). Sequence comparisons with databases were performed using the Basic Local Alignment Search Tool program at NCBI gene information network (Altschul *et al.*, 1999; <http://www.ncbi.nlm.nih.gov/blast/>).

2.2.2. Transformation methods for bacteria and yeast

2.2.2.1. *Escherichia coli*

Escherichia coli was transformed as described (Nishimura *et al.*, 1990).

2.2.2.2. *Agrobacterium tumefaciens*

For preparation of competent cells a single colony of *Agrobacterium* GV3101 grown on Broth plates with appropriate antibiotics was inoculated in 5 mL liquid Broth with antibiotics over night. This preculture was used for 1:100 inoculation of 500 mL Broth medium with

antibiotics. Cultures were grown to an OD₆₀₀ of ~0.5. Cells were pelleted for 5 min at 3840 g (JA14 rotor, J2-MC Centrifuge (Beckman, München, Germany)) and resuspended in 100 mL 0.15 M NaCl. Centrifugation was repeated and cells were resuspended in 10 mL of 20 mM ice-cold CaCl₂. Aliquots of 200 µL were immediately stored on ice and frozen at -70 °C. For transformation, aliquots of cells were thawed on ice and 10 µL of plasmid preparations (~ 1 µg/µl DNA) were added. Tubes were left on ice for 5 min, frozen for 5 min in liquid nitrogen and then incubated for 5 min at 37 °C. 1 mL of Broth was added and tubes were shaken for 2 hours at 27 °C before plating on Broth with antibiotics.

2.2.2.3. *Saccharomyces cerevisiae*

Yeast was transformed as described (Dohmen *et al.*, 1991; Gietz and Schiestl, 1995; Fusco *et al.*, 1999).

2.2.3. DNA-work

Maps of constructs are available in the appendices.

2.2.3.1. Cloning of *AtUPS* cDNAs

The *E. coli* strain DH5α was used for cloning. PCR reactions for cloning were performed with Pfu Turbo (Stratagene, La Jolla, California). *AtUPS2* was amplified by PCR from a cDNA library from 5-day-old seedlings of *Arabidopsis thaliana* (ecotype Col-0) with primers P1 and P2 and cloned into pCR4TopoBlunt. Sequencing revealed mutations of A to T (at position 276 of the open reading frame relative to the start codon) and A₆₇₈ to G not resulting in an altered protein sequence. In addition, T₃₀₈ was mutated to C, causing valine to alanine exchange. This mutation was reverted by site-directed mutagenesis using the Quick Change Kit (Stratagene, La Jolla, California) according to the manufacturer's instructions. *AtUPS5* and *AtUPS5s*⁴ were amplified with primers P3 and P4, cloned into pCR4TopoBlunt and sequenced.

2.2.3.2. Oocyte expression constructs

The *E. coli* strain DH5α was used for cloning. The *AtUPS2*, *AtUPS5* and *AtUPS5s* coding sequences were excised with *Bam*HI/*Xba*I from pCR4TopoBluntUPS2, pCR4TopoBluntUPS5 and pCR4TopoBluntUPS5s and cloned into the oocyte expression vector pOO2 (Ludewig *et al.*, 2002) linearized with *Bam*HI/*Xba*I. The *UPS1* expression construct was described before (Desimone *et al.*, 2002). Amino acid exchanges in *AtUPS1* and *AtUPS2* were generated by site-directed mutagenesis using the Quick Change Kit (Stratagene, La Jolla, California) according to the manufacturer's instructions as summarized in Table 1. Mutations were confirmed by sequencing.

Tab. 1: Templates and primers used to generate mutations on oocyte expression constructs.

Mutagenized Template	Primers used	Generated mutation	Name of final clone
pOO2UPS1	P5/P6	K215I	pOO2UPS1_K215I
pOO2UPS1	P7/P8	K219I	pOO2UPS1_K219I
pOO2UPS1	P9/P10	K219R	pOO2UPS1_K219R
pOO2UPS2	P11/P12	K227I	pOO2UPS2_K227I

⁴ *AtUPS5s* (short) is a shorter splicing variant of *AtUPS5*.

2.2.3.3. Yeast expression constructs

The *E. coli* strain DH5 α was used for cloning. pDR199UPS1 was obtained by amplifying *UPS1* from the cDNA library with primers P13 and P14, and co-transformation of the PCR-product with the *EcoRI/BamHI*-linearized vector pDR199 into a yeast *dal4 dal5* knock out strain (Desimone *et al.*, 2002), following the *in vivo* cloning technique (Dohmen *et al.*, 1991). After selection on uracil-free medium, plasmids were isolated and the cDNA insertion verified by sequencing. Two T to C mutations (positions 997 and 1152 of the open reading frame relative to the start codon), which did not alter the protein sequence, were found in the coding sequence. The *UPS2*, *UPS5* and *UPS5s* coding sequences were each excised with *BamHI/XhoI* from pOO2UPS2, pOO2UPS5 and pOO2UPS5s and subcloned into the yeast expression vector pDR199. pMD200 is a modification of pDR195 (Rentsch *et al.*, 1995) by disruption of the *URA3* gene by an *ApaI/NcoI* digestion and introduction of the *LEU2* gene. *LEU2* was PCR amplified with primers P15 and P16 from pACT2 (BD Biosciences, Mississauga, Canada). The *UPS1* (*UPS2*) coding sequences were excised from pCR4TopoBluntUPS1 (pCR4TopoBluntUPS2) and cloned into pMD200: *UPS1* (*UPS5s*) was excised *EcoRI*, blunted and introduced into the blunted *NotI* site of pMD200; *UPS2* and *UPS5* were excised by *XbaI/NotI*, *XbaI* was blunted and the constructs were introduced into pMD200 (*BamHI* blunted/*NotI*).

Yeast expression constructs for split ubiquitin assays were amplified by PCR of *UPS2*, *UPS5* and *UPS5s* coding sequences from pCR4TopoBluntUPS2, pCR4TopoBluntUPS5 and pCR4TopoBluntUPS5s with primers P17 and P18 for *UPS2* and P19 and P20 for *UPS5* and *UPS5s*. The PCR products were purified on a 1% agarose gel using a QIAquick Gel Extraction Kit (Qiagen, Düsseldorf, Germany) according to the manufacturer's instructions. For NubG-fusions, vectors pNXgate3HA and pXNgate3HA (Obrdlik *et al.*, 2004) were linearized by *EcoRI/SmaI* digest. PCR-products and linearized vectors (pNXgate3HA in combination with either *UPS2*, *UPS5* or *UPS5s* and pXNgate3HA with either *UPS2*, *UPS5* or *UPS5s*) were introduced into the yeast strain THY.AP5 (Obrdlik *et al.*, 2004) and *in vivo* cloning (Fusco *et al.*, 1999) and the transformants were selected on synthetic complete medium (SC) lacking tryptophan and uracil. In addition, the THY.AP5 yeast mutant was transformed with the vectors pNXgate3HA and pNubWT-2 and the expression constructs NubG-KAT, KAT1-NubG, NubG-Sut2 and Sut2-NubG (Gietz and Schiestl, 1995; Obrdlik *et al.*, 2004). For Cub-fusions, the vector pMetYCGate (Obrdlik *et al.*, 2004) was linearized by *PstI/HindIII* digest and introduced into the yeast strain THY.AP4 for *in vivo* cloning together with either *UPS2*, *UPS5* or *UPS5s*. In addition, the THY.AP4 yeast mutant was transformed with the vector pMetYCGate and the expression constructs KAT1-Cub and Sut2-Cub (Gietz and Schiestl, 1995; Obrdlik *et al.*, 2004).

2.2.3.4. GFP-fusion constructs

The *E. coli* strain XL1blue was used for cloning. Coding sequences without stop codon were amplified from pCR4TopoBluntUPS1, pCR4TopoBluntUPS2, pCR4TopoBluntUPS5 and pCR4TopoBluntUPS5s with primers P21 and P22 for *UPS1*, P23 and P24 for *UPS2* and P25 and P26 in case of *UPS5* and *UPS5s*. After sequencing, the constructs were excised with *BamHI/SacI* and translational C-terminal fusions to the green fluorescent protein (GFP) were created by cloning into CF203 digested with *BamHI/SacI*. CF203 is a derivative of pPZP212 (Hajdukiewicz *et al.*, 1994) allowing C-terminal fusion with GFP5.

2.2.3.5. Promoter-GUS constructs

The *E. coli* strain DH5 α was used for cloning. The promoter region containing genomic DNA extending from the 3'-UTR of the preceding gene to start codon was PCR'd out from genomic DNA (Table 2), cloned into pCR4TopoBlunt and sequenced. The promoters were excised and introduced into pCB308 (Xiang *et al.*, 1999).

Tab. 2: Cloning of *AtUPS* promoter regions

Gene name	Promoter length	PCR template	Primers used	Restriction sites
AtUPS1	647	genomic DNA	P27 and P28	SpeI/BamHI
AtUPS2	721	BAC T4M8	P29 and P30	XbaI/BamHI
AtUPS3	582	genomic DNA	P31 and P32	XbaI/SpeI
AtUPS4	504	BAC T4M8	P33 and P34	XbaI/BamHI
AtUPS5	700	BAC T1K7	P35 and P36	XbaI/BamHI

2.2.3.6. *UPS1* PTGS construct

The *E. coli* strain DH5 α was used for cloning. A 521 bp *AtUPS1* fragment ('sense') was amplified by PCR from pFL61UPS1 using primers P37 and P38. A similar 521 bp fragment ('antisense') was amplified using primers P39 and P40. An 882 bp fragment of the second intron of *AtAAP6* (At5g49630) was amplified from BAC K6M13 using primers P41 and P42. All the fragments were cloned into pCR4TopoBlunt and sequenced. The *UPS1* 'antisense' fragment was excised with *XbaI/XhoI* and ligated into the pCR4TopoBluntAAP6intron construct. The resulting construct was subsequently cleaved with *HindIII/SpeI* and the *UPS1* 'sense' fragment excised by *HindIII/SpeI* was introduced. The complete *UPS1*'sense'*AAP6*intron*UPS1*'antisense' construct was subcloned into pCB302.3 (Xiang *et al.*, 1999) using *SpeI/XbaI*.

2.2.3.7. *UPS5s* overexpression construct

The *UPS5s* coding sequence was *BamHI/XbaI* excised from pCR4TopoBluntUPS5s and introduced into pCB302.3.

2.2.3.8. Sensor cloning

The *E. coli* strain Top10F' was used for cloning of *PurR* constructs. *PurR1* (*PurR59*) from *E. coli* was PCRed out from genomic DNA (strains DH5 α , K12) with primers P43 and P44 (P45 and P46) resulting in clones for expression of the PurR protein from amino acids V56 to R341 (T59 to R328; according to full length amino acid sequence), cloned into pCR4TopoBlunt (pGEM[®]Teasy) and sequenced. Both clones had two T to C transitions in positions 534 and 788 of the open reading frame, causing mutation of Leu²⁶³ to Pro (number confers to complete PurR amino acid sequence). pCR4TopoBluntPurR1R190Q was obtained by site-directed mutagenesis on pCR4TopoBluntPurR1 using primers P47 and P48 and confirmed by sequencing. *PurR1* and *PurR1R190Q* were *KpnI* excised from pCR4TopoBluntPurR1 and pCR4TopoBluntPurR1R190Q respectively, and cloned into pRSET_FLIP derived by excising sequence encoding the binding protein from Flip_{rib}-250n (Lager *et al.*, 2003) by *KpnI* digestion and subsequent gel purification and ligation of linearized pRSET_FLIP. This resulted in an in frame fusion constructs of a His-Tag, ECFP, the PurR construct, and EYFP. PurR59 was excised with *KpnI* from pGEM[®]Teasy and cloned into pRSETVenusF16AmglB (Okumoto, S., personal communication) by *KpnI* digestion, thereby replacing the F16AmglB moiety (Fehr *et al.*, 2003). In this construct the EYFP was replaced by a less pH and chloride sensitive and faster maturing YFP mutant variant (Venus) (Nagai *et al.*, 2002).

2.2.4. Yeast methods

2.2.4.1. Complementation and uptake assays with yeast

The yeast *dal4 dal5* double mutant strain was transformed with pDR199 or pDR199UPS1 (pDR199UPS2, pDR199UPS5 and pDR199UPS5s) (Gietz and Schiestl, 1995). Growth tests were performed on medium (SD without ammonium sulfate) with 5 mM allantoin. The yeast strain CEN.PK 2-1C (Euroscarf, Frankfurt, Germany) was used to generate a *fur4* knockout

mutant strain by using a loxP-KanMX-loxP disruption cassette (Güldner *et al.*, 1996). The *fur4* mutant strain was selected on SD (with 38 mM ammonium sulfate, 200 mg/L G418, 0.1 mM L-histidine, 0.1 mM L-tryptophan, 0.2 mM uridine), confirmed by PCR and subsequently transformed with pMD200 or pMD200UPS1 (pMD200UPS2, pMD200UPS5, pMD200UPS5s). Growth tests were performed on medium with 0.2 mM uracil instead of uridine. The *dal4* knockout mutant yeast strain Y05963 (Euroscarf) was transformed with a series of plasmids: pDR199/pMD200, pDR199UPS2/pMD200, pDR199UPS2/pMD200UPS5, pDR199UPS2/pMD200UPS5s, pDR199UPS5s/pMD200UPS5, pDR199UPS5s/pMD200 and pDR199UPS5/pMD200 (Gietz and Schiestl, 1995). Selection was performed on SC medium without uracil and leucine. ¹⁴C-Allantoin for uptake assays was prepared from 8-¹⁴C uric acid (ACR, St. Louis, USA, specific activity 50 mCi/mmol) with uricase (Sigma, München, Germany) following the protocol with modifications (Desimone *et al.*, 2002). 4.55 µmol 8-¹⁴C uric acid were dissolved in 25 µL 1 M KOH at room temperature and immediately diluted with 375 µL 100 mM sodium phosphate buffer pH 7 resulting in pH ≈ 8.5. Fifty-five µL of a solution of 2.4 mg uricase in 1 mL water were added, incubated for 13 hours at room temperature and afterwards immediately frozen at -20 °C. The reaction was detected spectrophotometrically following the decrease of uric acid absorption at the absorption maximum of 293 nm. Purity of allantoin was checked by HPLC and determined to be ~93%. A NH₂-Phase column (NAK 50927, Spherisorb 5 NH₂; Kontron, Basel, Switzerland) was used. Solvent system A (92 % acetonitrile and 0.1 % acetic acid) and solvent system B (60 % acetonitrile and 0.1 % acetic acid) at a flow rate of 1 mL/min were used for the separation of allantoin and uric acid, respectively. No ¹⁴C-uric acid could be observed with solvent system B, while a major peak of ¹⁴C-allantoin was observed with solvent system A at a retention time of 6.17 min. The detection was performed with a DAD photometer (Kontron, Basel, Switzerland) and a LB50+B radioactivity monitor (Berthold, Bundoora, Australia). The yeast *dal4 dal5* double mutant strain was grown on SD medium, the strain Y05963 was grown on SD medium supplemented with 0.10 mM histidine and 0.13 mM methionine. 5 mL precultures were inoculated, grown over night and used for inoculation of 50 mL cultures in a ratio 1:100. Cultures were grown to OD 0.2-0.5. The cells were harvested by 6 min 30 s centrifugation at 2500 g (Jouan GR422 centrifuge) 4 °C, washed with 45 mL double distilled water and the centrifugation step repeated. The cells were subsequently suspended to OD 4 (*dal4 dal5*) or OD 5 (*dal4*). Uptakes were performed in 100 mM potassium phosphate solutions with yeast (*dal4 dal5* or *dal4*) resuspended to OD 2.2. Prior to uptake experiments with 200 µM ¹⁴C-allantoin, yeast cells were incubated for 5 min at 30 °C (shaking at 1000 rpm) with 100 mM D-glucose. Assays were started by addition of substrate at 30 °C (shaking at 1000 rpm). Aliquots of 100 µL were subsequently filtered through whatman filters (GF/C Glass Microfibre filters, Whatman, UK) under vacuum using a Hoefers collector (Pharmacia Biotech Model FH225V, San Francisco, USA) and washed with 12 mL of ice-cooled water. After addition of scintillation cocktail (High flash point LSC-cocktail, Ultima Gold, Perkin Elmer, Wellesley, USA), samples were counted in a Perkin Elmer Wallac Win Spectral 1414 Liquid Scintillation counter using Wallac LSC software.

2.2.4.2. Split ubiquitin assays (Obrdlik *et al.*, 2004)

a) Mating: 30 colonies of yeast strain THY.AP5 with pNXgate3HA-UPS2, pXNgate3HA-UPS2, pNXgate3HA-UPS5, pXNgate3HA-UPS5, pNXgate3HA-UPS5s, pXNgate3HA-UPS5s; 10 colonies of yeast strain THY.AP5 transformed with NubG-Kat, Kat-NubG, NubG-Sut2, Sut2-NubG, pNXgate3HA, pNubWT-2 (Obrdlik *et al.*, 2004); 30 colonies of yeast strain THY.AP4 transformed with pMetYCGate-UPS2, pMetYCGate-UPS5, pMetYCGate-UPS5s, and 10 colonies of yeast strain THY.AP4 transformed with KAT1-Cub, SUT2-Cub and pMetYCGate (Obrdlik *et al.*, 2004) were collected and suspended in 100 µL double distilled water. Fifty µL of each suspension were used to inoculate 5 mL cultures in SC/AHL

and SC/AHL G418 (200 µg/mL) for THY.AP5 or SC/AHTU and SC/AHTU G418 (200 µg/mL) for THY.AP4. Two mL of cells grown on medium without G418 (except for pNXgate3HA2 transformed yeast) were spun down for 1 min at 3830 g in a micro centrifuge (Eppendorf Centrifuge 5417R, Hamburg, Germany) and resuspended in 200 µL YPD. Two 15 µL aliquots of transformed THY.AP4 and THY.AP5 cells were mixed in a microtiter plate (96 wells) and 10 µL were dotted on YPD plates.

b) Growth assays: After a mating time of ~10 hours at 27 °C, the cells were replica plated on SC/AH and tested for growth at 27 °C for 5 days before replica plating on SC/AH with alternatively 0 µM, 50 µM, 150 µM and 1 mM methionine.

c) X-Gal overlay assay: 0.25 g agarose (Seakem® LE Agarose, Cambrex, East Rutherford, USA) was heated with 50 mL of Z-buffer in a microwave and cooled down to 50 °C before adding 1 mL of 10 % SDS and 1 mL of X-Gal solution. The solution was poured on a plate and incubated at 37 °C for ~1 hour.

2.2.5. Expression and electrophysiology in *Xenopus laevis* oocytes

2.2.5.1. Expression in *Xenopus laevis* oocytes

Oocytes were surgically removed from female *Xenopus laevis*. Follicular cell layers and connective tissues were removed by digesting with 2 mg/mL collagenase A (Roche, Basel, Switzerland) for 1.5-2 hours at 22 °C in a Ca²⁺-free solution (solution 1). Oocytes were subsequently washed 5-8 times with ND96 solution. Healthy oocytes at developmental stages V-VI were selected and maintained at 16 °C in ND96 solution supplied with 50 mg/l of gentamycin and 2.5 mM sodium pyruvate (ND96-G). Capped cRNAs were transcribed *in vitro* using the mMessage mMachine mRNA SP6 kit (Ambion, Huntingdon, Cambridgeshire, UK) from linearized plasmids pOO2UPS1, pOO2UPS2, pOO2UPS5 and pOO2UPS5s, according to the manufacturer's instructions. RNA yields were estimated by agarose gel electrophoresis and the concentrations were finally adjusted to approximately 1 µg/µL with nuclease-free water. Oocytes were microinjected with 50 nl of cRNA (20-50 ng/oocyte) and incubated at 16 °C in ND96-G solution to allow the expression of *AtUPS* genes. For injection with two expression constructs, equal concentrations of both cRNAs were mixed prior to microinjection.

2.2.5.2. Electrophysiology

Two-electrode voltage-clamp was performed starting 2 days after injection. Chemicals were dissolved in the standard perfusion solution to final concentrations of 200 µM and the pH values were adjusted to 5.5 with MES or Tris. For voltage-current analysis, currents were recorded while clamping the oocytes at -100 mV or by applying an I/V protocol. The I/V protocol consisted of 200 ms pulses of voltages ranging from -140 mV to 0 mV in steps of 20 mV. Substrate evoked currents were constant during these short pulses. Net currents induced by substrates were obtained by subtracting the background currents (measured with "wash solution" alone) before and after the addition of substrates. To avoid endogenous currents, which were slowly activated at more negative voltages, currents elicited at more negative voltages than -120 mV were not analyzed except when stated otherwise (in some cases only voltages in the range of 0 to -100 mV were analyzed). No differences between non-injected and water-injected oocytes were observed, thus in most cases uninjected oocytes were used as controls. K_m values were fitted using the equation $I = I_{max} / (1 + K_m/c)$ with I_{max} , maximal current at saturating concentration; K_m , substrate concentration at half maximal current and c , concentration of substrate used in the experiment.

2.2.6. Cell cultures

Cell cultures of tobacco BY-2 were grown at 26 °C in darkness on a shaker at 120 rpm with 70 mL of BY-2 medium in a 250 mL Erlenmeyer flask. They were inoculated once a week with 2 mL of culture per flask.

2.2.7. Preparation of protoplasts and expression of GFP constructs

Cultured cells of tobacco BY-2 were used 3 days after sub-cultivation. The cells were spun down at 400 g (Jouan GR422) for 5 min. The cells were washed with cell wall digestion buffer without enzymes before resuspending each pellet in 7 mL of cell wall digestion solution (with cellulase and Macerozym R-10). Samples were shaken for 6 hours at 50 rpm in the dark prior to centrifugation at 100 g for 5 min. Protoplasts were washed in cell wall digestion solution without enzymes and spun down by centrifugation for 5 min at 100 g. The pellet was slowly dissolved in 10 mL of solution W5, an aliquot was taken for counting and protoplasts were stored for 20 min at 4 °C in the dark. Protoplasts were spun down for 5 min at 100 g and suspended at a density of 2×10^6 protoplasts per mL with MMM solution. 250 μ L aliquots of protoplast suspension were taken and 30 μ g of plasmids CF203, CF203UPS1, CF203UPS2, CF203UPS5, CF203UPS5s (in 10 μ L water) were added for transformation. 250 μ L of PEG solution were slowly added and mixed gently before incubation for 15–20 min. Ten mL of W5 solution were slowly added. After centrifugation of the protoplasts for 5 min at 100 g, the pellet was suspended in 2 mL of K3 solution. The protoplasts were incubated in the dark for 1-4 days prior to investigation.

2.2.8. Plant growth and transgenic lines

2.2.8.1. Plant growth

For growth on plates, seeds were vernalized at 4 °C for 2 days before imbibition. The seeds were sterilized by shaking in 1 ml 70 % EtOH for 5 min, and afterwards for 20 min in 1 ml sterilization solution. They were then washed twice with sterile water. Plants were grown in a Percival Scientific growth chamber under a 16/8 h (light/dark) photoperiod at 22 °C and a light intensity of 100-150 μ E m⁻²s⁻¹, unless that otherwise stated. Plates with MS medium (Gibco™) were used. For Basta™ selection on plates 7 μ g/mL Phosphinotricin (Basta, Hoechst Schering AgrEvo GmbH, Berlin, Germany) were added to the MS medium. For growth assays on 5-FU (Sigma-Aldrich, München, Germany), the medium was supplemented with 200 μ M of this compound. Variations of the C:N ratio and nitrogen source were achieved by using a modified MS medium mixed from stock solutions supplemented or not with 1 % (w/v) of sucrose. Equal concentrations of ammonium (ammonium sulfate) and nitrate (potassium nitrate) were supplied. Alternatively plants were grown on MS medium with different heterocycles as sole source of 20 mM nitrogen (allantoin, xanthine, uric acid, uracil, thymine) or without nitrogen source. To test possible modulations of expression levels with supplemental heterocycles in the medium, plants were either grown on modified MS medium with 8 mM of nitrogen without sucrose and additional 200 μ M of either uracil, thymine, uric acid, xanthine, dihydrouracil, or allantoin, or on MS medium with sucrose with supplemental 1 mM thymine or uracil. For stress induction assays, plants were grown on plates with modified MS medium (20 mM nitrogen and 1 % (w/v) sucrose) for 13 days and transferred to liquid medium with modified MS medium (20 mM nitrogen with or without 1 % (w/v) sucrose, without nitrogen, or without sucrose but with 150 mM sodium chloride, and placed in a growth chamber with a 14/10 h (light/dark) photoperiod at 21.5 °C and a light intensity of 30-50 μ E m⁻²s⁻¹ for 1 day. Plants grown on soil were either grown under greenhouse conditions or in a growth chamber with a 16/8 h (light/dark) photoperiod at 22 °C and a light intensity of 70-80 μ E m⁻²s⁻¹.

2.2.8.2. Plant transformation and recovery of transgenic lines

pCB302.3 and pCB308 constructs were introduced into *Agrobacterium tumefaciens* strain GV3101 for plant transformation. *Arabidopsis thaliana* (ecotype Col-0) plants grown in the greenhouse were transformed with *Agrobacterium* using the floral dip method (Clough and Bent, 1998). Precultures of *Agrobacterium tumefaciens* GV3101 previously transformed with binary plasmids were grown in 5 mL of LB or Broth with appropriate antibiotics selection for 1-2 days at 28 °C. 400 mL cultures with antibiotics were inoculated from precultures and grown to OD ~ 2-4 at 28 °C. Cells were harvested by centrifugation for 10 min with 4420 g (JA10 rotor, J2-MC Centrifuge (Beckman, München, Germany)) at 20 °C and resuspended in 450 mL infiltration medium and distributed to 4 preserving jars. Another 150 mL of infiltration medium was added per preserving jar. *Arabidopsis* plants (4-5 pots with ~50 plants each) were dipped in this bacteria suspension for 15 min. Seeds of dipped plants were harvested and pooled. Transgenic plants (T1 to T3 generation) were selected by BASTA™ (phosphinothricin). In the case of the *UPS5s* over-expression line, only T1 generation was selected. For analysis of GUS activity T3 lines of the translational fusions of *UPS1*-, *UPS2*-, *UPS3*-, *UPS4*- or *UPS5*-promoter regions with the *uidA* gene were used for further investigation. Among the *UPS1* PTGS lines, fifty from T1 to T4 generation were analyzed for phenotypic alterations. BASTA™ resistance segregation and mRNA levels were determined for several lines. For growth assays with 5-FU, five T3 or T4 lines containing the *UPS1*-PTGS construct and chosen randomly (three homozygous and two heterozygous, based on BASTA™ resistance segregation) were analyzed for mRNA levels and phenotypic alterations.

2.2.8.3. T-DNA insertion Lines

Arabidopsis thaliana ecotype Col-0 was used throughout this study. Seeds of the T-DNA insertion lines Salk_143013 (designated *ups2-1*), Salk_044551 (designated *ups2-2*) and Salk_044810 (designated *ups5*) were obtained from the Arabidopsis Biological Resource Center (ABRC, Ohio, USA (Alonso *et al.*, 2003). Homozygous plants were isolated from T3 plants and confirmed in the T4 generation. Genomic DNA was prepared as described previously (<http://www.dartmouth.edu/~tjack/TAILDNAprep.html>). Homozygous lines were screened by two serious of PCR. PCR1 was performed with two gene specific primers and PCR2 with the left border primer P73 and the appropriate gene specific primer, as summarized in Table 3 :

Tab. 3: PCR for analysis of Salk-lines

Salk line	Primers for PCR1	Primers for PCR2
Salk_044551	P49/P50	P55/P50
Salk_143013	P51/P52	P55/P52
Salk_044810	P53/P54	P55/P53

Plants were considered homozygous if no PCR product was obtained by the first PCR reaction (PCR1) and fragments of expected size confirming the T-DNA insertion were amplified by the second PCR (PCR2). Position of T-DNA insertions in the gene sequence was analyzed by sequencing. Homozygous lines were subsequently taken for further investigations. Homozygous plants of each of the 3 Salk lines and two *UPS1* PTGS lines were backcrossed with *Arabidopsis thaliana* Col-0 wild type plants, and plants of different lines were crossed to obtain double knockout or silencing mutants of *UPS1* and *UPS2*, *UPS1* and *UPS5* or *UPS2* and *UPS5*. For this purpose, two homozygous *UPS1* PTGS lines were crossed with *ups2-1*, *ups2-2* or *ups5*, and *ups2-1* and *ups2-2* were each crossed with *ups5*.

2.2.9. Promoter GUS assays

Plants from plates were harvested from day 1 to day 14 after imbibition; plants from soil were harvested after 5-6 weeks and analyzed for β -glucuronidase activity (Martin *et al.*, 1992). Staining was performed for ~15 hours at 37 °C with GUS-staining solution 1 (whole plants) or 2 (tissues for sectioning). For root or leaf sections 6-day-old plants were prefixed in 50 mM phosphate buffer pH 7.2 containing 1.4 % (v/v) formaldehyde. Plants were washed in 50 mM phosphate buffer pH 7.2 followed by GUS staining for 8 h at 37 °C and subsequent fixation in 50 mM phosphate buffer (pH 7.2) containing 2 % (w/v) p-formaldehyde and 1 % (v/v) glutaraldehyde. Dehydration was performed in an series of solutions containing increasing concentrations of ethanol, followed by embedding in hydroxyethyl methacrylate (Technovit 7100, Heraeus Kulzer GmbH, Wehrheim, Germany). 6 μ m or 4 μ m thick sections were prepared with a LKB Ultratome. The tissue was counterstained in purple with periodic acid-Schiff solution.

2.2.10. RT-PCR analysis

Total RNA from agar-grown seedlings of *Arabidopsis* was extracted (Chang *et al.*, 1993). Plant material (50–100 mg) was ground to fine powder in liquid nitrogen and added frozen to 900 μ L CTAB buffer at 65 °C, vortexed for 30 s and incubated at 65 °C for ~1-2 min. A chloroform : isoamylalcohol mixture (24 : 1) (900 μ L) was added and the sample was spun at 10620 g at room temperature for 20 min. The supernatant was extracted with 900 μ L of the chloroform : isoamylalcohol mixture and spun at 10620 g at room temperature for 15 min. LiCl solution was added to the supernatant to a final concentration of 2 M prior to precipitation for ~12 hours at 4 °C. The sample was spun for 20 min at 4 °C and 20800 g. The supernatant was discarded and the pellet washed with 500 μ L 70 % EtOH and subsequently 500 μ L 100 % EtOH. The pellet was dissolved in 500 μ L TE and extracted with 900 μ L of the chloroform : isoamylalcohol mixture and spun at 10000 at room temperature for 15 min. 1/10 of the volume of 3 M sodium acetate (pH 5.2) and 2 times the volume of 100 % EtOH were added to the supernatant. After incubation at –20 °C for 5 hours, the sample was spun down for 20 min at 4 °C and 20800 g and subsequently washed with 70 % and 100 % EtOH. Samples were resuspended in 20–30 μ L DEPC treated water and the RNA concentration was determined. cDNA synthesized with RevertAid™ H Minus M-MuLV Reverse Transcriptase (MBI Fermentas, St. Leon Roth, Germany) was used as template for PCR-reactions. PCR-reactions are summarized in Table 4 :

Tab. 4 : Summary of RT-PCR assays

Template (gene)	Primers	size of fragment in bp	number of PCR-cycles
AtACT2 (cDNA)	P56/P57	641	26
AtUPS1 (cDNA)	P58/P59	481	30
AtUPS2 (cDNA)	P60/P61	484	32
AtUPS5, AtUPS5s (cDNA)	P62/P63	510	27
AtUPS5 (gen. DNA)	P3/P4	1595	27
AtUPS5 (cDNA)		1272	
AtUPS5s (cDNA)		1164	

The *AtACT2* gene was used as an internal control. No discrimination of *AtUPS5* and *AtUPS5s* is possible with primers P83/P84, since they anneal downstream of the additional splicing site of *AtUPS5s*.

2.2.11. Protein expression and purification

Constructs in pRSET-vectors were introduced into BL21Gold(DE3) cells. Colonies were inoculated in 200 mL of LB medium with ampicilin (100 µg/mL) and tetracylin (12 µg/mL) and grown for 3 days in darkness at room temperature with shaking at ~180 rpm before protein purification according to the method described (Fehr *et al.*, 2002). One mL of culture was spun down. The supernatant was discarded and the pellet re-suspended in 1 mL 20 mM MES buffer pH 7 (adjusted with KOH). Two µL of cell suspension were pipetted into 200 µL of 20 mM MES- or sodium-phosphate buffer pH 7 on a 96 well flat bottom microtiter plate (Nalge Nunc International, Rochester, USA) and emission spectra between 460 and 560 nm were recorded on a Sapphire Tecan Instrument using the Tecan software V3.12. The excitation wavelength was determined at 433 nm.

If CFP and YFP emission peaks were observed, cell cultures were spun down for 15 min at 4 °C with 2450 g (JA14 rotor and a J2-MC Centrifuge (Beckman, München, Germany)). The pellets were kept on ice and re-suspended in 5-8 mL ice-cold 20 mM Tris-HCl buffer (pH 7.9). The cells were broken by ultrasonification with a Branson Sonifier B-12 Cell Disruptor (Branson Sonic Power Company, Danbury, Connecticut, USA) while kept on ice for 6 times 15 s with 15 s of interruption in between. The samples were transferred to glass tubes and centrifuged for 45 min at 7750 g (JA20 rotor) and 4 °C. The supernatant was subsequently filtered through a 0.2 or 0.45 µm filter (Schleicher & Schuell GmbH, Dassel, Germany) and purified by His-bind chromatography (Novagen, San Diego, USA). The samples were shaken with 1 mL of resin on a planar shaker for ~1 hour at 4 °C in the dark for binding to the resin material and subsequently put back into the column (at 4 °C). The column was washed with 10 mL of 20 mM Tris-HCl (pH 7.9) and 3 mL of 20 mM Tris-HCl (pH 7.9) with 20 mM of imidazol. Proteins were eluted from the resin with 2 mL of 20 mM Tris-HCl (pH 7.9) with 200 mM of imidazol and stored on ice in darkness over night before starting functional assays. Ni²⁺ was released from the resin material by washing with a buffer containing 20 mM Tris-HCl (pH 7.9), 100 mM EDTA and 0.5 M NaCl. Spectra of proteins were recorded as described above. Titrations were made using 96-well microtiter plates with a Safire (Tecan) fluorometer and the software XFLUOR4 Version: V 4.50. The emission was recorded from the bottom of the plate, temperatures varied between 24 °C and 30 °C, and the gain was manually set between 65–75. The excitation wavelength was 433 nm and emission was recorded at 485 nm and at 530 nm. Bandwidths for excitation and emission were set to 12 nm, 10 flashes were given without lag time, the time between flash and move was 1 ms. Measurements were made with various concentrations of hypoxanthine dissolved in 20 mM MES-KOH buffer (pH 7). Using the changes in steady-state ratios upon different substrate concentrations, the K_d was determined as described by fitting the substrate titration curves to the equation $S = (r - R_{\min}) / (R_{\max} - R_{\min}) = [S]_{\text{bound}} / [P]_{\text{total}} = n[S] / (K_d + [S])$ with [S], substrate concentration, [S]_{bound}, concentration of bound substrate, n, number of equal binding sites, [P]_{total}, concentration of repressor, r, ratio, R_{min}, minimum ratio in absence of repressor, R_{max}, maximum ratio in presence of repressor coefficients were determined using the Hill equation $S = (n[S]^p / (K_d + [S]^p))$ (Fehr *et al.*, 2002). Three independent protein preparations were analyzed.

3. Results

3.1. Investigation of the *Arabidopsis thaliana* UPS family

3.1.1. The *AtUPS* family

The *AtUPS* family consists in 5 members in *Arabidopsis*. *AtUPS1* has recently been identified in a screen for an allantoin transporter (Desimone *et al.*, 2002). Two sets of two *AtUPS* genes are present in tandem orientation on chromosome 2 in the genome: *AtUPS1* and *AtUPS3* as well as *AtUPS2* and *AtUPS4* (Fig. 8). They might thus derive from recent gene duplications.

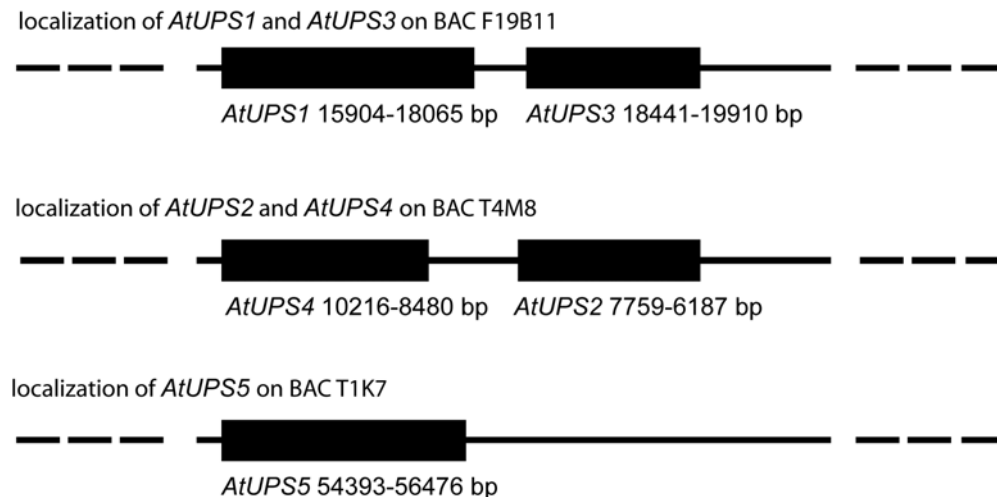


Fig. 8: Localization of *AtUPS* sequences on BACs.

AtUPS1 and *AtUPS3* as well as *AtUPS2* and *AtUPS4* seem to have arisen from recent gene duplications.

AtUPS have high levels of sequence similarities; *AtUPS1* shares 74 % sequence identity on the amino acid level with *AtUPS2*, 82 % with *AtUPS3*, 64 % with *AtUPS4* and 63 % with *AtUPS5*. *AtUPS2* and *AtUPS4* share 64 % of sequence identity on amino acid level (Fig. 9A, B). Related genes were also identified in legumes (<http://www.ncbi.nlm.nih.gov/blast/>).

A

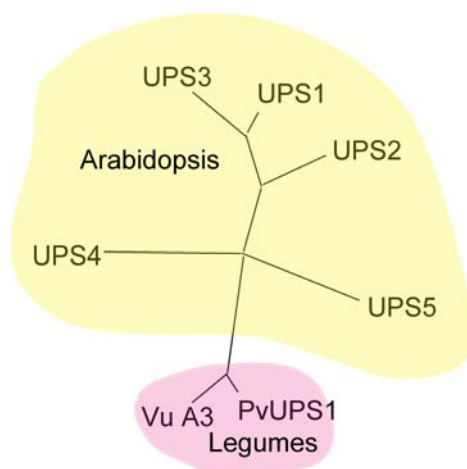


Fig. 9: Phylogenetic Tree (A) and alignment (B).

Phylogenetic analysis of *AtUPS* and related proteins in legumes. Maximum parsimony analyses were performed using PAUP4.0b4a informative (<http://paup.csit.fsu.edu/index.html>) (A). *AtUPS1*, 2, 3, 4 and 5 from *Arabidopsis*, *PvUPS1* from French bean and *VuA3* (X90487) from cowpea were used to create a sequence alignment by Clustal algorithm (LASERGENE software; DNASTAR, Madison, WI). Black backgrounds show identical amino acids, dashes indicate gaps in the sequence to allow maximal alignment (B).

```

[ 1 60]
PvUPS1 M-----YLVESKGGAI GCMFLALFFLGTWPALLTMLERRGRLPQHTYLDYSITNFFA
UPS1 M-----YMTESKGGAIACMLLALLFLGTWPAIMTLTERRGRLPQHTYLDYTLTNLLA
UPS2 M-----LLALLSLGTWPAVLTLLERRGRLPQHTYLDYSITNLLA
UPS3 M-----YVIESKGGTITCMLLALLFLGTWPAIMTLTERRGRLPQHTYLDYTLTNLLA
UPS4 M-----IISLCCLGSWPAITLTLERRGRLPQHTFLDFATANLLA
UPS5 MMIAQELGIYVVESKGGAILCLLLSLLCLGTWPALMALLERRGRLPQHTYLDYSITNFLA
Vu_A3 M-----FLALFFLGTWPALLTMLERRGRLPQHTYLDYSITNFFA

```

```

[ 61 120]
PvUPS1 ALLIAFTFGEIGKGPDEPNFLAQLAQ--DNWPSVLFAMGGGVVLSLGNLSSQYAFAFVG
UPS1 AVIIAFTLGEIG---PSRPNFFTQLSQ--DNWQSVMFAMAGGIVLSLGNLATQYAWAYVG
UPS2 AIIIAFTFGQIGSTKPDSPNFITQLAQ--DNWPSVMFAMAGGIVLSLGNLSTQYAWALVG
UPS3 AVIIAFTLGEIS---PSRPNFFTQLSQ--DNWPSVMFAMAGGIFLSLGLTLATQYAWAFVG
UPS4 AIVIAFSLGEIGKSTFLKPDFTTQLPQ--DNWPSVLLAVAGGVLLSIGNLATQYAFAFVG
UPS5 AIFIAFVEGGIGESTHEAPSFITQLTQIQDNWPSVLFAMAGGVGLSIGNLATQYSLAFVG
Vu_A3 ALLIAFTFGEIGKGPDEPNFLAQLAQ--DNWPSVLFAMGGGVVLSLGNLSSQYAFAFVG

```

```

[ 121 180]
PvUPS1 LSVTEVITASITVVIGTTVNYFLDDKINKAEILFPGVGCFLIAVFLG-SAVHSSNASDNK
UPS1 LSVTEVITASITVVIGTTLNYFLDDRINRAEVLFPGVACFLIAVCFG-SAVHKSNAADNK
UPS2 LSVTEVITSSITVVIGSTLNYFLDDKINKAEILFPGVACFLIAVCLG-SAVHRSNADDNK
UPS3 LSVTEVITASIAVVIGTTLNYFLDDRINRAEVLFPGVACFLIAVCFG-SAVHKSNAADNK
UPS4 LSVTEVITASITVVIGTTLNYFLDNKINKAEILFPGVGCFLIAVFLG-AAVHASNAADVK
UPS5 LSVTEVITASITVVIGTTVNYFLDNGLNRAIDILFSGVGCFFMVAVCLG-SAVHSSNSADIK
Vu_A3 LSVTEVITASITVVIGTTLNYFLDDKINKAEILFPGVGCFLIAVFLGFCRFNSSNASDNK

```

```

[ 181 240]
PvUPS1 AKLNNYSNDYKEAAI-SSKERDLVKSKDLERGSSSADNVEAGTAVFLIELEERRAIKVFG
UPS1 TKLQNFKSLETTSSFEMETISASNGLTK-----GKAKEGTAAFLIELEKQRAIKVFG
UPS2 AKLRDFETAKQEASG- PSTEIGTNSKDL E--TNVTTKPKEGTARFLIELENTRAIKVFG
UPS3 SKLQGFKSLETTSSFQMET----SSIKE-----GKAKVGTADFLIEVEKQRAIKVFG
UPS4 EKLSLPSSELYSSIENGEDKPEIEKTDVESQEKLAEKAKAGTAGFYVELENKRAIKVFG
UPS5 AKLGLKSGDCETVTPPECQR--LFGVEEEEEEEKEMENVKEGSAAFLIALENKRAIKVLG
Vu_A3 AKLSNYTSDYKEVAI-SSKESDLVKSKDLERGSSSADNVEAGTAVFLLELEERRAIKVFG

```

A****G

```

[ 241 300]
PvUPS1 KSTLIGLSLTFSSAGLCFSMFSPAFNLATNDQWHTLEKGIPLHTVYTAFFYFSISCFVIAI
UPS1 KSTIIGLVITFFAGICFSLFSPAFNLATNDQWHTLKHGVPKLN VYTAFFYFSISAFVVAL
UPS2 KRRIIIGLAITFFAGLCFSLFSPAFNLATNDQWNRLKQGVPKLVYTAFFYFSVSCFIIAL
UPS3 KSTIIGLAITFFA-----VPKLN VYTAFFYFSISSFGVGL
UPS4 KSIIMIGLFIITLFFAGISLFLFSPAFNLATNDQWSTLPKGVPKLVYTAFFYFSIAGFLISL
UPS5 KSMVVGLGITFFAGLSFSLFSPAFNLATNDQWHTLQGVPKLIVYTAFFYFSLSCFVIAV
Vu_A3 KSTLIGLALTFSSAGLCFSMFSPAFNLATNDQWHTLPNGIPLHTVYTAFFYFSISCFVIAI

```

KS

```

[ 301 360]
PvUPS1 ILNITFLYHPVLNLPKSSLKAYLADSDGRMWALLAGLLCGFGNGLQFMGGQAAGYAAADA
UPS1 ILNIRFLYWPILGLPRSSFAYLNDWNGRGWSFLAGFLCGFGNGLQFMGGQAAGYAAADA
UPS2 ILNVVFLYYPVLGPKSSFKAYLNDWNGRYWAFFLAGFLCGFGNGLQFMGGQAAGYAAADS
UPS3 ILNIIFLYWPILGLPRSSFAYLNDWNGRGWSFLAGFLCGFGNGLQFMGGQAAGYAAAGA
UPS4 ILNLIIFLYRPMVGLARSSLKKYIYDSKGRGWAVFAGFLCGFGNGLQFMGGQAAGYAAADS

```


3.1.2. Cloning of members of the *AtUPS* family

AtUPS2 and *AtUPS5* were isolated from a cDNA library from 5-day-old *Arabidopsis thaliana* seedlings (ecotype Col-0). No EST for *AtUPS3* could be found in the public databases, while for *AtUPS4* two ESTs are identified. Attempts to clone full length cDNAs for *AtUPS3* and *AtUPS4* have failed so far. This might be due to very low or conditional expression of *AtUPS4*. In addition to the predicted coding sequence for *AtUPS5*, a shorter cDNA was also cloned. This is a splicing variant of the longer *AtUPS5* coding sequence. Since the start of this work, ESTs became available for both splicing variants, supporting our results. Consequently the longer *AtUPS5* clone was named *AtUPS5*, while the shorter version was named *AtUPS5s* (for short). The coding sequences of *AtUPS1*, 2, 5 and 5s were cloned into the yeast expression vectors pDR199 and pMD200 and the vector pOO2 to generate cRNA for expression in *Xenopus* oocytes.

3.1.3. *AtUPS1*, 2 and 5 mediate transport of purine degradation products and pyrimidines

3.1.3.1. *AtUPS1*, *AtUPS2* and *AtUPS5* mediate uptake of allantoin

The *dal4 dal5* yeast double mutant strain deficient in the uptake of allantoin and allantoic acid was used to isolate *AtUPS1* (Desimone *et al.*, 2002). The strain was used to test if *AtUPS2*, *AtUPS5* and *AtUPS5s* are also able to suppress the mutant phenotype in a growth assay with 5 mM allantoin as the sole nitrogen source. The yeast mutant transformed with *AtUPS2* was able to grow in a similar fashion as *AtUPS1* transformed yeast (Fig. 10A). *AtUPS5* and *AtUPS5s* failed to complement the mutant phenotype (not shown). Background growth of the *dal4 dal5* yeast mutant strain transformed with the empty vector is relatively high. Thus, the uptake of ^{14}C -allantoin by the yeast *dal4 dal5* strain transformed with *AtUPS1*, *AtUPS2*, *AtUPS5*, or the empty vector pDR199 as a control, was measured (Fig. 10B).

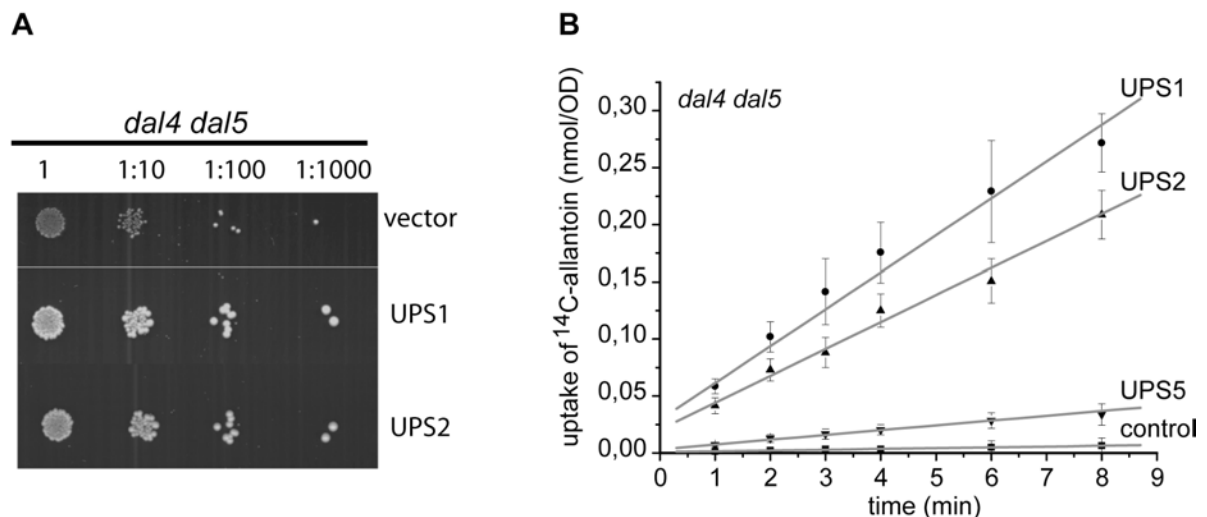


Fig. 10: Functional expression of *AtUPS1* and *AtUPS2* in yeast mutants.

The yeast *dal4 dal5* mutant strain transformed with either pDR199UPS1, pDR199UPS2 constructs or empty vector (pDR199) was tested for growth on medium with 5 mM of allantoin as sole nitrogen source (A). Uptake of 200 μM ^{14}C -allantoin in the yeast *dal4 dal5* knockout mutant strain transformed with either pDR199UPS1, pDR199UPS2, pDR199UPS5 or pDR199 as control (B).

All three proteins mediated the uptake of allantoin, although with different efficiencies. Cells transformed with the empty vector take up allantoin at a rate of 3 % of that of *AtUPS1* expressing cells. *AtUPS2* and *AtUPS5* mediate uptakes at rates of ~73 % and 13 % of *AtUPS1* expressing cells. The low uptake efficiency due to *AtUPS5* expression together with the background growth of yeast *dal4 dal5* mutant colonies might explain why *AtUPS5* expressing yeast could not be distinguished from yeast expressing the empty vector in the complementation assay. Thus *AtUPS1*, *AtUPS2* and *AtUPS5* allow allantoin import when expressed in yeast. In contrast, *AtUPS5s* cannot transport allantoin when expressed in yeast as will be confirmed below (Chapter 3.1.4.2.).

3.1.3.2. *AtUPS1*, *AtUPS2* and *AtUPS5* also act as uracil transporters

Since there is no evidence that *Arabidopsis* uses allantoin as a long distance transport form of organic nitrogen, it was conceivable that *AtUPS* have (a) different physiological substrate(s) in *Arabidopsis*. Previous studies had shown that *AtUPS1* recognizes *oxo*-derivatives of *N*-heterocycles (Desimone *et al.*, 2002). Also, uracil has some structural similarities to allantoin. Since uracil transport was observed, while transporters were not identified, it was tested whether *AtUPS1*, *AtUPS2* or *AtUPS5* are able to mediate uracil uptake.

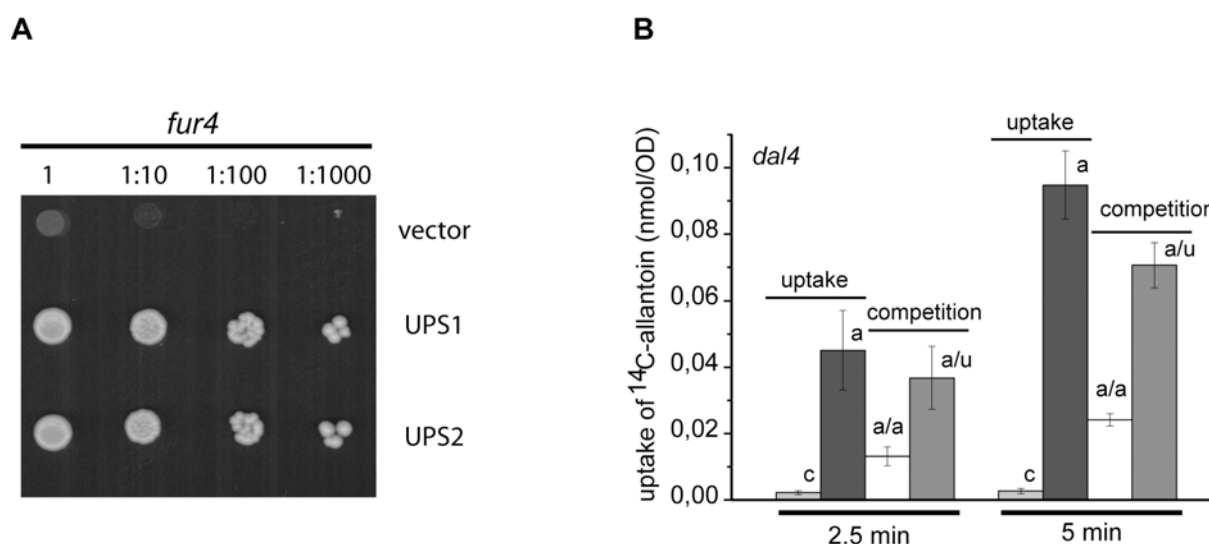


Fig. 11: Uptake and inhibition studies in yeast.

The yeast *fur4* mutant strain transformed with either pMD200UPS1 or pMD200UPS2 or empty vector (pMD200) was tested for growth on 0.2 mM uracil as sole source of pyrimidines (A). Uptake of 200 μ M 14 C-allantoin in the yeast *dal4* knockout mutant strain transformed with (a) *UPS5* (pDR199UPS5/pMD200) or (c) pDR199/pMD200 as control; and competition of uptake of (a/a) 14 C-allantoin and allantoin (200 μ M each), or (a/u) 14 C-allantoin and uracil (200 μ M each) due to *UPS5* (pDR199UPS5/pMD200) expression (B).

The yeast mutant *fur4*, deficient in uracil uptake, grew on 0.2 mM of uracil as sole source of pyrimidines when expressing *AtUPS1* or *AtUPS2*, demonstrating that both transporters mediate uracil uptake (Fig. 11A). In contrast, no growth of the *AtUPS5* or pMD200 transformed *fur4* was observed (not shown).

Nevertheless, a competition study of 14 C-allantoin (200 μ M) uptake in the presence of equal concentrations of uracil (200 μ M) or allantoin (200 μ M) in the yeast *dal4* mutant⁵ strain expressing *AtUPS5* showed that allantoin transport is inhibited by uracil, though not with the

⁵ The yeast *dal4* mutant strain is deficient in allantoin uptake.

same efficiency as by allantoin itself (Fig. 11B). This suggests that AtUPS5 is able to transport or bind uracil.

3.1.3.3. *AtUPS1* and *AtUPS2* were functionally expressed in *Xenopus laevis* oocytes

3.1.3.3.1. AtUPS1 and AtUPS2 mediate transport of a range of substrates

To test the substrate specificities and features of transport in more detail, *AtUPS* were expressed in *Xenopus laevis* oocytes. Functional expression of *AtUPS1* has previously been demonstrated (Desimone *et al.*, 2002). Functional expression was achieved for *AtUPS2*, while it could not be demonstrated for *AtUPS5* (not shown). Since in yeast uptake rates due to *AtUPS5* expression are significantly lower than for *AtUPS1* or *AtUPS2*, a similar situation upon *AtUPS5* expression in oocytes might yield currents below the detection limit. However, the possibility that *AtUPS5* might not be functionally expressed or targeted to the plasma membrane in oocytes cannot be excluded. *AtUPS5s* was also tested, but no allantoin dependent currents could be observed. Thus, *AtUPS5s* might not function as an importer for known UPS substrates, or was not expressed or correctly targeted to the plasma membrane in *Xenopus* oocytes.

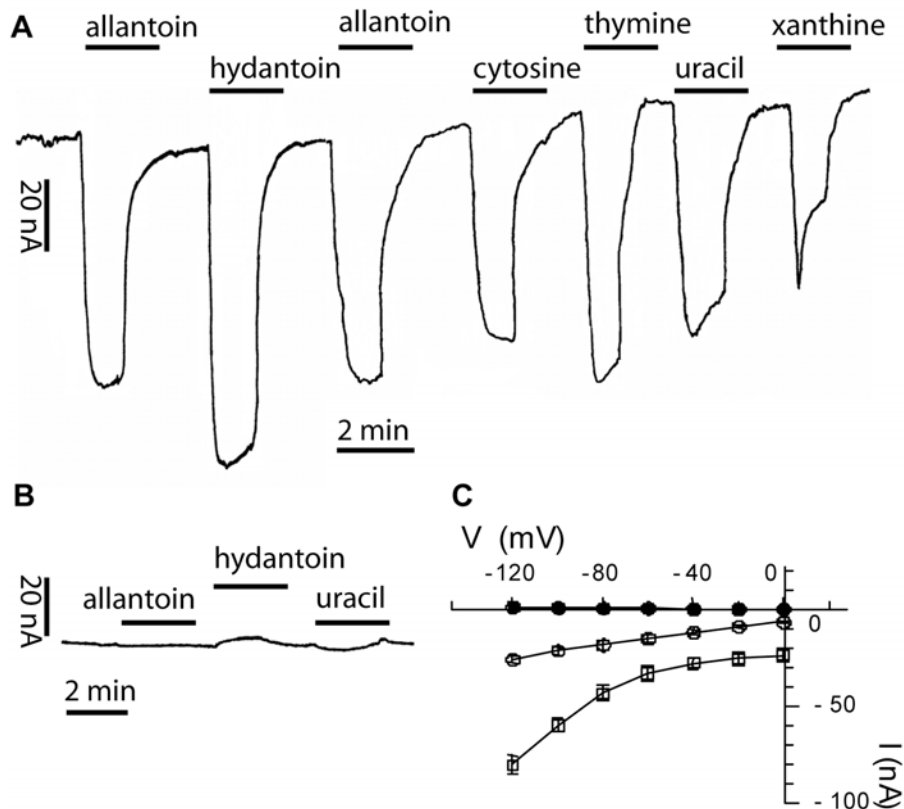


Fig. 12: Functional expression of *AtUPS2* in *Xenopus* oocytes.

AtUPS2 expressing oocytes (A) or non-injected oocytes (B) were flushed with solutions containing 200 μ M of the indicated substances (pH 5.5) and inward currents were recorded at -100 mV. (C) Allantoin-induced currents were recorded with an I/V protocol for control oocytes (filled circles), *AtUPS1* expressing oocytes (open circles) and *AtUPS2* expressing oocytes (open squares) (C). Data points represent means \pm SD from at least 3 oocytes of different batches.

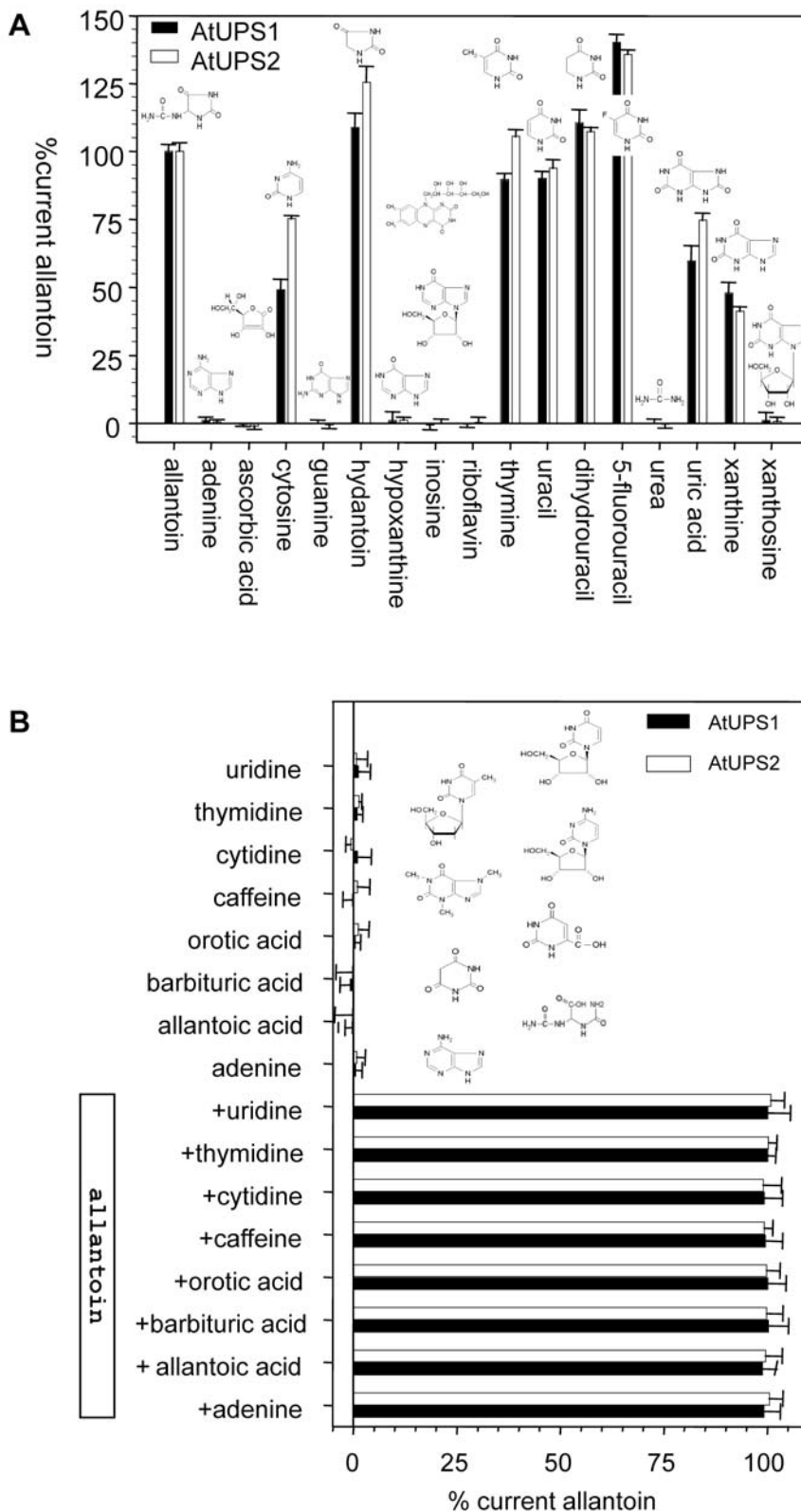


Fig. 13: Substrate specificity of AtUPS1 and AtUPS2, AtUPS1 (filled bars) and AtUPS2 (open bars) expressing oocytes were flushed with solutions containing 200 μ M of the indicated substances (pH 5.5) (A). Competition experiments were performed with equal concentrations (200 μ M) of allantoin and tested compounds in a mixture (pH 5.5). Currents determined at -100 mV with an I/V protocol are presented as the percentages of the currents induced by 200 μ M of allantoin alone (B). Data points represent means \pm SD from at least 3 oocytes of different batches. Structural formulas are given accordingly.

Expression of *AtUPS1* and *AtUPS2* induced inward currents in oocytes clamped at -100 mV when bathed in buffer with allantoin in a flow system (Fig. 12A), while no significant currents were detected in non-injected control oocytes (Fig. 12B and C).

To investigate substrate specificities, compounds were selected by different criteria: they are either structurally related, or belong to the metabolic pathways of nucleobases and derivatives, or known as substrates for other nucleobase transporters. Various cyclic purine degradation products and pyrimidines were found to induce currents. In the cases of allantoin, hydantoin, cytosine, thymine or uracil, the induced currents remained stable or slowly decreased until washout of the substrates. However, when flushed with xanthine, the evoked current decreased within 10 seconds to a lower steady state level (Fig. 12A). A similar effect was found for uric acid (not shown). Despite lower current levels, *AtUPS1* behaved in a manner similar to *AtUPS2*. Clamping oocytes to -100 mV for longer periods of time resulted in small shifts of the baseline (Fig. 12A). To minimize the errors conferred by this process, further investigations were done using brief substrate flushing periods and the I/V protocol described in the methods section. The allantoin-induced currents recorded from *AtUPS1* or *AtUPS2* expressing oocytes increased in response to further hyperpolarization of the membrane potential (Fig. 12C) and displayed clear voltage dependence.

Steady-state currents induced by different substances were plotted as percentage of the allantoin effect (Fig. 13A and B). The cyclic purine degradation products uric acid and xanthine induced currents in *AtUPS1* and *AtUPS2* expressing oocytes ($\sim 60\%$ and 50% for *AtUPS1*, 75% and 40% for *AtUPS2*, respectively). All pyrimidines and their tested derivatives (cytosine, uracil, thymine, dihyouracil and 5-FU) induced currents of different magnitude (Fig. 13A). Slight differences were found between *AtUPS1* and *AtUPS2* in response to thymine and cytosine ($\sim 92\%$ and 105% for thymine, 50% and 75% for cytosine, respectively), whereas uracil, dihydrouracil and 5-FU were transported at comparable rates ($\sim 91\%$, 110% and 140% , respectively). In contrast, several compounds did not induce currents, e.g. nucleosides, the secondary metabolite caffeine, or the purine bases adenine, hypoxanthine, and guanine (Fig. 13A and B). Other transporters (*AtENT* and *AtPUP*) for these compounds have already been identified in plants. Moreover, ascorbic acid (a substrate for mammalian NAT transporter) failed to produce currents (Fig. 13B). No inward currents could be recorded for barbituric acid and orotic acid, even though they are structures similar to those of the pyrimidines, but with additional substitutions in *meta*-position to the *oxo*-residues (Fig. 13B). Allantoic acid, having an ureido-moiety and urea itself, both being linear degradation products of purines, were not transported. In contrast hydantoin, a synthetic compound lacking the ureido-substitution at position 5 of allantoin, induced currents in *AtUPS1* and *AtUPS2* expressing oocytes ($\sim 108\%$ and 127% , respectively) (Fig. 13A). This confirms that the ureido-residue is not a structural determinant for substrates.

To elucidate whether compounds are binding to the transporters without being transported, competition experiments were performed. Allantoin and other compounds were mixed at equal concentrations ($200\ \mu\text{M}$), resulting in almost the same current levels as induced by allantoin alone. These results indicate that these compounds (e.g. nucleosides, caffeine, orotic acid, barbituric acid) are not transported or bound by *AtUPS1* or *AtUPS2* (Fig. 13B).

In summary, all the transported substrates were heterocyclic compounds with similar electron density distribution established by the *N*-hetero-atoms and the substituents (Fig14). *AtUPS1* and *AtUPS2* transport a similar set of substrates covering cyclic purine degradation products and pyrimidines, but no nucleosides, secondary metabolites like caffeine nor purine bases like adenine, guanine or hypoxanthine.

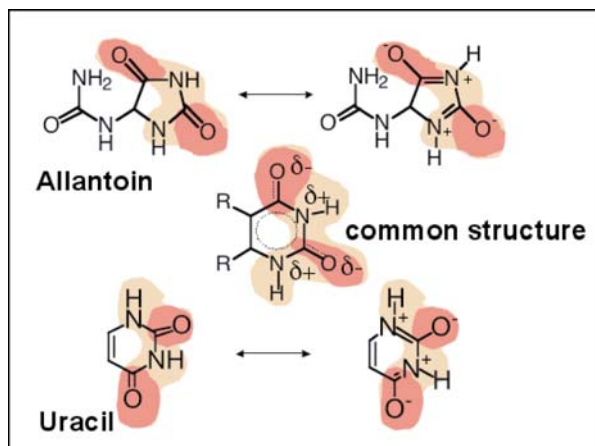


Fig. 14: Common structural features of AtUPS substrates.

Selected mesomeric structures of two AtUPS substrates, uracil and allantoin. Both are heterocycles with a similar electron density distribution established by the substituents.

3.1.3.3.2. Affinities of *AtUPS1* and *AtUPS2* are higher to uracil than to allantoin

Since substrates for *AtUPS1* and *AtUPS2* consist mainly of the two groups of pyrimidines and cyclic purine degradation compounds, kinetic parameters of the transport were investigated for representative molecules. Uracil was chosen as the pyrimidine base important in salvaging, while allantoin was selected for its importance in legumes. For a better understanding of the structural features determining transport, the affinity of *AtUPS2* for xanthine was also investigated. Xanthine, in contrast to uracil and allantoin, is a double ring system like non-degraded purine bases. Currents mediated by allantoin, uracil or xanthine depended on the concentrations of the compounds and displayed saturation kinetics (Fig. 15). Variations in dependence of the voltage were observed (Table 5). For *AtUPS1*, at -100 mV, an apparent K_m for allantoin of 75.3 ± 2.7 μM was determined. *AtUPS2* had a ~ 3 -fold lower K_m of 26.1 ± 5.4 μM . The affinity of *AtUPS2* for xanthine was in the range of the affinity for allantoin with a K_m value of 24.0 ± 5.7 μM (Table 5). Thus differences of these compounds in the ring structures are not of major importance for the transport. Both transporters had a higher affinity for uracil with K_m values of 6.2 ± 1.6 μM (*AtUPS1*) and 5.9 ± 0.7 μM (*AtUPS2*; Fig. 15). Thus, *AtUPS1* and *AtUPS2* have ~ 11 - and 5 -fold higher affinity for uracil than for allantoin.

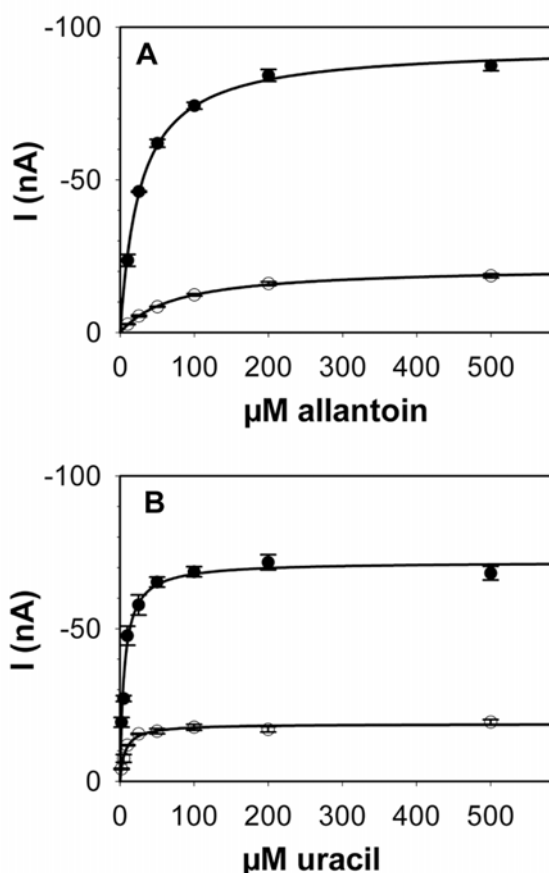


Fig. 15: Affinities of *AtUPS1* and *AtUPS2* to uracil and allantoin.

AtUPS1 (open circles) and *AtUPS2* (filled circles) expressing oocytes were flushed with solutions containing different concentrations of allantoin (A) or uracil (pH 5.5) (B). Currents determined at -100 mV with an I/V protocol. Data points represent means \pm SD from at least 3 oocytes of different batches.

Tab. 5: K_m values for the substrates allantoin, uracil and xanthine were determined in *AtUPS1* or *AtUPS2* expressing oocytes.

		K _m (μM)			
		V (mV)	Allantoin	Uracil	Xanthine
AtUPS1	-120		69.3 ± 4.6	5.9 ± 0.8	
	-100		75.3 ± 2.7	5.9 ± 0.7	n.d.
	-80		85.0 ± 3.0	6.6 ± 1.1	
	-60		106.5 ± 14.1	7.6 ± 1.5	
AtUPS2	-120		28.5 ± 5.2	6.5 ± 1.7	12.4 ± 4.0
	-100		26.1 ± 5.4	6.2 ± 1.6	24.0 ± 5.7
	-80		24.9 ± 5.7	6.9 ± 1.7	28.0 ± 6.5
	-60		27.2 ± 7.4	8.6 ± 2.9	27.4 ± 9.0

3.1.4. Transport Mechanism and Regulation

3.1.4.1. The currents mediated by AtUPS1 and AtUPS2 are proton dependent

Previous findings proposed that AtUPS1 mediates a transport of uncharged substrates coupled to a proton co-transport. To address the question whether the same mechanism applies for AtUPS2, its transport mechanism was studied. The uptake of ¹⁴C-allantoin was measured in the *dal4 dal5* yeast mutant transformed with *AtUPS2* (Fig. 15A). The rates of ¹⁴C-allantoin depended on the pH of the external medium and were maximal at pH ~5. This conforms with previous reports for UPS1 dependency on pH with a maximum uptake in yeast at pH 4.75 (Desimone *et al.*, 2002). Allantoin-induced currents were investigated at different pH values for oocytes expressing *AtUPS1* and *AtUPS2* (Fig. 15B, C). The induced currents decreased with increasing pH of substrate solutions. At alkaline pH (pH 8.5), there was almost no current in oocytes expressing either *AtUPS1* or *AtUPS2* (Fig. 15B and C). Moreover, increasing concentrations of other monovalent cations (potassium and sodium) did not stimulate allantoin transport (not shown). Since allantoin (pK_a ~8.9) is predominantly neutral (99,6 %) at pH 5.5, a proton-co-transport of uncharged substrate can be suggested for AtUPS2 as for AtUPS1.

The percentage of neutral and charged molecules at pH 5.5 varies between substrates used in the assays: In the case of hydantoin and uracil, more than 99 % of all the molecules are uncharged, while in the case of cytosine, uric acid, and xanthine, respectively 89 %, 80 % and 20 % of all the molecules are negatively charged. At least 99.9 % of orotic- and barbituric-acid carry one negative net charge.

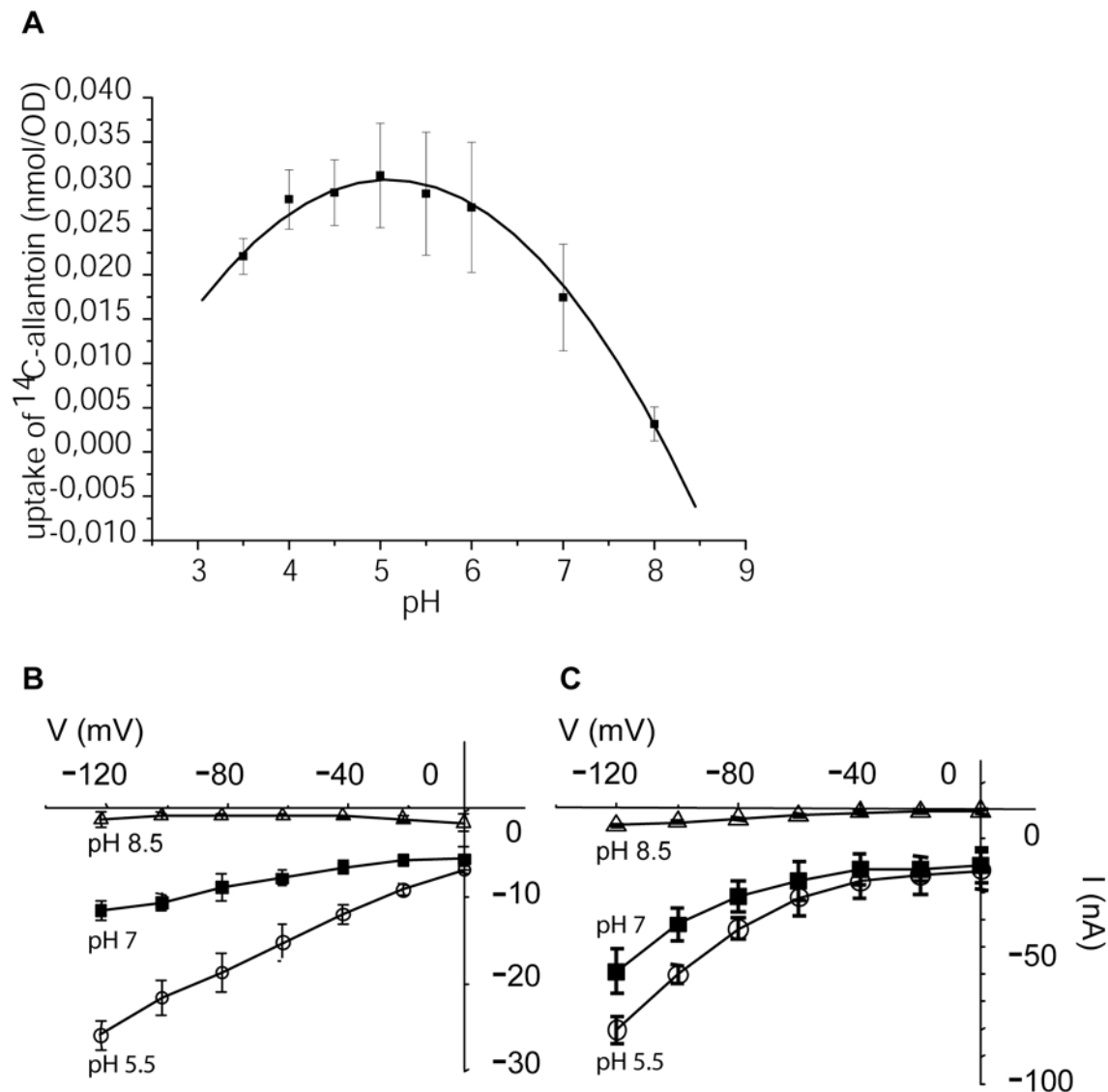


Fig. 16: pH dependency of allantoin transport.

Uptake of ¹⁴C-allantoin in the yeast *dal4 dal5* knockout mutant strain transformed with pDR199UPS2 at different pH values (A). Currents were recorded from *AtUPS1* (B) or *AtUPS2* (C) expressing oocytes perfused with 200 μM of allantoin; open circles, pH 5.5; filled squares, pH 7; open triangles, pH 8.5. The relation between currents and proton concentration at -120 mV was fitted to a saturable hyperbola (insets). Data points represent means ± SD from at least 3 oocytes of different batches.

3.1.4.2. Mutations in ATP/GTP-binding motifs of *AtUPS1* and similar sequences of *AtUPS2* affect transport

Since a secondary active transport mechanism was found for *AtUPS1* and *AtUPS2*, the presence of a Walker A motif in *AtUPS1* seemed surprising. Conserved residues of the Walker A motif mediate binding of the phosphate moiety of ATP or GTP (Lutkenhaus and Sundaramoorthy, 2003). It has previously been shown that mutations of the conserved lysine residue (to alanine or arginine) can impair the functionality of ATP binding proteins (Hishida *et al.*, 1999). In analogy, mutations of *AtUPS* proteins were designed to test the function of the predicted Walker A motif. Different situations were compared: (i) two different mutants of the conserved lysine residue of the UPS1 Walker A motif (K219I, K219R), (ii) a mutation of a non-conserved lysine residue of the UPS1 Walker A motif (K215I), and (iii) a mutation

of the lysine residue of UPS2 aligning with the conserved lysine residue of AtUPS1 (K227I), although AtUPS2 does not have a completely conserved Walker A motif.

Mutant proteins were subsequently expressed in *Xenopus* oocytes and currents induced by allantoin (pH 5.5) were tested. For comparison, currents induced in oocytes expressing the non-mutated proteins (WT) were followed under the same experimental conditions.

Currents induced in oocytes expressing the *UPS1_K219I* and *UPS1_K219R* mutants were respectively only 15 % and 40 % of the currents induced by expression of non-mutated *UPS1* (WT) (Fig. 17A). Since for the *UPS1_K219R* mutant the positive charge of the residue is conserved, the probability of structural changes due to this mutation might be lower than for *UPS1_K219I*.

Currents induced in oocytes expressing the *UPS1_K215I* construct were 10 % of the currents induced in *UPS1* (WT) expressing oocytes (Fig. 17A).

Induced currents upon expression of *UPS2_K227I* in oocytes were 10 % of the currents induced in *UPS2* expressing oocytes (Fig. 17B).

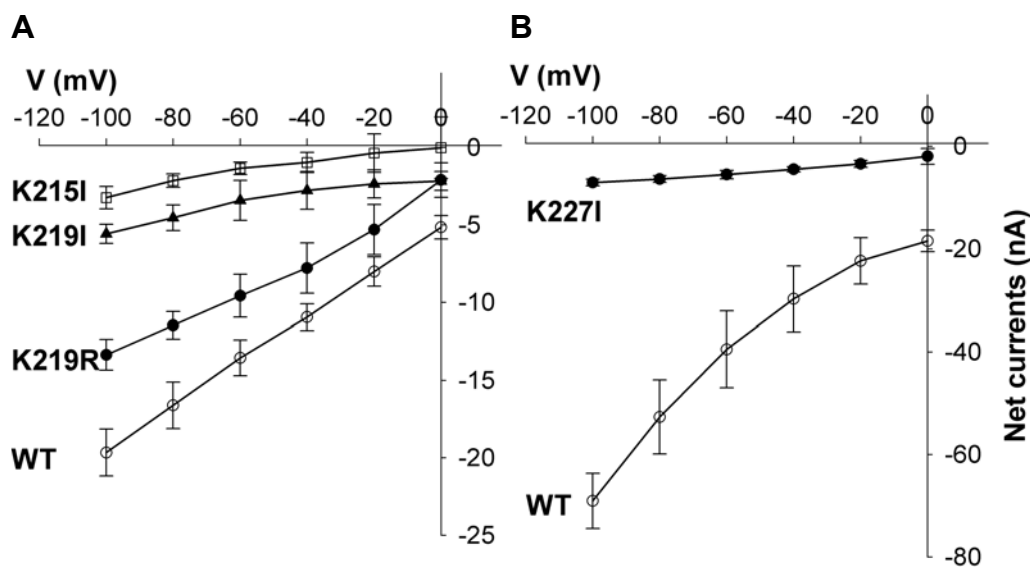


Fig. 17: Effect of mutations in the Walker A motif of UPS1 (A) and a similar residue in the AtUPS2 (B) coding sequence on transport.

Currents induced by 200 μ M of allantoin at pH 5.5 were determined at different voltages ranging from 0 to -100 mV. Data points represent means \pm SD from at least 3 oocytes of different batches.

For all mutant proteins transport rates were significantly decreased (~10-40 % of WT). Concerning the mutations of the conserved lysine residue of the Walker A motif of UPS1, this might be the result of an impaired ATP/GTP binding, with consequences for the functionality of the protein. On the other hand, Lys²¹⁵ is not a conserved residue of the Walker A motif and might thus not be essential for binding of ATP/GTP. In addition, AtUPS2 does not have a completely conserved Walker A motif. Thus, there is no evidence that ATP/GTP binding might play a role for AtUPS2. Since all mutations severely affected the transport rate of AtUPS1 and AtUPS2, other possible explanations have to be taken into account: structural changes, changes in membrane integration, effects on substrate recognition, etc. Thus, it can be concluded, that all mutated residues of AtUPS1 and AtUPS2 seem to be of some structural or functional importance for the protein. Further investigations will be needed to elucidate whether ATP/GTP binding plays a role for AtUPS1 (and other AtUPS).

3.1.4.3. Is AtUPS5s involved in regulation of transport?

As a special feature of *AtUPS5*, two different splicing variants *AtUPS5* and *AtUPS5s* are expressed (Fig. 18A). The *AtUPS5s* processed mRNA, in comparison to *AtUPS5*, lacks the basepairs 300 to 404 due to an additional splicing event (relative to the start codon of the *AtUPS5* cDNA). From EST analysis, there is also a differential splicing in the 5' UTR.

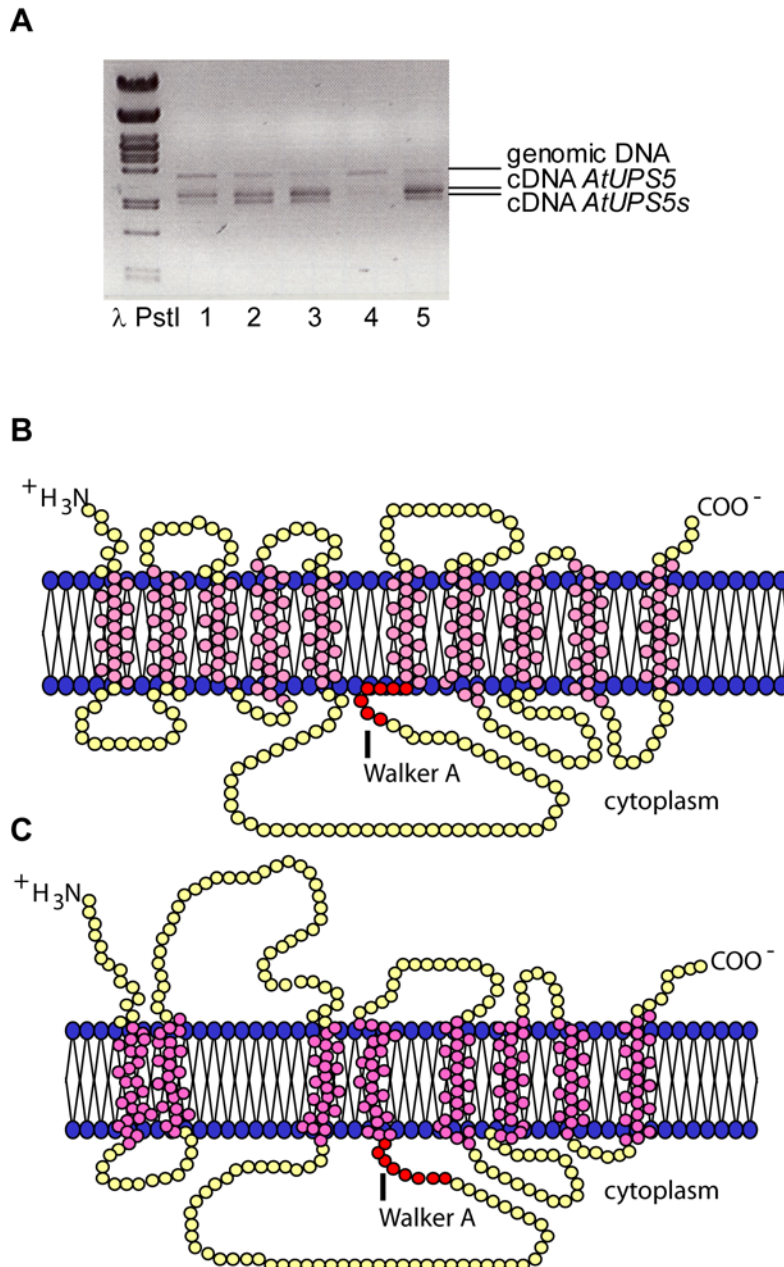


Fig. 18: Splicing variants of *AtUPS5* and structural consequences. RNA was extracted from 14-day-old seedlings transferred at day 13 of growth on plates with modified MS medium (20 mM N, 1 % (w/v) sucrose) to liquid medium without sucrose and with different nitrogen sources: (1), 10 mM NH_4NO_3 ; (2), 10 mM glutamine, (3), no nitrogen; (4), 20 mM NH_4^+ ; (5), 5 mM allantoin. RNA was converted to cDNA by reverse transcription. A 1595 bp fragment of genomic DNA of *AtUPS5*, a 1272 bp fragment of the coding region of *AtUPS5* and a 1164 bp fragment of the coding region of *AtUPS5s* were amplified by PCR (27 cycles) (A). Structural models of AtUPS proteins were created using topology predictions (TMHMM version 2.0, <http://www.cbs.dtu.dk/services/TMHMM-2.0/>). The structural model for AtUPS1 is similar to that for AtUPS5 or AtUPS2 (B). In the structural model for AtUPS5s, two transmembrane helices of the protein are missing compared to AtUPS1, 2 and 5 (C).

The missing basepairs in *AtUPS5s* correspond to amino acids forming two transmembrane domains in *AtUPS5*. As a structural consequence, although all other AtUPS proteins are predicted to have 10 transmembrane domains, *AtUPS5s* would only have 8 (Fig. 18B) (TmHMMv2.0; Krogh *et al.*, 2001)⁶. Moreover, while *AtUPS1*, *AtUPS2* and *AtUPS5* (the long version) are importers of allantoin, uracil, and other oxo-*N*-heterocycles when expressed

⁶ Several prediction programs are available in the Aramemnon database <http://aramemnon.botanik.uni-koeln.de>. In these prediction programs, signal peptides are predicted for UPS, resulting in 9 transmembrane domains in case of AtUPS1, 2, 4 and 5 and 7 transmembrane domains in case of AtUPS3.

in oocytes or yeast (Fig. 9, 10; Baumann, N., Desimone, M., personal communication), no transport mediated by AtUPS5s was observed. Thus, AtUPS5s might have a different function. There is compelling evidence that the formation of homo- or heteromeric complexes is often involved in regulation of transporters (Reinders *et al.*, 2002a; Reinders *et al.*, 2002b; Ludewig and Frommer, 2003). Thus, it was tested if AtUPS5s might form complexes with other AtUPS, and would therefore regulate AtUPS transport activity. AtUPS2, AtUPS5 and AtUPS5s were therefore tested in a split-ubiquitin assay (Ludewig *et al.*, 2003; Obrdlik *et al.*, 2003). It is based on the interaction of Nub and Cub, the N- and C-terminal halves of ubiquitin, which can reconstitute a functional protein (Obrdlik *et al.*, 2004). Interactions were observed between all N-terminal Nub-UPS fusion proteins with all UPS-Cub fusion proteins. This might indicate that UPS proteins form complexes. In contrast, no interactions could be observed for C-terminal UPS-Nub fusion proteins with UPS-Cub fusion proteins, although interactions of C-terminal Nub-fusion proteins seem to be more specific (Obrdlik *et al.*, 2004). However, yeast expressing *KATI* or *SUT2* (as controls), and *AtUPS* grew suggesting that the putative interactions of AtUPS proteins might have resulted from background growth. Thus, the split-ubiquitin assay does not give clear evidence for complex formation of AtUPS proteins (not shown).

3.1.4.4. Coexpression in yeast and *Xenopus* oocytes

A second functional approach was taken to test if complex formation between AtUPS proteins might play a role in transport regulation. Two *AtUPS* were co-expressed in the yeast *dal4* knockout mutant strain, which was tested for ¹⁴C-allantoin uptake. For each uptake assay, yeast was transformed with two different plasmids (pDR199, pMD200) with different selection markers (*ura*, *leu*, respectively). Since pMD200 is a derivative of pDR195, both vectors have the same promoter to drive expression (PMA, Plasma Membrane ATPase) and there should not be significant differences in copy numbers. For expression of only one *AtUPS*, yeast was transformed with one expression construct and an empty vector. To minimize the probability of recombination events between two similar constructs in yeast, the presence of both plasmids and/or expression constructs in yeast cells was tested prior to the uptake assays. This was done either by PCR or by rescuing plasmids into *Escherichia coli*. Uptake of ¹⁴C-allantoin by the yeast *dal4* mutant expressing *AtUPS2*, *AtUPS5* or *AtUPS5s* alone was compared to uptake by yeast expressing *AtUPS2/AtUPS5*, *AtUPS2/AtUPS5s* and *AtUPS5/AtUPS5s*. No significant rate of ¹⁴C-allantoin uptake by yeast cells transformed with *AtUPS5s* was observed (~1 % of uptake rate due to UPS2 and similar to empty vectors control).

The uptake rates of yeast co-expressing *AtUPS2/AtUPS5* or *AtUPS2/AtUPS5s* were decreased in comparison to rates observed with *AtUPS2* alone (~88 % and ~79 % respectively), but the decrease was not statistically significant due to sample to sample variations (Fig. 19A). In the case of *AtUPS5/AtUPS5s* co-expression, uptake rates were ~16 % of rates mediated by *AtUPS5* expression alone (Fig. 19A).

In addition, the oocyte expression system was used, in which protein expression can be more directly controlled due to the injection of different cRNA amounts. Similar cRNA amounts were injected for expression of *AtUPS2*, *AtUPS5s*, or *AtUPS2/AtUPS5s*. Oocytes were perfused with allantoin (200 μ M, pH 5.5) and the induced currents were recorded with the I/V protocol. As previously tested, no uptake could be shown for oocytes expressing *AtUPS5s*; uptake in oocytes expressing *AtUPS2* and *AtUPS5s* was slightly lower than in oocytes expressing *AtUPS2* alone, but again not in significantly (Fig. 19B). This conforms with the results of the yeast assay.

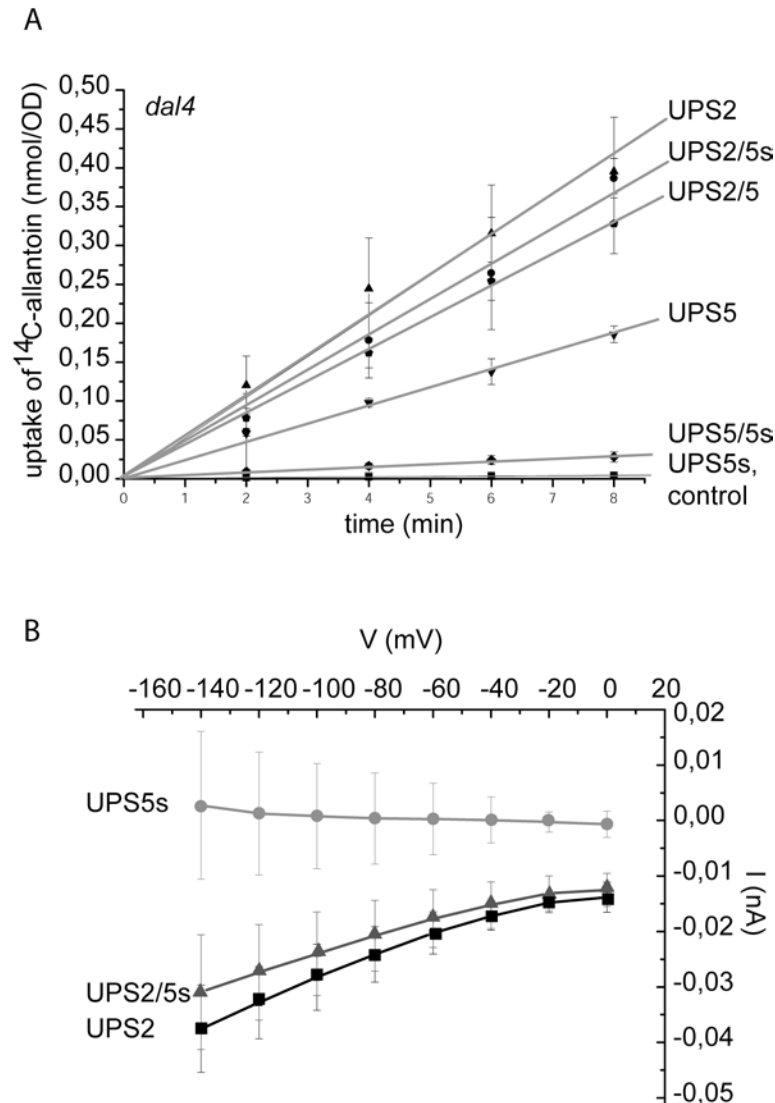


Fig. 19: Effects of UPS coexpression on transport efficiency in yeast and oocytes.

Uptake of ^{14}C -allantoin in the yeast *dal4* knockout mutant transformed with couples of plasmids: pDR199/pMD200, pDR199UPS2/pMD200, pDR199UPS2/pMD200UPS5, pDR199UPS2/pMD200UPS5s, pDR199UPS5s/pMD200UPS5, pDR199UPS5s/pMD200 and pDR199UPS5/pMD200 as control and for expression of *UPS2*, *UPS2/UPS5*, *UPS2/UPS5s*, *UPS5/UPS5s* and *UPS5s*, respectively (A). Currents induced by 200 μ M of allantoin at pH 5.5 were determined at different voltages ranging from 0 to -140 mV for *Xenopus oocytes* expressing either *AtUPS2*, *AtUPS5s* or both *AtUPS2* and *AtUPS5s* (B). Data points represent means \pm SD of at least 3 oocytes.

Thus, no clear evidence was given for regulation of *AtUPS* transport due to specific complex formation of *AtUPS2* and *AtUPS5/5s*. In contrast, the significant reduction of the *AtUPS5* transport rate observed upon co-expression with *AtUPS5s* in yeast might suggest that *AtUPS5s* can interact with *AtUPS5* and regulate the transport activity.

3.1.5. Members of the *AtUPS* family are differentially expressed and regulated in plants

The high affinity of AtUPS1 and AtUPS2 to uracil suggests that members of the AtUPS family might play a role in the salvaging of uracil in plants. Salvaging activity is high when cells or tissues have an elevated demand for nucleotides. To study tissue specific expression of members of the *AtUPS* family, promoter regions⁷ of *AtUPS1*, *AtUPS2*, *AtUPS3*, *AtUPS4* and *AtUPS5* were isolated and cloned into the pCB308 vector to drive expression of the *uidA* gene of *Escherichia coli*. pCB308 is a binary vector for plant transformation. No differentiation between *AtUPS5* and *AtUPS5s* is possible, since the construct comprised 700 bp of genomic sequence upstream from start codon to drive expression of the β -glucuronidase. *Arabidopsis thaliana* (Col 0) were transformed with these constructs and transgenic plants were recovered. Plants of different ages and grown under different conditions were analyzed. GUS-activity driven by the *AtUPS1*-, 2-, 4- of 5-promoters was observed. However, GUS-activity driven by the *AtUPS3*-promoter could not be observed under any tested conditions for plants grown on soil or on agar plates.

3.1.5.1. Mature plants

Bolting plants grown on soil under greenhouse conditions or in growth chambers were harvested. No GUS-activity driven by *AtUPS1*-promoter could be observed, whatever the organ tested (leaves, stems, or reproductive organs). GUS-activity driven by the *AtUPS2*-promoter was observed in leaf blades and petioles (Fig. 20D), in trichomes, and in stems (Fig. 20A). In flowers, GUS-activity was observed in the stigma and the upper part of the style as well as in sepals (Fig. 23A, B). GUS-activity was present in the top and bottom parts of carpels in siliques, but not in seeds.

GUS-activity driven by the *AtUPS4*-promoter was present in flowers: in filaments of the androecium and in stigma and style (Fig. 21E). No staining was observed in leaves or stems. Staining in siliques of bolting plants resembled staining driven by the *AtUPS2*-promoter (Fig. 21D). Moreover, GUS-activity driven by the *AtUPS5*-promoter was observed in stems and leaves and stipules (Fig. 22). In younger leaves it was present in the vasculature (Fig. 22G, K), and in older leaves all over the blade and in the petiole. This change in expression pattern started from the tip of the leaf (Fig. 22D, G, H, L). Staining in flowers was observed in stigma and style as well as in the connective tissue between pollen sacks (Fig. 22I, J).

⁷ For *AtUPS1*, 2, 3 and 4, the sequence upstream of the start codon to the 3'UTR of the preceding gene was taken. For *AtUPS5*, a 700 bp fragment upstream of the start codon was cloned.

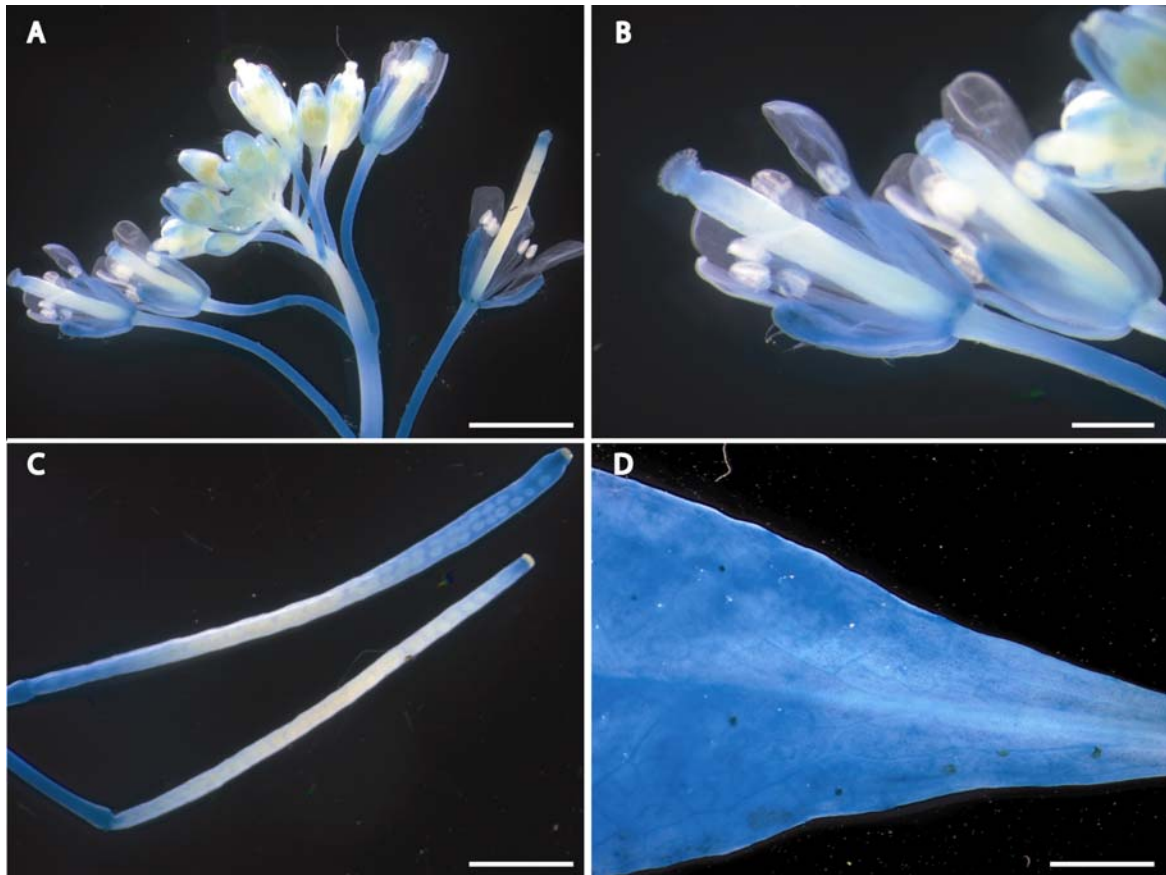


Fig. 20: Gus-expression driven by the *AtUPS2* promoter in bolting plants.

The *uidA* gene from *E. coli* was expressed in *Arabidopsis* under the control of the *AtUPS2*-promoter. Plants were grown on soil in the greenhouse for ~5-6 weeks prior to harvest and analysis of GUS-activity (scale bar = 0.25 cm).

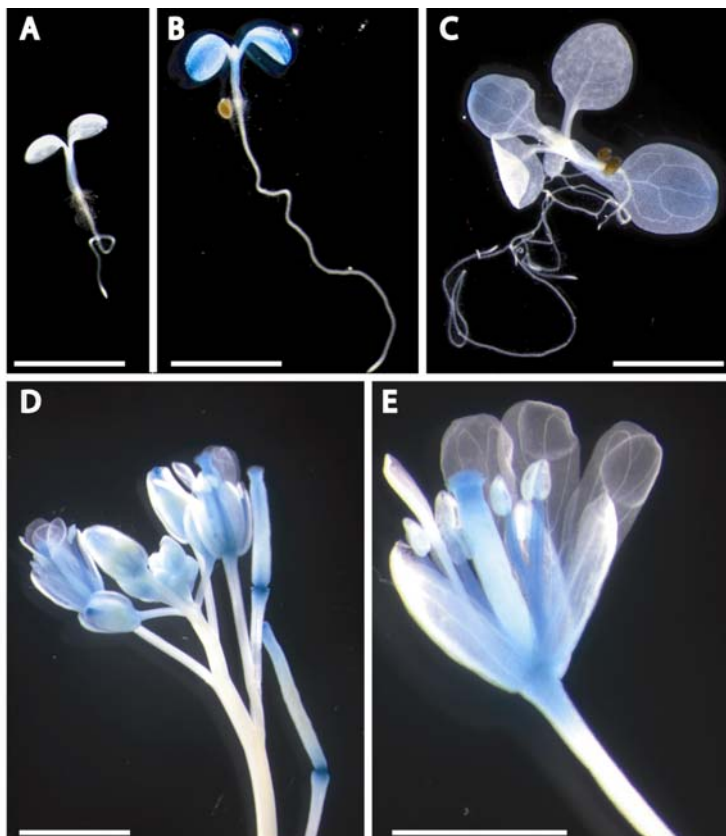


Fig. 21: Gus-expression driven by the *AtUPS4*- promoter.

The *uidA* gene from *E. coli* was expressed in *Arabidopsis* under the control of the *AtUPS4* promoter. Seedlings grown on plates with MS medium for 4 days (A), 6 days (B) and 9 days (C) were harvested and analyzed for GUS-activity. Plants grown on soil in the greenhouse for ~5 weeks prior to harvest were analysed for GUS-activity (D,E, scale bar = 0.25 cm).

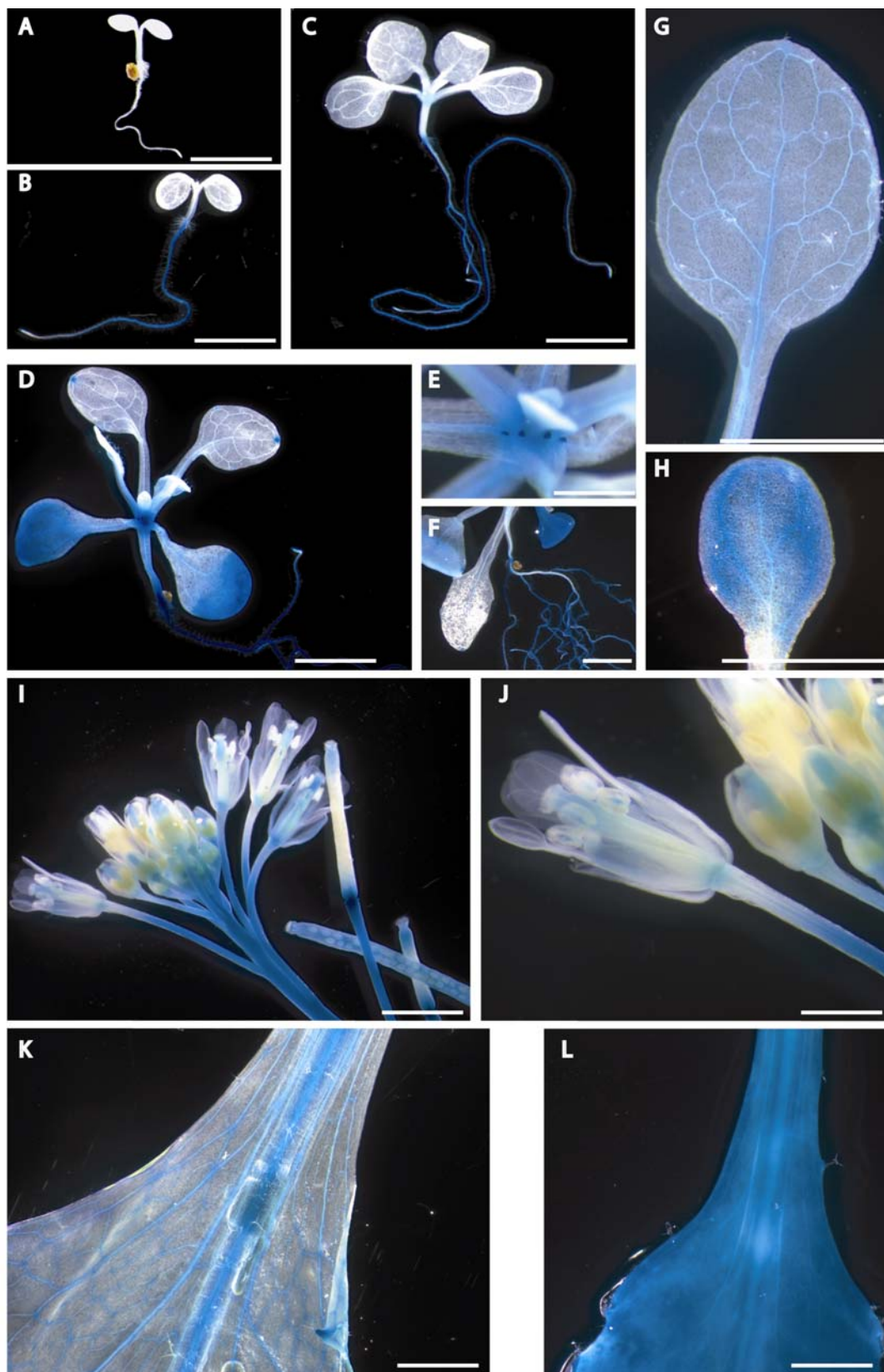


Fig. 22: GUS-expression driven by the *AtUPS5* promoter.

The *uidA* gene from *E. coli* was expressed in *Arabidopsis* under the control of the *AtUPS5*-promoter. Seedlings grown on plates with MS medium for 4 days (A), 6 days (B) and 9 days (C) and 13 days (D-H) were harvested and analyzed for GUS-activity. Plants grown on soil in the greenhouse for ~5 weeks prior to harvest were analysed for GUS-activity (A-D, G-L, scale bar = 0.25 cm; E, F, scale bar 1 cm).

3.1.5.2. Germination and early seedling development

Since the salvaging of nucleobases from storage tissues plays a role during germination and early seedling development, accumulation of the mRNA of *AtUPS1* and *AtUPS2* were studied in seedlings during the first two weeks of development. *AtUPS1* levels were high at day 1, declining continuously to steady levels after day 5 (Fig 23). In contrast, expression of *AtUPS2* was hardly detectable during the first two days of seedling development, but the expression levels increased afterwards until day 9.

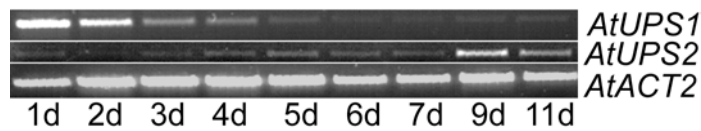


Fig. 23: Expression of *AtUPS1* and *AtUPS2* during seedling development.

RNA was extracted from *Arabidopsis* seedlings germinated on MS medium and converted to cDNA by reverse transcription. A 481 bp *AtUPS1* and a 484 bp *AtUPS2* fragment were amplified by PCR (30 and 32 cycles, respectively). As control, a 641 bp *AtACT2* fragment was amplified by PCR (26 cycles).

GUS expression driven by the *AtUPS1*-promoter was observed in two-day-old seedlings after the seedling emerged through the seed coat (Fig. 24A). GUS staining was detected in the whole seedling with the exception of the radicle. At day 3, GUS activity was present in the hypocotyl and in cotyledons. It was limited to hypocotyl and hydathodes (staining of hydathodes was not always observed) from day 4, further decreasing with age. GUS-activity driven by the *AtUPS2*-promoter was observed starting at day 4, the blue staining being present in cotyledons, increasing in intensity and distribution during the following days (Fig. 24B). At later stages (11 days), GUS-activity was high in cotyledons and primary leaves. In addition, from day 5 staining was observed in the stele of roots (Fig. 24B and 25A). The observed GUS-activity was conformed with the RT-PCR.

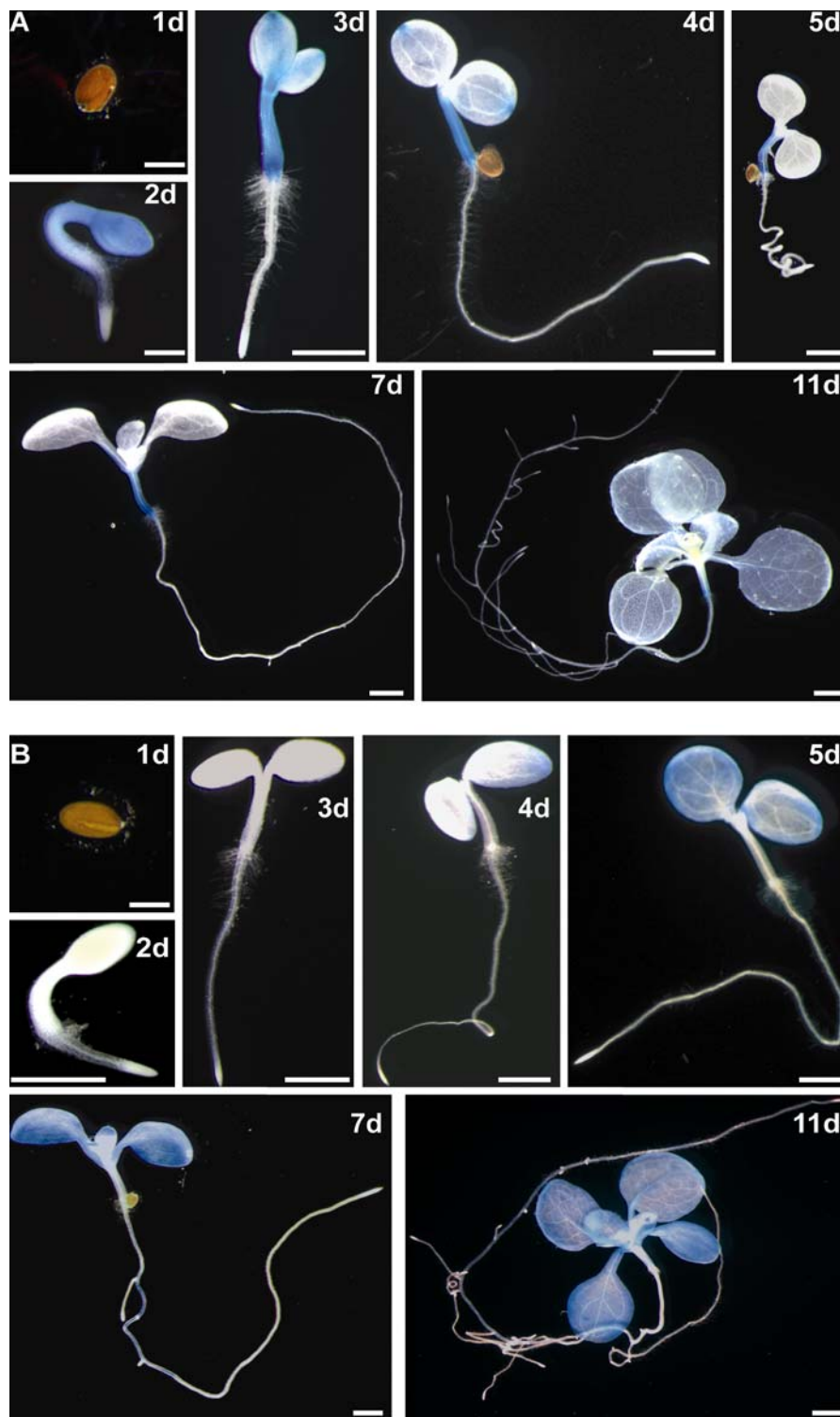


Fig. 24: GUS-expression in Arabidopsis seedlings driven by the promoters of *AtUPS1* and *AtUPS2*.

The *uidA* gene from *E. coli* was expressed in *Arabidopsis* under the control of the *AtUPS1*-(A) and the *AtUPS2*-(B) promoter. Seedlings grown on plates with MS medium were harvested 1, 2, 3, 4, 5, 7 and 11 days after imbibition and analyzed for GUS-activity (scale bar = 1.2 mm).

GUS-activity driven by the *AtUPS5*-promoter was observed starting from ~day 5 in roots and in older leaves from ~day 13 (Fig. 22A-H). To localize *AtUPS2* and *AtUPS5* expression patterns in roots at the cellular level, transverse sections were analyzed. The highest GUS

activity driven by the *AtUPS2*-promoter was found in the pericycle, weaker activity was detectable in all cells of the stele, except in mature xylem tracheary elements (Fig. 25A). GUS-activity driven by the *AtUPS5*-promoter was high in the epidermis, cortex and endodermis of the roots, and present in pericycle cells (Fig. 25B). Promoter activity of *AtUPS5* in roots was limited to lateral roots in older seedlings and plants (Fig. 25F). Staining resulting from the activity of the *AtUPS4*-promoter was transiently observed in leaves between day five and day nine (Fig. 24A-C).

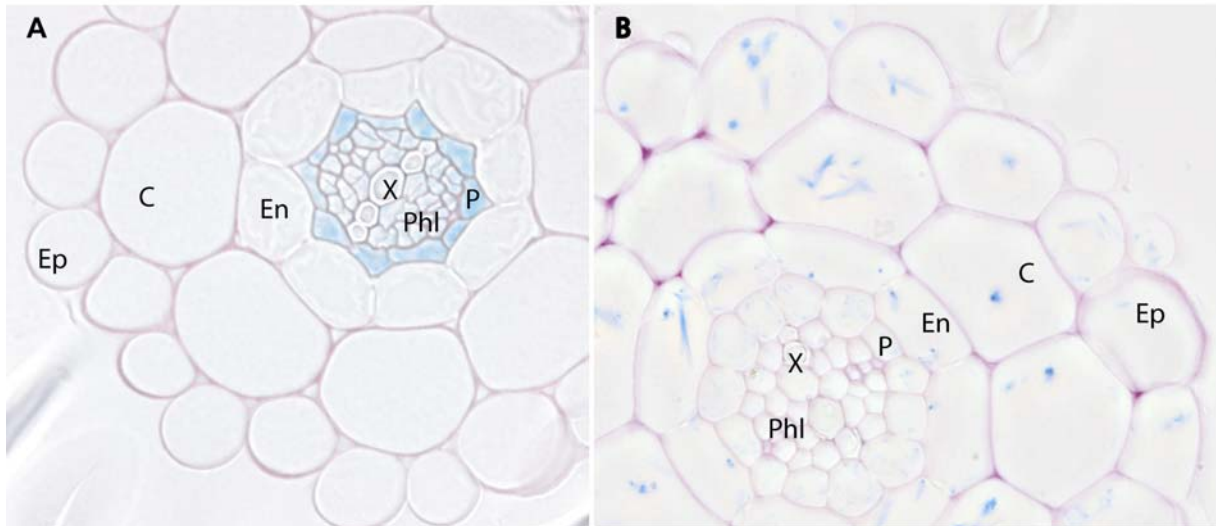


Fig. 25: Tissue specific GUS-expression driven by the *AtUPS2*- and *AtUPS5*-promoters in roots.

The *uidA* gene from *E. coli* was expressed in *Arabidopsis* under the control of the *AtUPS2*- and the *AtUPS5*-promoter. GUS-activity driven by the *AtUPS2*-promoter (A) or by the *AtUPS5*-promoter (B) was determined in roots of *Arabidopsis* seedlings grown on plates with MS medium for 6 days. Sections (6 μ m (A) or 4 μ m (B), 100x magnification) were generated after fixation and resin embedding. Staining was observed in the root stele, except in mature xylem tracheary elements. Abbreviations: Ep: epidermis; C: cortex; En: endodermis; P: pericycle; Phl: phloem; X: mature xylem tracheary elements.

3.1.5.3. Expression of *AtUPS* is modulated by nutritional and stress conditions

Regulation between nucleotide *de novo* synthesis and salvaging of nucleobases and nucleosides depends on a variety of physiological conditions, e.g. carbon and nitrogen availability. Thus, promoter activities of *AtUPS* members were studied in seedlings grown under different nutritional and stress conditions.

In agreement with previous assays (Desimone *et al.*, 2002), GUS-activity driven by the *AtUPS1*-promoter is high under nitrogen starvation. Staining was observable in cotyledons and primary leaves of 8- and 11-day-old seedlings grown on 5 mM allantoin as a sole nitrogen source or without nitrogen supply. In contrast, no staining in leaves was observable when seedlings were grown on MS medium (Fig. 26A,B). In 11-day-old seedlings grown on allantoin as sole nitrogen source, induction of GUS-activity was also observed in the root (Fig. 26B).

AtUPS4 expression was also elevated under nitrogen deficiency. GUS-activity driven by the *AtUPS4*-promoter was present in the hypocotyl in the zone of emergency of the lateral root formation of 11-day-old plants grown on MS medium. The supply of allantoin as a sole nitrogen source or complete nitrogen privation led to induction of promoter-activity in the stele of the root (Fig. 26C,D).

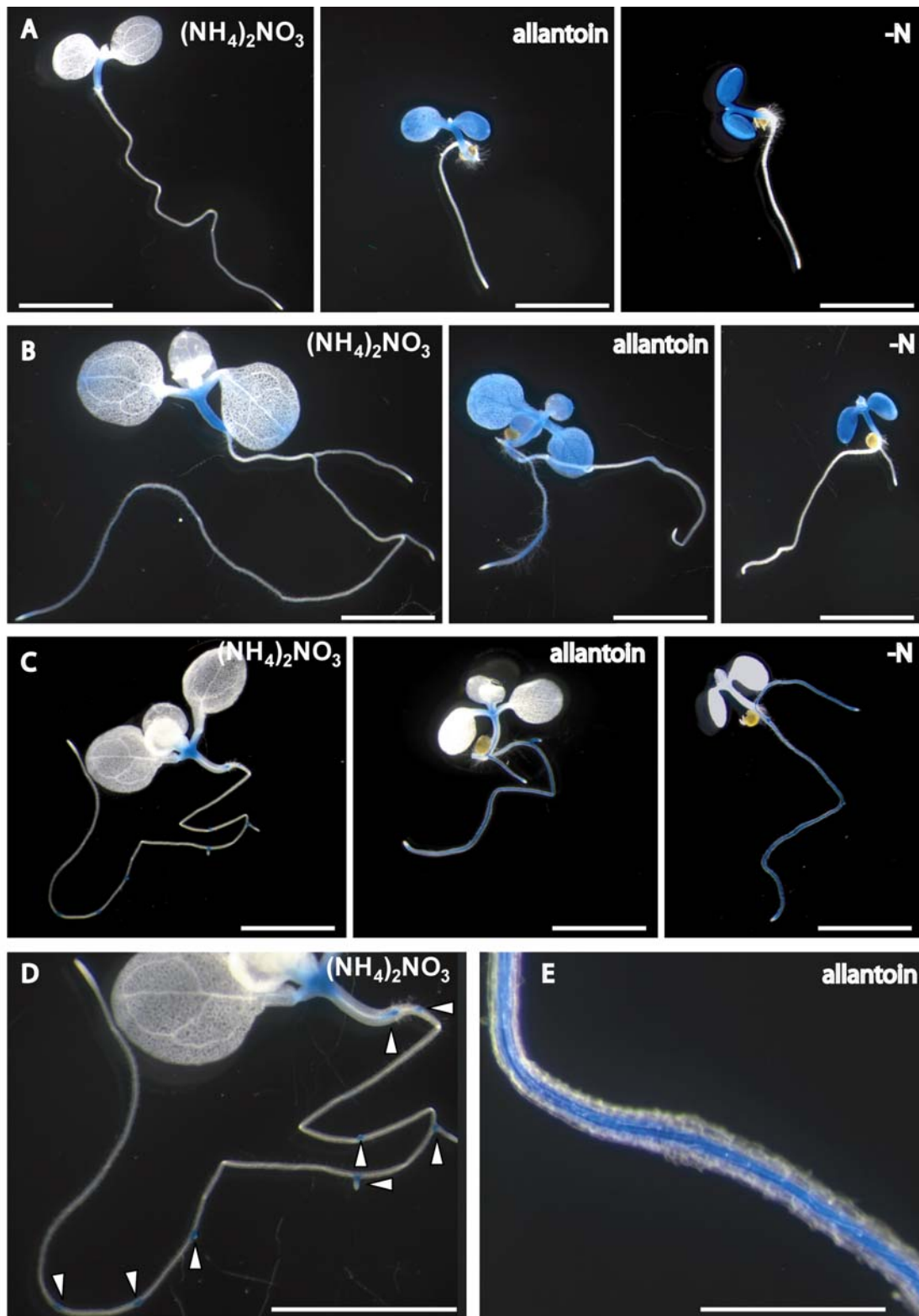


Fig. 26: Elevation of GUS-expression driven by the *AtUPS1*- and *AtUPS4*-promoter under nitrogen deficiency.

The *uidA* gene from *E. coli* was expressed in *Arabidopsis* under the control of the *AtUPS1*-(A, B) and the *AtUPS4*-(C, D) promoter. Seedlings were grown on MS medium, or modified MS medium with 5 mM allantoin as a sole nitrogen source, or modified MS medium without nitrogen source for 8 or 11 days prior to harvest. GUS-activity was analyzed. (A-C, scale bar = 0.25 cm; D, scale bar = 6.25 mm).

In another experiment, 13-day-old plants were transferred from plates to liquid modified MS-medium with either 20 mM nitrogen and 1 % (w/v) sucrose, 20 mM nitrogen without sucrose, or 20 mM nitrogen without sucrose, plus additional 150 mM of sodium chloride. GUS-activity driven by the *AtUPS2*-promoter was elevated in plants transferred to medium without supplemental sucrose in comparison to control plants transferred to medium with sucrose; an additional slight increase in staining intensity could be observed under salt stress (Fig. 27A-C). Moreover, a variation of expression pattern within the root system was observed. In plants transferred to MS medium with 20 mM nitrogen without sucrose staining was mainly observed in the main root. In contrast, expression in lateral roots was mainly observed for salt stressed plants. GUS-activity driven by the *AtUPS4*-promoter was induced in the stele of the root in salt stressed plants (Fig. 27D,E).

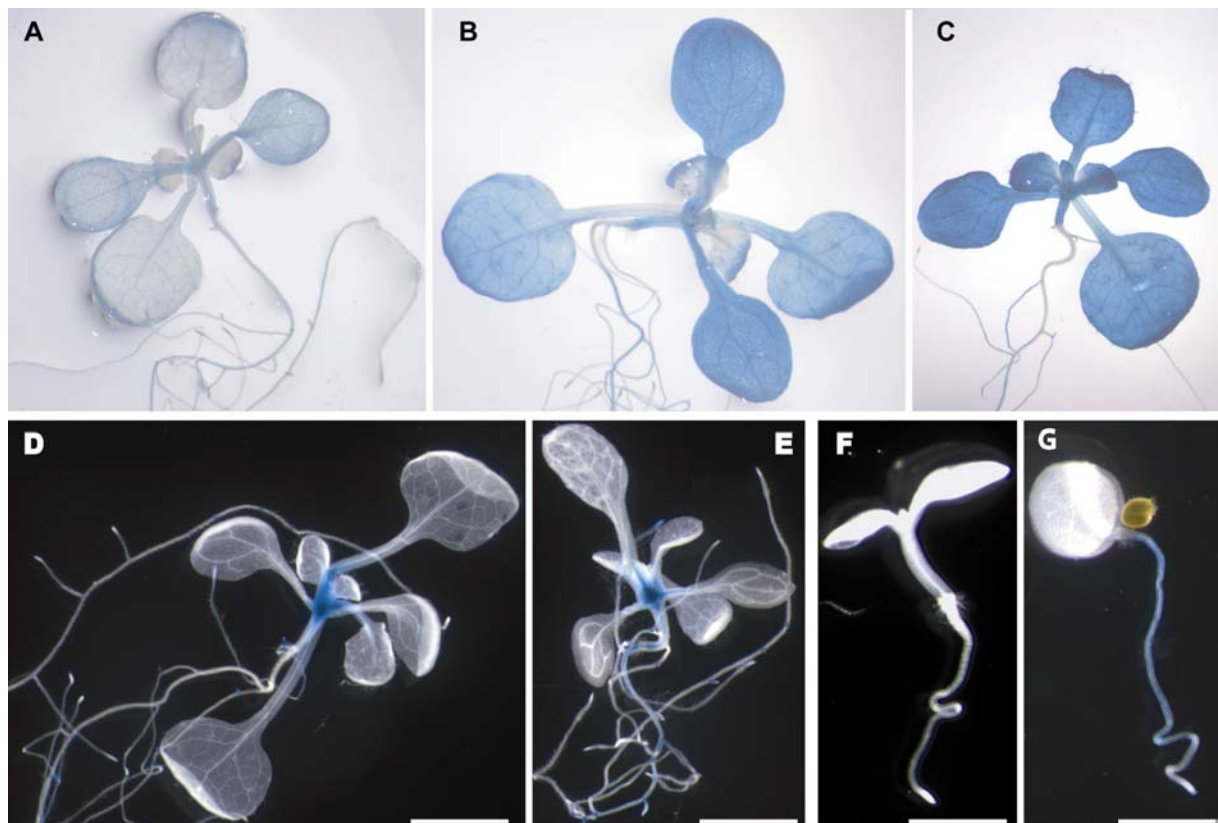


Fig. 27: Gus-activity driven by the *AtUPS1*-, *AtUPS2*- and *AtUPS4*-promoter upon different nutritional conditions and salt stress.

The *uidA* gene from *E. coli* was expressed in *Arabidopsis* under the control of the *AtUPS1*- (F, G), the *AtUPS2*- (A-C) and the *AtUPS4*- (D, E) promoter. 13-day-old seedlings grown on modified MS medium (20 mM N, 1 % (w/v) sucrose) were transferred to liquid medium with either 20 mM nitrogen with 1 % (w/v) sucrose (A, D), 20 mM nitrogen without sucrose (B), or 20 mM nitrogen without sucrose with additional 150 mM of sodium chloride (C, E) for one day prior to analysis of GUS activity (scale bar = 0.25 cm). Seedlings were grown for 6 days on modified MS medium with 8 mM of nitrogen without sucrose (F) and supplemental 200 μM of either uracil (G) before analysis of GUS-activity (scale bar = 0.5 cm).

Since induction of expression might be due to decreased nucleobase availability resulting from *de novo* synthesis, it was tested if supplementation of selected UPS substrates directly affects expression. GUS-activity driven by the *AtUPS1*-promoter was followed for 1- to 5-day-old seedlings grown on MS medium with 1 % (w/v) sucrose with or without the addition of 1 mM

thymine, 1 mM uracil, or 100 μ M 5-FU. No changes in expression pattern or staining intensity were observed. This was confirmed by RT-PCR (not shown). GUS-activity driven by the *AtUPS1*-, 2-, 4-, or 5-promoter was not significantly affected in plants grown on modified MS medium with 8 mM of nitrogen without sucrose and a supplemental 200 μ M of either uracil, thymine, uric acid, xanthine, dihydrouracil, or allantoin, with one exception: slight staining was observed in roots of 6-day-old plants expressing GUS under the control of the *AtUPS1*-promoter upon addition of 200 μ M uracil to the medium (Fig 27F,G).

In summary, the expression of *AtUPS* members seems to be differentially regulated during the different developmental stages, and displays tissue specificity. *AtUPS1* is mainly expressed during germination and early seedling development, implying a role in nucleobase mobilization from storage tissues. *AtUPS2* and *AtUPS5* expression might play a role in long distance transport of nucleobases in later stages of seedling and plant development. *AtUPS4* might be involved in supply to dividing cells in the zone of emergency of the lateral roots, as well as in nucleobase uptake in pollen, in the latter case potentially together with *AtUPS5*. No indication for expression of *AtUPS3* has been found. Moreover, *AtUPS1*, *AtUPS2* and *AtUPS4* expressions were sensitive to nutritional conditions like C: N ratio, abundance of nitrogen, as well as the presence of salt. GUS-activity driven by *AtUPS*-promoters is summarized in Tables 6 and 7.

Tab. 6: GUS-activity driven by *AtUPS*-promoters; +: GUS-activity detected; ++; high GUS-activity detected; -: no GUS-activity detected; n. d., not determined

promoter	bolting plants on soil						seedlings on MS plates		
	stems	leaves	flowers	shoots	seeds	roots	<3-4days	~5-13days	>13 days
<i>AtUPS1</i>	-	-	-	-	-	n.d.	cotyledons, hypocotyl	hypocotyl, hydatodes	hypocotyl, hydatodes
<i>AtUPS2</i>	+	++	+	+	-	n.d.	-	leaves, root	leaves, root
<i>AtUPS3</i>	-	-	-	-	-	n.d.	-	-	-
<i>AtUPS4</i>	-	-	+	+	-	n.d.	-	leaves, hypocotyl	side roots, (leaves, hypocotyl)
<i>AtUPS5</i>	++	++	+	+	-	n.d.	-	roots	roots, leaves

Tab. 7: GUS-activity driven by *AtUPS*-promoters; -: no elevation of GUS-activity detected; +: elevation of GUS-activity; ++, stronger elevation of expression; GUS-activity driven by *AtUPS*-promoters of 11-day-old seedlings grown with different sources or no source of nitrogen in comparison to seedlings grown on MS medium (A); GUS-activity driven by *AtUPS*-promoters of 14-day-old plants transferred from plates (MS, 20 mM nitrogen, 1 % (w/v) sucrose) to liquid medium (MS, 20 mM nitrogen)

A		B		C:N ratio; salt stress	
promoter	5 mM allantoin (sole N-source)	no N-source	promoter	no sucrose	no sucrose, 150 mM NaCl
<i>AtUPS1</i>	+ leaves	+ leaves, roots	<i>AtUPS1</i>	-	-
<i>AtUPS2</i>	-	-	<i>AtUPS2</i>	+ leaves	++ leaves
<i>AtUPS3</i>	-	-	<i>AtUPS3</i>	-	-
<i>AtUPS4</i>	+ root vasculature	+ root vasculature	<i>AtUPS4</i>	+ root vasculature	+ root vasculature
<i>AtUPS5</i>	-	-	<i>AtUPS5</i>	-	-

3.1.6. Analysis of *AtUPS1* PTGS lines and *AtUPS2* or *AtUPS5* T-DNA insertion lines

To study the physiological role of AtUPS proteins in plants, *AtUPS2* T-DNA insertion lines *ups2-1*, *ups2-2*, and one *AtUPS5* T-DNA insertion line *ups5* were analyzed. The insertion in *ups2-1* is localized in the first exon, 16 bp downstream of the start codon. Line *ups2-2* carries a T-DNA insertion in the third intron of *AtUPS2*. The T-DNA insertion in *ups5* is localized in the 5'UTR, 149 bp upstream of the start codon (Fig. 28A). For plants of the *ups2-1* and *ups2-2* lines, no *AtUPS2* mRNA was detectable by RT-PCR indicating that both T-DNA insertions prevent the generation of stable full-length transcripts (Fig. 28B). For *ups5* plants, no *AtUPS5* or *AtUPS5s* mRNA was observed, indicating that the T-DNA insertion prevents generation of a stable transcript (Fig. 28C).

In addition, *AtUPS1*-PTGS lines were generated to silence expression of *AtUPS1*. Efficient silencing of *AtUPS1*-PTGS lines seems to depend on lines and age of plants (Appendices Tab. 1-3). Due to the high sequence similarity of all members of the *AtUPS*-family in the region used for the PTGS construct, mRNA-levels of *AtUPS2* and *AtUPS5* were also reduced for some lines (Appendices Tab. 1-3). In five independent PTGS-lines taken for further growth assays, *AtUPS1* mRNA levels were severely reduced as shown by RT-PCR (Fig. 28B). *AtUPS2* levels were also reduced in 2 of the lines (Fig. 28B) while *AtUPS5* mRNA level was hardly affected (Fig. 28C).

Plants were grown on soil or agar and tested for phenotypic alterations. Since nucleotide synthesis is dependent on carbon and nitrogen availability, the growth of knockout and PTGS lines was tested on MS or modified MS medium with different concentrations of nitrogen (equal amounts of NH_4^+ and NO_3^- and sucrose). No evident phenotypic alteration was found for any of the lines when plants were grown in soil or on agar, with exception of *ups5*. Root development of *ups5* plants was delayed in comparison to wild type plants (Fig. 29A), when grown on MS medium (40 mM nitrogen) without sugar supply. This phenotype was not observed when 1 % of sucrose was present in the medium or when plants were grown on MS medium without sugar supplied with only 2.5 mM or 10 mM of nitrogen (not shown). Thus, root development of *ups5* plants was influenced by the C:N ratio in the medium. To exclude effects that could result from the insertion of more than one T-DNA in the plant genome, plants were backcrossed with wild type. Homozygous plants need to be generated from the backcrossed line to confirm the phenotypic alteration.

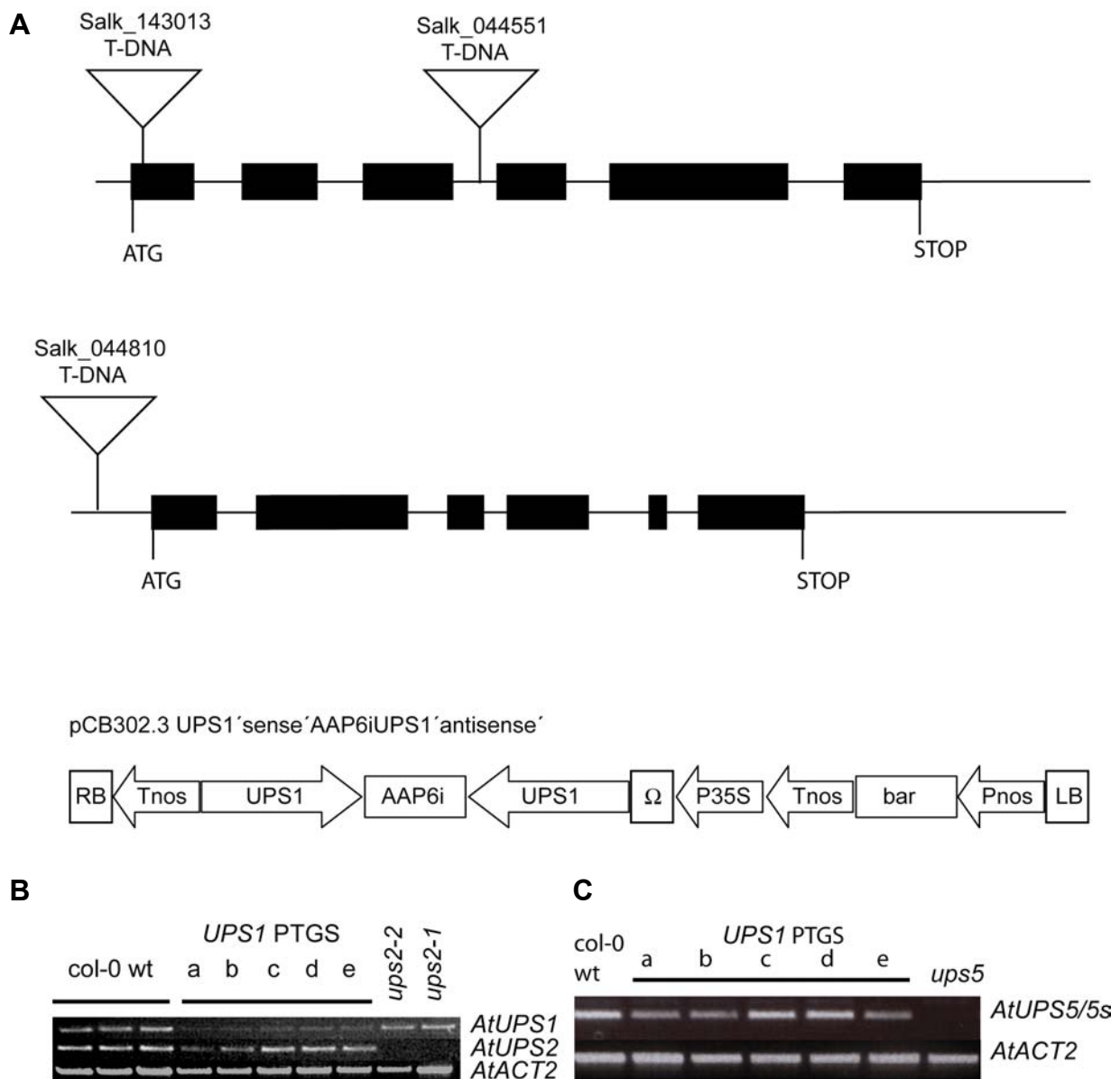


Fig. 28: Analysis of *AtUPS2* and *AtUPS5* T-DNA insertion lines and *UPS1* PTGS lines.

Two *AtUPS2* T-DNA insertion lines Salk_143013 (designated *ups2-1*) and Salk_044551 (designated *ups2-2*) were analyzed. The insertion in *ups2-1* is localized in the first exon, 16 bp downstream of the start codon. Line *ups2-2* carries a T-DNA insertion in the third intron of *AtUPS2*. The *AtUPS5* T-DNA insertion line Salk_044810 (*ups5*) is localized in the 5'UTR, 149 bp upstream of the start codon. The *AtUPS1* PTGS (*UPS1*'sense'*AAP6iUPS1*'antisense') construct was obtained by fusing a 521 bp *AtUPS1* fragment ('sense') to a 882 bp fragment of the second intron of *AtAAP6* and a 521 bp fragment of *AtUPS1* ('antisense') and cloned into the vector pCB302.3 (A). Expression levels were analyzed by RT-PCR (B). RNA was extracted from 12-day-old seedlings grown on plates with MS medium and converted to cDNA by reverse transcription. A 481 bp *AtUPS1* fragment, a 484 bp *AtUPS2* and a 510 bp *AtUPS5/5s* fragment were amplified by PCR. A 641 bp *AtACT2* fragment was used as control (C).



Fig. 29: Effect of different nutritional conditions and of 5-FU on the development of *ups5* mutants.

5-day-old seedlings grown on MS medium without sucrose under 24 hours illumination a day (A) and 7-day-old seedlings grown on plates with MS medium with 1 % (w/v) sucrose supplemented with 200 μ M 5-FU (B, scale bar = 1 mm).

5-FU is a toxic analogue of uracil and, like uracil, a good substrate at least for AtUPS1 and AtUPS2 and presumably also for other members of the AtUPS family. When germinated on 5-FU (200 μ M), wild type seedlings showed severe developmental retardation (Boyes *et al.*, 2001), while *AtUPS1* PTGS plants, *ups2-1*, *ups2-2*, and *ups5* mutants grew significantly better (Fig. 29B, Fig. 30). This suggests that UPS1, UPS2 and UPS5 are able to mediate transport of 5-FU. Since all *UPS* T-DNA insertion lines or PTGS lines supposedly behaved in the same manner in the presence of 5-FU, this might suggest all investigated members of the *UPS* family in *Arabidopsis* are involved in the same process.

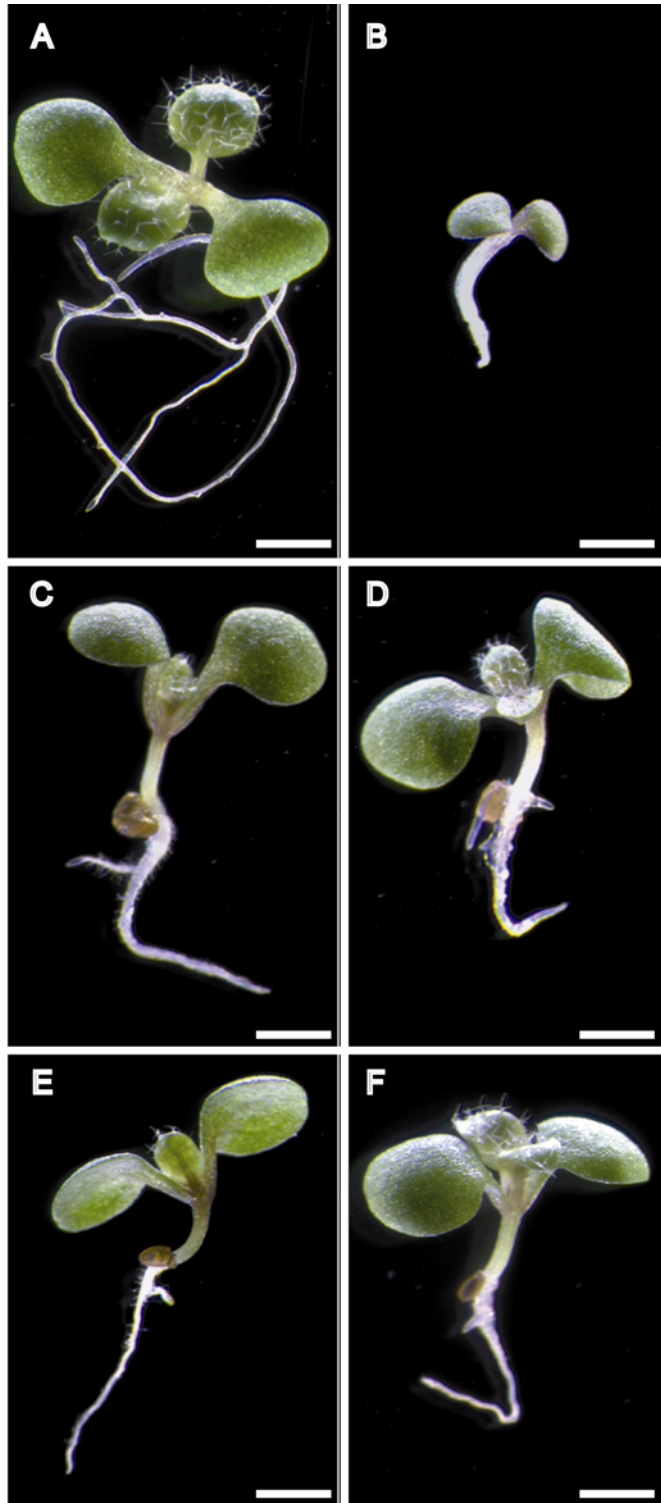


Fig. 30: Effect of 5-FU on the development of *ups2* mutants and *AtUPS1* PTGS lines.

7-day-old seedlings grown on plates with MS medium (A) and MS medium supplemented with 200 μ M 5-FU (B-F). A, B: *Arabidopsis* wt; C: *ups 2-2*; D: *ups2-1*; E: *UPS1* PTGS line b; F: *UPS1* PTGS line d (scale bar = 2 mm).

3.2. Towards establishment of a nucleobase sensor

3.2.1. Constructs with different backbones

The *Escherichia coli* Purine Repressor (PurR) was chosen as a target protein for development of a nucleobase sensor, because of its structural relationships to PBPs. FRET efficiency is dependent on the distance between fluorescent partners (Förster, 1948) and the relative orientations of the donor and acceptor fluorophores. Thus, two different constructs differing in N- and C-termini and subsequently in protein backbone were created for the development of nucleobase sensors: PurR1 (amino acids 56-341), and PurR59 (amino acids 59-328) (Fig. 31B). PurR1 includes a part of the

flexible hinge connecting the nucleotide binding domain (NBD) and the corepressor binding domain (CBD) (Choi and Zalkin, 1994; Swint-Kruse *et al.*, 2002), while PurR59 was designed to get the highest possible structural similarity to the ribose binding protein (RBP) used to generate the ribose sensor (Lager *et al.*, 2003) (Fig. 30A,B). Both constructs were amplified from *Escherichia coli* DH5 α (*PurR1*) or K12 (*PurR59*) genomic DNA. Furthermore, to generate a mutant differing in substrate specificity, site-directed mutagenesis of PurR1 was performed to generate PurR1_R190Q. Since the side chain of Arg¹⁹⁰ participates directly in the binding of 6-oxo-purines (e.g. hypoxanthine), a ~75 fold increase of the affinity to adenine has been described for a PurR mutant with an R190Q mutation (Fig. 30C) (Lu *et al.*, 1998b; Huffman *et al.*, 2002). In analogy to the described maltose and ribose nanosensors (Fehr *et al.*, 2002; Lager *et al.*, 2003), the N-termini of the respective PurR-variants were fused to ECFP as donor fluorophore while the C-termini were fused to EYFP as acceptor fluorophore. In the case of the *PurR59* expression construct, the *EYFP* encoding sequence was replaced by the sequence encoding for a mutant YFP called Venus. The Venus protein has several advantages for *in vivo* applications: its maturation time is shorter, and the protein is less sensitive to changes of pH and chloride concentration in comparison to EYFP (Nagai *et al.*, 2002).

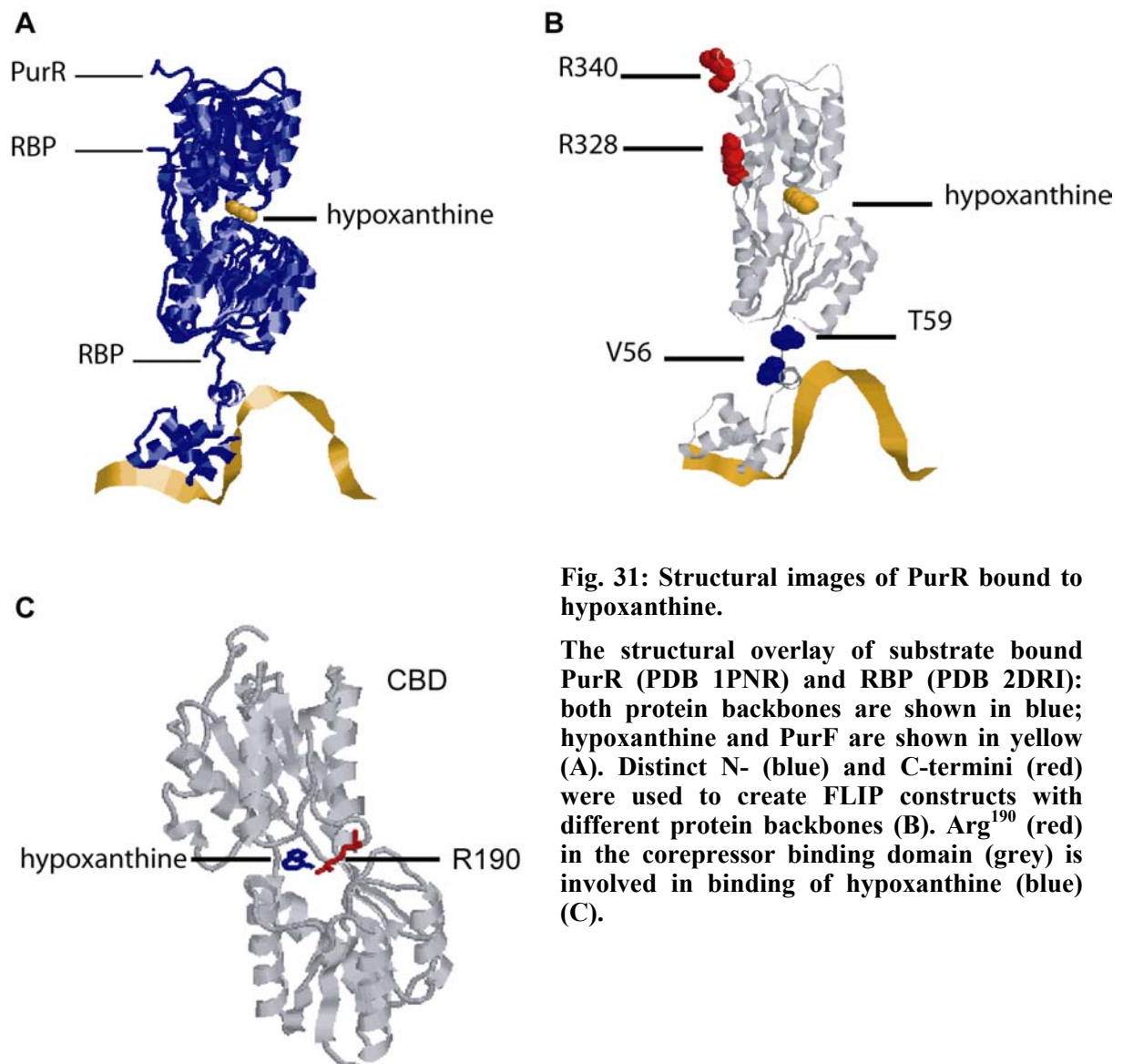


Fig. 31: Structural images of PurR bound to hypoxanthine.

The structural overlay of substrate bound PurR (PDB 1PNR) and RBP (PDB 2DRI): both protein backbones are shown in blue; hypoxanthine and PurF are shown in yellow (A). Distinct N- (blue) and C-termini (red) were used to create FLIP constructs with different protein backbones (B). Arg¹⁹⁰ (red) in the corepressor binding domain (grey) is involved in binding of hypoxanthine (blue) (C).

3.2.2. Repressor mutants affected protein expression and maturation

The proteins FLIP_{PurR1} as well as FLIP_{PurR59} caused problems in expression and maturation in *Escherichia coli* (BL21Gold(DE3)) cells. In the case of FLIP_{PurR1}, fluorophores were detected in less than 50 % of all transformed and inoculated bacterial cultures. Maturation of YFP (Venus) took considerably longer (1-2 days) for FLIP_{PurR59} compared to Flip_{glu-600μ} (Fehr *et al.*, 2003) under the same conditions.⁸ This suggests that the FLIP_{PurR}-proteins tested might have problems with expression or folding. In contrast, expression and maturation of the mutant protein FLIP_{PurR1}R190Q was always achieved after ~3 days of bacterial growth. This implies that problems in expression and maturation might have been abolished due to this mutation in the binding site.

3.2.3. Nucleobases can serve as quenchers for fluorescence

When substrates (e.g. hypoxanthine) bind to PurR, conformational changes should lead to changes in distance and presumably orientation of the donor CFP and the acceptor YFP, and consequently to changes in FRET efficiency. To record steady-state changes in FRET efficiency upon binding of substrate, different ways can be followed: (i) upon excitation of the donor fluorophore, emission of the donor and the acceptor can be followed by monitoring the emission spectra of both fluorophores. (ii) Alternatively, changes in emission can be measured at emission maxima for donor and acceptor molecules, and the value of the ratio (acceptor emission intensity/donor emission intensity) can be recorded. It is expected that when the donor and acceptor molecules get closer, donor emission decreases while acceptor emission increases. In contrast, in the presence of 1 mM of hypoxanthine, emission intensity of both CFP and YFP decreased for FLIP_{PurR1}, FLIP_{PurR59} and Flip_{glu-600μ} (control) (Fig. 32, not shown).

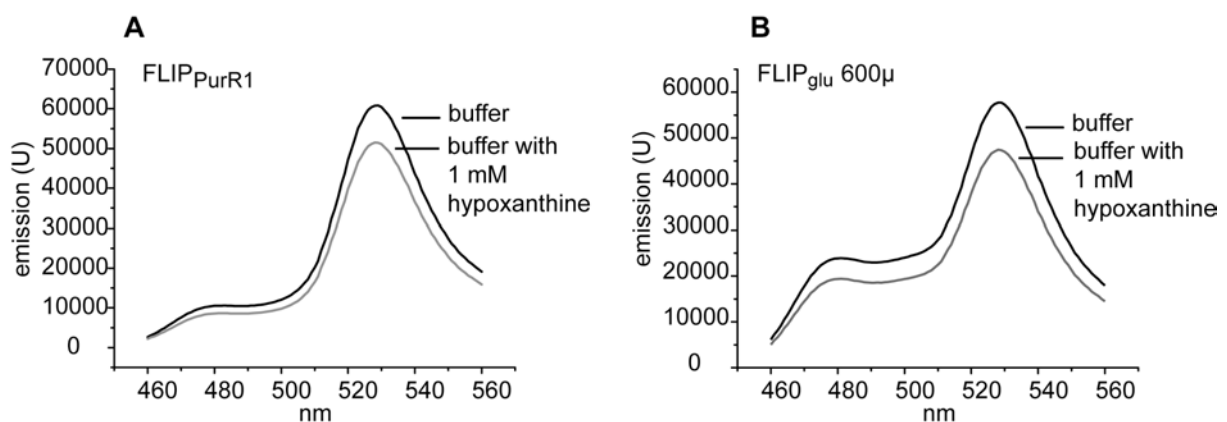


Fig. 32: Presence of hypoxanthine effects emission spectra.

Emission spectra were recorded for different sensor proteins, PurR1 and Flip_{glu600μ} (B) in 20 mM sodium phosphate buffer (pH 7.0) in the absence or presence of 1 mM hypoxanthine. Excitation wavelength was 433 nm.

Thus, the lower emission was not specifically due to hypoxanthine binding to PurR but to a more general mechanism. Nucleobases are described to be quenchers of fluorescence (Seidel *et al.*, 1996), thus, the observed effect might be due to quenching. In order to quantify the background noise resulting from the quenching effects, a sensor based on the histidine binding protein (FLIP_{his}, Persson, J., personal communication) was tested. Different buffer

⁸ For expression of Flip_{glu-600μ}, the EYFP coding sequence was replaced by Venus (Okumoto, S., personal communication).

conditions (20 mM sodium phosphate buffer pH 7, 50 mM MES-KOH buffer pH 7 and 20 mM MES-buffer pH 7) were chosen to analyze ratios of emission of YFP/CFP (528 nm/485 nm) upon excitation of CFP at 433 nm. The lowest background was obtained with 20 mM MES-buffer pH 7. Hypoxanthine concentrations of 0 to 500 μM did not result in significant effects on the ratio of emission intensity (Fig. 33A).

3.2.4. Changes in steady-state FRET efficiency were observed for a mutant repressor

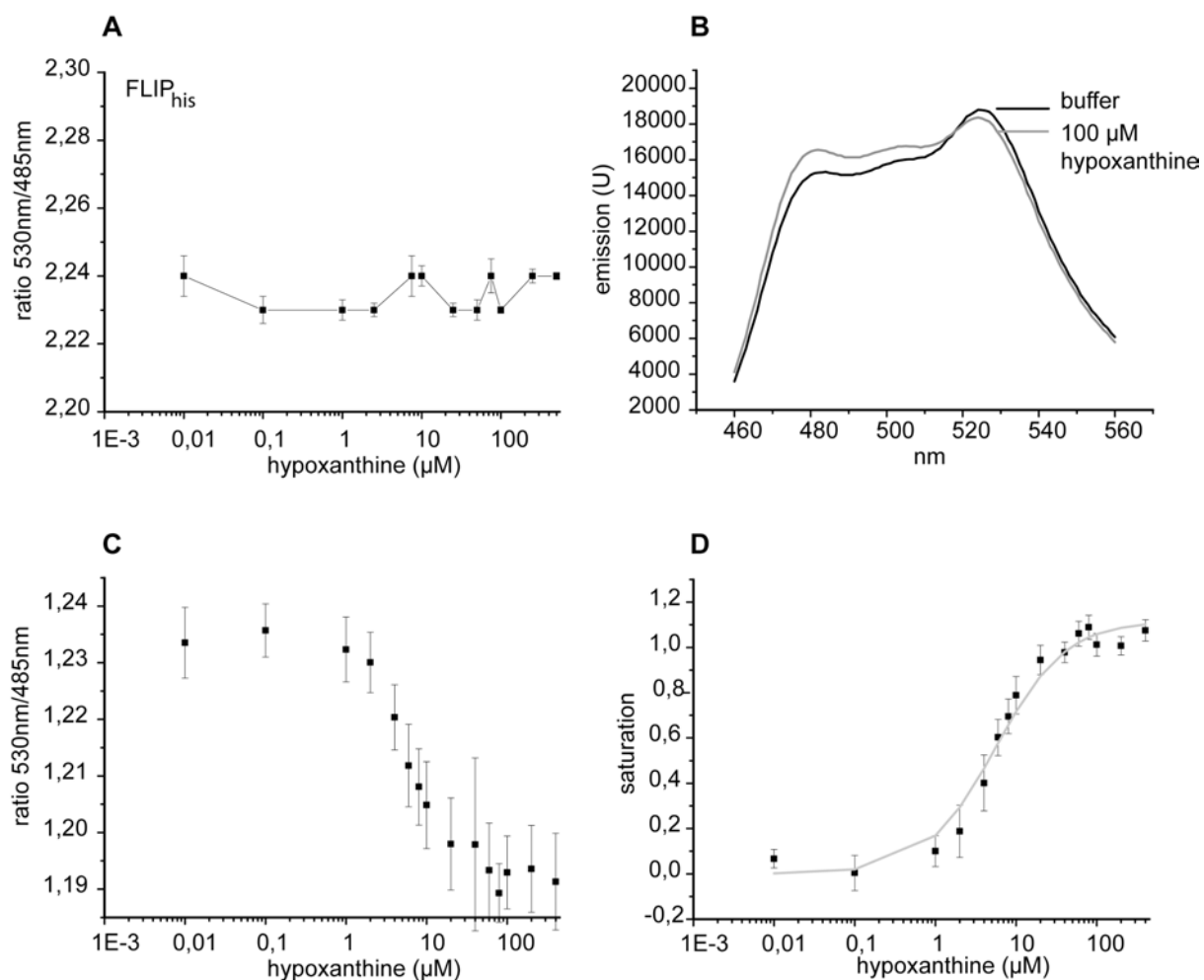


Fig. 33: *In vitro* substrate titrations of purified nanosensors.

Possible background due to quenching effects was tested with a FLIP_{his} in 20 mM MES-KOH buffer at pH 7 with concentrations of hypoxanthine ranging from 0-500 μM (data points represent means \pm SD of 3 independent measurements) (A). Emission spectra were recorded for PurR1_{R190Q} in 20 mM MES-KOH buffer (pH 7) in absence or presence of 100 μM hypoxanthine. Excitation wavelength was 433 nm (B). Decrease of the emission intensity ratio (530 nm/485 nm) was recorded with concentrations ranging from 0-400 μM of hypoxanthine in 20 mM Mes-KOH buffer (pH 7). Ratios at 0 μM hypoxanthine concentration were set to the same value (C). By transforming the hypoxanthine dependent ratio change into a saturation of PurR with the corepressor, the K_d for hypoxanthine binding was determined by a non-linear regression fit. Data points represent means \pm SD of three measurements each of 3 independent protein purifications (C,D).

Steady-state FRET efficiency of FLIP_{PurR1} or FLIP_{PurR59} was analyzed at different concentrations of hypoxanthine (between 0 μ M and 500 μ M). No significant change in the ratio of emission intensity (530 nm/485 nm) was observed (not shown). Ratios of emission intensities (530 nm/485 nm) for different proteins were different with ~ 5.6 for FLIP_{PurR1} and ~ 1.2 for FLIP_{PurR59}. This might indicate conformational differences resulting in closer proximity of CFP and YFP in the case of FLIP_{PurR1} compared to FLIP_{PurR59}, or effects of orientation of fluorophores.

For the purified FLIP_{PurR1}R190Q protein, an emission spectrum recorded in presence of 100 μ M hypoxanthine showed higher emission intensity of ECFP (donor) and lower emission intensity of EYFP (acceptor) compared to the spectrum recorded in buffer without additional hypoxanthine (Fig. 33B). These changes are presumably due to conformational changes of the protein upon binding of hypoxanthine, resulting in changes of FRET efficiency. Thus, either the distance between ECFP and EYFP might decrease, or the decrease in emission intensity of EYFP might be caused by changes in orientations of donor and acceptor dipoles. Since an affinity of $K_d = 5.5 \pm 3.1$ μ M was reported for PurR with a R190Q exchange (Lu *et al.*, 1998b), 100 μ M of substrate should be saturating for the enzyme. Significant effects due to quenching should not be obtained at this concentration (Fig. 32A). To determine the binding constant of the FLIP_{PurR}R190Q protein, the ratios in emission intensities of YFP/CFP were recorded for different concentrations of hypoxanthine between 0 and 400 μ M. The ratio of emission intensity (530/485 nm) decreased by ~ 0.04 (taken as difference between maximum and minimum ratios of emission intensity, Δr_{\max}). The ratio change depending on hypoxanthine concentrations was transformed in a saturation curve using the formula described in the methods. A K_d for hypoxanthine of 5.6 ± 0.7 μ M (Fig. 33C,D) was derived by a non-linear regression fit. The value is in agreement with the results described in (Lu *et al.*, 1998b), who determined an affinity of $K_d = 5.5 \pm 3.1$ μ M for PurR with a R190Q exchange. Since the total ratio change was relatively small ($\Delta r_{\max} \sim 0.04$ in comparison to Δr_{\max} between 0.19 and 0.38, as reported for wild type or affinity mutants of the ribose nanosensor (Lager *et al.*, 2003)), our sensor would have to be improved prior to *in vivo* applications. Nevertheless changes in total ratio of this sensor mutant are promising, since they indicate that PurR can practically be used as a nanosensor.

4. Discussion

4.1. Transport of uracil by *Arabidopsis* UPS transporters

AtUPS1 and *PvUPS1* from *Arabidopsis thaliana* and *Phaseolus vulgaris* have recently been identified as transporters of allantoin and other oxo-*N*-heterocycles. However, there was no evidence of the importance of the long distance transport of allantoin in *Arabidopsis*. The present study shows that *Arabidopsis* UPS members (*AtUPS1*, 2, 5 and presumably also *AtUPS4*) transport uracil and other pyrimidines when expressed in *Xenopus* oocytes or yeast. In addition, at least *AtUPS1* and *AtUPS2* display a high affinity for uracil (~6 μ M). Moreover, a decreased sensitivity of *ups2*, *ups5* and *UPS1* PTGS lines suggests that these *AtUPS* proteins are major transporters of 5-FU and probably uracil in *Arabidopsis*.

Although several putative uracil transporters are predicted in the *Arabidopsis* genome, they have not been described to date, like members of the NAT family and the gene *At5g03555* (Ward, 2001). *At5g03555* shares 30 % of sequence identity with the uracil transporter *FUR4* of *Schizosaccharomyces pombe* on the protein level (de Montigny *et al.*, 1998). No phylogenetic relationships between *AtUPS* and these proteins has been observed, nor with uracil transporters that have been identified so far in bacteria, yeast or protozoa (Yoo *et al.*, 1992; Ghim and Neuhard, 1994; Andersen *et al.*, 1995; de Koning and Diallinas, 2000). In addition, no significant sequence similarity has been found with genes in organisms other than plants (Desimone *et al.*, 2002).

Thus members of the *AtUPS* family are the first investigated transporters in higher eukaryotes mediating high affinity transport of uracil. Moreover, *UPS* are a novel family of transmembrane transporters, possibly restricted to plants.

4.2. *PvUPS* and *AtUPS* – two plant families, two different roles of *UPS*-transporters?

Transport of considerable amounts of allantoin and other ureides is known to play an important role in the long distance transport of organic nitrogen in nodulated legumes (Pélissier *et al.*, 2004). This suggests, that allantoin is the physiological substrate for *PvUPS*. Since allantoin and allantoic acid are degradation products of nucleic acids, it is conceivable that they might also be present in soils. Although the composition of soils is highly variable, the presence of organic nitrogen compounds has been demonstrated, including amino acids, amino sugars, *N*-heterocycles and others. *N*-heterocycles can make up to ~30 % of nitrogen compounds present in soil (Schulten and Schnitzer, 1998). It is known that under agricultural cultivation plants mainly use ammonium and nitrate as nitrogen sources (von Wirén *et al.*, 2000). In contrast, availability of nitrogen in natural habitats is often limiting. Since plants are likely to use all possible sources of nitrogen, a role for *AtUPS* transporters in the utilization of *N*-heterocycles present in soils has been suggested (Desimone *et al.*, 2002). *Arabidopsis* seedlings are able to grow on allantoin as a sole nitrogen source. This indicates that *Arabidopsis* is able to take up this compound when supplied in the medium. But plants present severe phenotypic alterations; they generally remain smaller than plants grown on ammonium and nitrate as nitrogen sources, and have smaller leaves and longer roots (Desimone *et al.*, 2002). Similar or even more severe phenotypes were observed with other oxo-*N*-heterocycles as sole nitrogen source, e.g. uracil, hydantoin or xanthine (not shown). Increased root surface can have several different reasons, one of them being nitrogen deficiency (Gazzarrini *et al.*, 1999). *AtUPS1* expression is elevated in plants grown on allantoin as a sole nitrogen source, as well as under nitrogen deficiency, as shown by RT-PCR (Desimone *et al.*, 2002). In addition, higher GUS-activity driven by the *AtUPS1* promoter was observed in leaves of seedlings grown either on allantoin as a sole nitrogen source or without a nitrogen source. This indicates that increased expression levels may result from nitrogen

deficiency rather than the presence of allantoin. Thus, it is conceivable that UPS transporters serve different roles in nodulated legumes and *Arabidopsis*: While legumes might have taken advantage of the broad substrate specificity of UPS transporters to develop an allantoin transporter, according to their needs, UPS might have other functions in *Arabidopsis*, like the transport of uracil for salvaging. Nevertheless, it cannot be excluded that the physiological substrate might be another *N*-heterocyclic compound, that might not even be identified.

4.3. Regulation at protein level

4.3.1. Does the Walker A motif play a role in nucleotide sensing?

Local metabolite concentrations have to be maintained to fit the cellular needs and to avoid concentrations that might be cytotoxic, as have been for example discussed for high concentrations of uracil in some legume species (Thran, 1999). For transporters playing a role in nucleobase salvaging, transport activities have to be adapted to a multitude of physiological changes at different periods of time, for example depending on developmental processes, cell cycle, activity of photosynthesis, nutritional changes, etc. Control of expression and protein stability provide a long term means of regulating protein activity. However, protein activity must also be regulated in an immediate fashion. Thus, some kind of signal is necessary for the transporter to recognize the metabolic state of cells or subcellular compartments.

A proton cotransport mechanism has been observed for two members of the AtUPS family, AtUPS1 and AtUPS2. Therefore it is unlikely that ATP/GTP binding and hydrolysis by the Walker A motif of AtUPS1 is directly involved in energizing transport. It is, thus, possible that the Walker A motif might play a role in regulation of transport by sensing the levels of nucleotides in cells or certain cellular compartments. It is worthwhile noting that CTP and UTP hydrolysis by proteins having a standard Walker motifs has been reported, although with lower efficiencies (Schneider and Hunke, 1998). Investigating the putative binding and hydrolysis of nucleotides to the UPS Walker A motif would help to understand the role of this motif in UPS proteins, and also presumably the differences in regulation between AtUPS2 and other AtUPS proteins.

Since all generated mutations caused a decrease in the efficiency of allantoin transport when *AtUPS1* or *AtUPS2* were expressed in *Xenopus* oocytes, all mutated residues are of structural or functional importance. Such decreased transport rates might result from mutations of residues directly involved in substrate recognition, or close to the substrate recognition site. Since Walker A motifs are reported to play a role in binding of the phosphate moieties of ATP or GTP, it seems unlikely that these residues are directly involved in the recognition of the heterocyclic UPS substrates. Based on structural predictions, the mutated residues are localized in a transition of a cytoplasmatic loop and a transmembrane helix. Thus the mutations might effect membrane integration or binding to phospholipids as well. Further investigations, e.g. by creating additional mutations, will be needed to completely understand the function of these residues.

4.3.2. Is AtUPS5s involved in regulation of AtUPS5?

Formation of homo- or heteromeric complexes between membrane proteins can be involved in modulation of activity (Schulze *et al.*, 2003; Ludewig *et al.*, 2003a; Ludewig *et al.*, 2003b). A special feature of *AtUPS5* is the presence of the shorter splicing variant, *AtUPS5s*. No function in solute transport was found upon expression in oocytes or yeast, implying that the protein might have a function different from the other characterized members of the family. This hypothesis is supported by the observation of the structural changes caused by the

splicing of the additional intron. AtUPS5s might be involved in the regulation of transport processes of other AtUPS proteins, presumably AtUPS5, by the formation of heteromeric complexes. This is indicated by the severe reduction of the rate of allantoin transport upon *AtUPS5/5s* co-expression in yeast. For more detailed understanding of interactions or complex formations involved in regulation of AtUPS, further analyses might focus on the determination of AtUPS protein levels in yeast membranes upon uptake, or modifications of expression levels by the use of inducible promoters, etc.

4.4. Correlations between *AtUPS* expression and uracil salvaging

AtUPS are differentially expressed, although there is no evidence of *AtUPS3* expression. This gene might not be expressed or might display very low or specific expression. Various expression patterns for *AtUPS1*, 2, 4, and 5 could be observed by RT-PCR or promoter-GUS studies. Expression of *AtUPS1* was mainly observed during germination and early seedling development, suggesting a role in uracil supply from seed storage tissues. In contrast, expression of *AtUPS2*, 4 and 5 is low or absent during the first ~4 days of seedling growth, suggesting that these proteins play a role in later developmental stages. *AtUPS4* and *AtUPS5* might be involved in the supply of uracil to pollen, since GUS-activity driven by the *AtUPS4*-promoter was observed in filaments of the androecium, while *AtUPS5* expression was observed in the connective tissue between pollen sacks. The salvaging of nucleobases and nucleosides might contribute to an elevation of the uracil nucleotide pool in preparation of pollen tube growth, in agreement with reports of nucleoside uptake into petunia pollen (Kamboj and Jackson, 1984; Kamboj and Jackson, 1985; Kamboj and Jackson, 1987). *AtUPS5* and *AtUPS2* might, in addition, play a role in long distance transport of metabolites, since *AtUPS2* expression was found in the stele of the root and *AtUPS5* expression in the vasculature of young leaves. While *AtUPS5* expression in leaves is restricted to veins in young tissues, overall staining of the blade of older leaves starting from the tip was observed. It can be assumed that this result is consistent with the high uracil salvaging activities in early senescent stages of tobacco leaves (Ashihara, 1981). GUS-activity driven by the *AtUPS5*- and *AtUPS2*-promoters was observed in roots. While expression of *AtUPS5* was observed in the epidermis, cortex, endodermis and pericycle of the root, *AtUPS2* expression was observed in the stele of the root, so both might be involved in uptake and transport of heterocycles from soil. Since pyrimidine synthesis is high in leaves and *AtUPS5* expression is observed in the veins of the leaves as well in the source tissues of older leaves, the opposite might be true and pyrimidine bases might be transported from source tissues to sink leaves and roots.

Interestingly, *AtUPS2* was found to be expressed all over the leaf. It might thus be involved in short distance transport processes or cellular nucleobase turnover due to compartmentalization of metabolic pathways. While the pyrimidine synthesis pathway is localized in chloroplasts and mitochondria, uracil salvaging enzymes are mainly found in the cytoplasm. RNA degradation as source of free bases predominantly takes place in the vacuole (Wagner and Backer, 1992). Nevertheless, as a 5'-nucleosidase was also localized to the outer surface of the plasma membrane and to plasmodesmata (Wagner and Backer, 1992), there might be a necessity of uptake of external nucleobases. The expression patterns of the members of the *AtUPS* family suggest roles in uracil salvaging. Since *AtUPS* have different expression patterns and presumably various regulation mechanisms, they probably do not have redundant functions.

Since metabolic pathways of nucleotide *de novo* synthesis, degradation and salvaging are highly compartmentalized, especially at the subcellular level, knowledge about subcellular localization of AtUPS transporters would help to understand their physiological roles. AtUPS members might be localized in different subcellular compartments. Targeting predictions for members of the AtUPS family are ambiguous, as summarized in the Aramemnon database

(<http://aramemnon.botanik.uni-koeln.de/>). Predictions mainly involve the secretory pathway or targeting to chloroplasts. But no experimental data on subcellular localization is available in plants to date. Expression of C-terminal *AtUPS1*-, *AtUPS2*-, *AtUPS5*- or *AtUPS5s*-GFP fusion constructs was analyzed in protoplasts but no GFP could be detected. Thus, future investigations will be needed to detect the subcellular localization of AtUPS in plants.

4.5. Stress conditions and effects of differences of the C:N ratio

A multitude of cellular functions is affected by the availability of nitrogen and carbon, as well as by stress due to high salt concentrations. Since nucleobase *de novo* synthesis depends on the availability of nitrogen and carbon, deficiency of these nutrients results in decreased *de novo* synthesis, as demonstrated for starved suspension cultured cells (Wagner and Backer, 1992). Elevation of *AtUPS1* expression under nitrogen deficiency has previously been reported (Desimone *et al.*, 2002). In addition, it was shown that *AtUPS4* expression is elevated under nitrogen deficiency. The same is described for members of the *AtENT* family, transporting nucleosides for salvaging (Li *et al.*, 2003). Thus, this elevation might be due to nucleobase deficiency. In this line a slight enhancement of expression levels of *AtUPS2* and *AtUPS4* under salt stress conditions might therefore result from decreased nucleotide *de novo* synthesis. In addition, the C:N ratio in the medium was shown to play a role. GUS-activity driven by the *UPS2*-promoter was elevated when plants were transferred from medium supplemented with 1 % (w/v) of sucrose to medium without sucrose. Root growth of *ups5* plants was detected to be sensitive to differences of the C:N ratio. For *ups5* plants grown with 40 mM nitrogen as ammonium and nitrate in the medium without an external sucrose supply, root growth was delayed in comparison with wild type. Cellular uracil and sucrose levels are connected in different ways. The synthesis rate of uracil nucleotides depends on cellular glucose levels, as shown for roots of squash plants (Wagner and Backer, 1992). This might be due to formation of PRPP, in a fashion depending on the availability of a carbon source (Wagner and Backer, 1992). Thus, the salvaging activity of uracil is presumably higher in plants without external sucrose supply. UDP-glucose is, in addition, needed for synthesis and utilization of sucrose. Without external sucrose source, root development might rely on uracil salvaging due to lower *de novo* synthesis, or regulation of pyrimidine transport processes might be impaired due to absence of *UPS5s*. *Arabidopsis UPS5s* over-expression lines were engineered that might help to elucidate the contribution of *UPS5s* in further investigations.

4.6. Effect of 5-FU on plants of *ups2*, *ups5* and *UPS1* PTGS lines

5-FU is a toxic analogue of uracil, because its metabolites can be incorporated into RNA or lead to inhibition of thymidylate synthetase (Lazar *et al.*, 1993), thus causing thymidylate starvation. In young seedlings supplied with 200 μ M of 5-FU phenotypes of *ups2*, *ups5* and *UPS1* PTGS lines are similar. Seedlings grow significantly better than *Arabidopsis* wild type plants under the same conditions, although development, especially of roots, is still delayed in comparison with plants grown without supplemental 5-FU. The members of the *AtUPS* family showed differential expression patterns depending on the developmental stages, tissue specificity and stress conditions. Several members of the *UPS* family might be involved in the transport of 5-FU to the location where toxicity occurs, presumably in a sequential manner. *AtUPS1* expression in plants grown on medium with abundant nitrogen was mainly observed during germination and early seedlings development. Thus it seems surprising, at first sight, that *UPS1* PTGS plants maintain their decreased sensitivity to 5-FU after the first days of

development. However, nothing is known about *AtUPS1* expression in the presence of 5-FU in seedlings older than 5 days.

UPS genes expression was observed to be elevated under several stress conditions, presumably in the context of nucleobase deficiency. Thus it is conceivable that expression levels of *UPS* members might be elevated in wild type plants under these conditions. In addition, the mRNA levels of other members of the *UPS* family are silenced to a certain extent. This is presumably due to the high sequence similarity of the open reading frames to the *UPS1* PTGS construct. Since all the tested knockout or PTGS lines supposedly behaved in the same manner, *UPS* members do not seem to be redundant. They all seem to play a role in the transport of 5-FU, and presumably also uracil, in plants.

4.7. Role of UPS transporters in *Arabidopsis* development

Although the decreased sensitivity of *ups2*, *ups5* and *UPS1* PTGS lines suggests that these UPS are the main transporters of 5-FU and presumably also of uracil, germination or development of *Arabidopsis* plants was not affected in any of these lines grown under greenhouse conditions or on agar plates. Since salvaging to uracil nucleotides is mainly mediated by uridine salvaging (Wagner and Backer, 1992), other transporters like members of the ENT family might compensate (Möhlmann *et al.*, 2001; Li *et al.*, 2003). In addition, other uracil transporters might exist that have not been characterized to date. Lines carrying mutations in at least four *UPSs* (1, 2, 4 and 5) and lines deficient in uridine transport will be required to determine the contribution of UPS proteins for salvaging, or to identify other potential functions of this family of *N*-heterocycle proton co-transporters. Double mutants for further investigations are already prepared.

4.8. Nucleobase nanosensors

To understand the role of transporters in nucleotide metabolism, and possible regulation by nucleosides/nucleotides, nucleobase sensors would be of great value. Different substrate specificities could be obtained by mutagenesis or computational design from only one sensor (Looger *et al.*, 2003). The purine repressor PurR was taken as a target protein because of its high structural similarity to RBP. Since FRET efficiency might depend on the rigidity of the protein backbone, different parts of the gene were cloned. Problems in expression and folding of FLIP_{PurR1} and FLIP_{PurR59} might result from bacterial toxicity (Rolfes and Zalkin, 1988; Lu *et al.*, 1998b) or limited solubility of PurR (Lu *et al.*, 1998a). A functional sensor was obtained by site-directed mutagenesis of FLIP_{PurR1} to FLIP_{PurR1}R190Q. The emission ratio of fluorescence intensity (530nm/485 nm) of this protein construct was much lower than for FLIP_{PurR1} (~1.4 in contrast to ~5.6). Thus the mutation might lead to structural changes of the overall protein backbone. The applicability of the FLIP_{PurR1}R190Q sensor in living cells is still limited, due to the small maximal changes in the fluorescence emission ratio ($\Delta r_{\max} \sim 0.04$ in comparison to Δr_{\max} between 0.19 and 0.38, as reported for wild type or affinity mutants of the ribose nanosensor (Lager *et al.*, 2003)). The differences in Δr_{\max} between the structurally highly related proteins might be due to the fact that the two proteins open differently upon substrate release, probably due to dimerisation of PurR. While the opening of RBP is nearly a pure hinge motion changing orientations of the two globular subdomains $\sim 43^\circ$ with respect to each other, the CBD of PurR opens with an angle of $\sim 17\text{-}24^\circ$ more in a twisting than in a hinge motion (Mowbray and Björkman, 1999). Differences in opening motions might be due to the presence of proline residues (Pro³²³ and Pro²⁹³), preventing rotations in PurR present in RBP (Mowbray and Björkman, 1999). Thus mutations of these proline residues might help to

elucidate the impact of opening motion on Δr_{\max} . In addition to the maximal conformational change, FRET efficiency is influenced by the distance between FRET partners and also probably by their orientation. Thus, variations in linkers and the rigidity of protein backbone might be used as a tools to optimize the sensor. In addition, other fluorescent proteins with different spectral overlap might be tried as FRET partners.

4.9. Conclusions and perspectives

The results presented in this study describe members of the *AtUPS* family as the first transporters of uracil and thymine characterized in higher eukaryotes. AtUPS1 and AtUPS2 display high affinity for uracil. Since *ups2*, *ups5* and *UPS1* PTGS lines are less sensitive to the toxic uracil analogue 5-FU, this suggests that AtUPS1, 2 and 5 are major transporters of 5-FU and also potentially of uracil in *Arabidopsis*. Nucleotide binding to the Walker A motif might play a role in the regulation of transport efficiency. Moreover, AtUPS5s might be involved in the regulation of transport efficiency of AtUPS5 by interaction or complex formation. Expression of members of the *AtUPS* family suggests involvement in supply of nucleobases to tissues having an elevated need of nucleotides. Lines carrying mutations in several *AtUPS* and also *AtENTs* might help to understand the physiological functions of UPS transporters.

Transport processes of nucleobases, nucleosides and derivatives requires regulation to fit the cellular needs under changing physiological conditions. Real time visualization of compounds involved in nucleotide metabolism in plants and other organisms would be of great value for detailed understanding of role and regulation of the transporters. In this study, a FRET-based nanosensor for hypoxanthine was developed and tested *in vitro*. The applicability of this sensor in living cells is still limited due to the small maximal changes in the fluorescence emission ratio. Nevertheless, it is a starting point for improvement of the maximum ratio change and generation of sensors with different substrate specificities.

5. References

- Adams, A., Gottschling, D.E., Kaiser, C. A., and Stearns, T. (1997). *Methods in Yeast Genetics*. Cold Spring Harbor Laboratory Press, N. Y.
- Alonso, J.M., Stepanova, A.N., Leisse, T.J., Kim, C.J., Chen, H., Shinn, P., Stevenson, D. K., Zimmerman, J., Barajas, P., Cheuk, R., Gadrinab, C., Heller, C., Jeske, A., Koesema, E., Meyers, C.C., Parker, H., Prednis, L., Ansari, Y., Choy, N., Deen, H., Geralt, M., Hazari, N., Hom, E., Karnes, M., Mulholland, C., Ndubaku, R., Schmidt, I., Guzman, P., Aguilar-Henonin, L., Schmid, M., Weigel, D., Carter, D. E., Marchand, T., Risseuw, E., Brogden, D., Zeko, A., Crosby, W. L., Berry, C. C., and Ecker, J. R. (2003). Genome-Wide Insertional Mutagenesis of *Arabidopsis thaliana*. *Science* **301**, 653-657.
- Altschul, S.F., Gish, W., Miller, W., Myers, E.W., and Lipman, D.J. (1999). Basic local alignment search tool. *J. Mol. Biol.* **215**, 403-410.
- Andersen, P.S., Frees, D., Fast, R., and Mygind, B. (1995). Uracil uptake in *Escherichia coli* K-12: isolation of *uraA* mutants and cloning of the gene. *J. Bacteriol.* **177**, 2008-2013.
- Argyrou, E., Sophianopoulou, V., Schultes, V., and Diallinas, G. (2001). Functional Characterization of a Maize Purine Transporter by Expression in *Aspergillus nidulans*. *Plant Cell* **13**, 953-964.
- Ashihara, H. (1981). Pattern of uracil metabolism during ageing of tobacco leaves. *Acta Physiol. Plant.* **3**, 77-84.
- Ashihara, H. and Nobusawa, E. (1981). Metabolic Fate of [8-¹⁴C]Adenine and [8-¹⁴C] Hypoxanthine in Higher Plants. *Z. Pflanzenphysiol.* **104**, 443-458.
- Ashihara, H., Takasawa, Y., and Suzuki, T. (1997). Metabolic fate of guanosine in higher plants. *Physiol. Plant.* **100**, 909-916.
- Atkins, C.A., Ritchie, A., Rowe, P. B., Mc. Crains, E., and Sauer, D. (1982). *De novo* purine-synthesis in nitrogen-fixing nodules of Cowpea (*Vigna unguiculata* [L.] Walp.) and Soybean (*Glycine max* [L.] Merr.). *Plant Physiol.* **70**, 55-60.
- Blattner, F.R., G. Plunkett, C. A. Bloch, N. T. Perna, V. Burland, M. Riley, J. Collado-Vides, J. D. Glasner, C. K. Rode, G. F. Mayhew, J. Gregor, N. W. Davis, H.A. Kirkpatrick, M. A. Goeden, D. J. Rose, B. Mau, and Y. Shao. (1997). The complete genome sequence of *Escherichia coli* K-12. *Science* **277**, 1453-1474.
- Boland, M.J. and Schubert, K.R. (1983). Biosynthesis of purines by a proplastid fraction from soybean nodules. *Arch. Biochem. Biophys.* **220**, 435-441.
- Boyes, D.C., Zayed, A.M., Ascenzi, R., McCaskill, A.J., Hoffman, N.E., Davis, K.R., and Görlach, J. (2001). Growth Stage-Based Phenotypic Analysis of *Arabidopsis* A Model for High Throughput Functional Genomics in Plants. *Plant Cell* **13**, 1499-1510.
- Bürkle, L., Cedzich, A., Döpke, C., Stransky, H., Okumoto, S., Gillissen, B., Kühn, C., and Frommer, W.B. (2003). Transport of cytokinins mediated by purine transporters of the PUP family expressed in phloem, hydathodes and pollen of *Arabidopsis*. *Plant J.* **34**, 13-26.
- Castro, A.H.F., Young, M.C.M., de Alvarenga, A.A. and Alves, J.D. (2001). Influence of Photoperiod on the accumulation of Allantoin in comfrey plants. *Rev. Bras. Fisiol. Veg.* **13**, 49-54.
- Chang, S., Puryear, J., and Cairney, J. (1993). A Simple and Efficient Method for Isolating RNA from Pine Trees. *Plant Mol. Biol. Rep.* **11**, 113-116.
- Choi, K.Y. and Zalkin, H. (1994). Role of the Purine Repressor Hinge Sequence in Repressor Function. *J. Bacteriol.* **176**, 1767-1772.
- Christensen, J.G. and LeBlanc, G.A. (1996). Reversal of multidrug resistance in vivo by dietary administration of the phytochemical indole-3-carbinol. *Cancer Res.* **56**, 574-581.
- Clough, S.J. and Bent, A.F. (1998). Floral dip: a simplified method for *Agrobacterium*-mediated transformation of *Arabidopsis thaliana*. *Plant J.* **16**, 735-743.
- de Koning, H. and Diallinas, G. (2000). Nucleobase Transporters (Review). *Mol. Membr. Biol.* **75**, 75-94.

- de Montigny, J., Straub, M. L., Wagner, R., Bach, M L., and Chevallier, M.R.** (1998). The uracil permease of *Schizosaccharomyces pombe*: A representative of a family of 10 transmembrane helix transporter proteins of yeasts. *Yeast* **14**, 1051-1059.
- Desimone, M., Catoni, E., Ludewig, U., Hilpert, M., Schneider, A., Kunze, R., Tegeder, M., Frommer, W.B., and Schumacher, K.** (2002). A novel superfamily of transporters for allantoin and other oxo derivatives of nitrogen heterocyclic compounds in *Arabidopsis*. *Plant Cell* **14**, 847-856.
- Diallinas, G., Gorfinkiel, L., Arst, H.N. Jr., Cecchetto, G., and Scazzocchio, C.** (1995). Genetic and molecular characterization of a gene encoding a wide specificity purine permease of *Aspergillus nidulans* reveals a novel family of transporters conserved in prokaryotes and eukaryotes. *J. Biol. Chem.* **270**, 8610-8622.
- Dohmen, R.J., Strasser, A. W., Honer, C. B., and Hollenberg, C.P.** (1991). An efficient transformation procedure enabling long-term storage of competent cells of various yeast genera. *Yeast* **7**, 691-692.
- Dudler, R. and Hertig, C.** (1992). Structure of an MDR-like gene from *Arabidopsis thaliana*. Evolutionary implications. *J. Biol. Chem.* **267**, 5882-5888.
- Dupre S, and Haguener-Tsapis, R.** (2003). Raft partitioning of the yeast uracil permease during trafficking along the endocytic pathway. *Traffic* **4**, 83-96.
- Fehr, M., Frommer, W. B., and Lalonde S.** (2002). Visualization of maltose uptake in living yeast cells by fluorescent nanosensors. *PNAS* **99**, 9846-9851.
- Fehr, M., Lalonde, S., Lager, I., Wolff, M.W., and Frommer, W.B.** (2003). *In vivo* Imaging of Dynamics of Glucose uptake in the Cytosol of COS-7 Cells by Fluorescent Nanosensors. *J. Biol. Chem.* **278**, 19217-19133.
- Felder, C.B., Graul, R.C., Lee, A.Y., Merkle, H.P., and Sadee, W.** (1999). The Venus Flytrap of Periplasmic Binding Proteins: An Ancient Protein Module Present in Multiple Drug Receptors. *AAPS Pharmsci.* **1**, 1-20.
- Förster, T.** (1948). Zwischenmolekulare Energieumwandlung und Fluoreszenz. *Ann. Phys.* **2**, 55-75.
- Fukami-Koboyashi, K., Tateno, Y., and Nishikawa, K.** (2003). Parallel Evolution of Ligand Specificity Between LacI/GalI Family Repressors and Periplasmic-Binding Proteins. *Mol. Biol. Evol.* **20**, 267-277.
- Fusco, C., Guidotti, E., and Zervos, A. S.** (1999). In vivo construction of cDNA libraries for use in the yeast two-hybrid system. *Yeast* **15**, 715-720.
- Galluhn, D. and Langer, T.** (2004). Reversible assembly of the ABC-transporter Mdl1 with the F1FO-ATP synthase in mitochondria. *J. Biol. Chem.* **6**, in press, **M405871200**
- Gazzarrini, S., Lejay, L., Gojon, A., Ninnemann, O., Frommer, W.B., and von Wirén, N.** (1999). Three Functional Transporters for Constitutive, Diurnally Regulated, and Starvation-Induced Uptake of Ammonium into *Arabidopsis* Roots. *Plant Cell* **11**, 937-948.
- Geisler, M., Kolukisaoglu, H.U., Bouchard, R., Billion, K., Berger, J., Saal, B., Frangne, N., Koncz-Kalman, Z., Koncz, C., Dudler, R., Blakeslee, J.J., Murphy, A.S., Martinoia, E., and Schulz, B.** (2003). TWISTED DWARF1, a unique plasma membrane-anchored immunophilin-like protein, interacts with *Arabidopsis* multidrug resistance-like transporters AtPGP1 and AtPGP19. *Mol. Biol. Cell.* **14**, 4238-4249.
- Ghim, S.Y. and Neuhard, J.** (1994). The pyrimidine biosynthesis operon of the thermophile *Bacillus caldolyticus* includes genes for uracil phosphoribosyltransferase and uracil permease. *J. Bacteriol.* **176**, 3698-3707.
- Gietz, R.D. and Schiestl, R.H.** (1995). Transforming Yeast with DNA. (Invited chapter). *Method Mol. Cell. Biol.* **5**, 255-269.
- Gillissen, B., Bürkle, L., André, B., Kühn, C., Rentsch, D., Brandl, B., and Frommer, W. B.** (2000). A New Family of High-Affinity Transporters for Adenine, Cytosine, and Purine Derivatives in *Arabidopsis*. *Plant Cell* **12**, 291-300.
- Gorfinkiel, L., Diallinas, G., and Scazzocchio, C.** (1993). Sequence and regulation of the *uapA* gene encoding a uric acid-xanthine permease in the fungus *Aspergillus nidulans*. *J. Biol. Chem.* **268**, 23376-233781.
- Graf, S.A., Haigh, S.E., Corson, E.D., and Shirihai, O.S.** (2004). Targeting, import, and dimerization of a mammalian mitochondrial ABC transporter, ABCB10 (ABCme). *J. Biol. Chem.* **Jun 23**, in press, **M405040200**

- Güldner, U., Heck, S., Fiedler, T., Beinhauer, J., and Hegemann, J. (1996). A new efficient gene disruption cassette for repeated use in budding yeast. *Nucl. Acids Res.* **24**, 2519–2524.
- Guranowski, A. and Barankiewicz, J. (1979). Purine salvage in cotyledons of germinating lupin seeds. *FEBS Lett.* **104**, 95–98.
- Hajdukiewicz, P., Svab, Z., and Maliga, P. (1994). The small, versatile pPZP family of *Agrobacterium* binary vectors for plant transformation. *Plant Mol. Biol.* **25**, 989–994.
- Hearn, J.D., Lester, R.L., and Dickson, R.C. (2003). The uracil transporter Fur4p associates with lipid rafts. *J. Biol. Chem.* **278**, 3679–3686.
- Hebert D.N. and Carruthers, A. (1992). Glucose transporter oligomeric structure determines transporter function. Reversible redox-dependent interconversions of tetrameric and dimeric GLUT1. *J. Biol. Chem.* **267**, 23829–23838.
- Heuberger, E.H.M.L., Veenhoff, L.M., Durkens, R.H., Friesen, R.H.E., and Poolman, B. (2002). Oligomeric state of membrane transport proteins analyzed with blue native electrophoresis and analytical ultracentrifugation. *J. Mol. Biol.* **317**, 591–600.
- Hishida, T., Iwasaki, H., Yagi, T., and Shinagawa, H. (1999). Role of Walker Motif A of RuvB Protein in Promoting Branch Migration of Holliday Junctions. *J. Biol. Chem.* **274**, 25335–25342.
- Huffman, J.L., Lu, F., Zalkin, H., and Brennan, R.G. (2002). Role of Residue 147 in the Gene Regulatory Function of the *Escherichia coli* Purine Repressor. *Biochemistry* **41**, 511–520.
- Jackson, J.H. and Linskens, H.F. (1978). Evidence for DNA repair after ultraviolet irradiation of *Petunia hybrida* pollen. *Mol. Gen. Genet.* **161**, 117–120.
- Jackson, J.H. and Linskens, H.F. (1980). DNA repair in pollen: Range of mutagens inducing repair, effect of replication inhibitors and changes in thymidine nucleotide metabolism during repair. *Mol. Gen. Genet.* **180**, 517–522.
- Kafer, C. and Thornburg, R. (1999). Pyrimidine Metabolism in Plants. *Paths to pyrimidines* **14**, 1–12.
- Kamboj, R.K. and Jackson, J.F. (1984). Divergent transport mechanisms for pyrimidine nucleosides in *Petunia* pollen. *Plant Physiol.* **75**, 499–501.
- Kamboj, R.K. and Jackson, J.F. (1985). Pyrimidine nucleoside uptake by *Petunia* pollen. *Plant Physiol.* **79**, 801–805.
- Kamboj, R.K. and Jackson, J.F. (1987). Purine nucleoside transport in *Petunia* pollen is an active, carrier-mediated system not sensitive to nitrobenzylthioinosine and not renewed during pollen tube growth. *Plant Physiol.* **84**, 688–691.
- Katahira, R. and Ashihara, H. (2002). Profiles of pyrimidine biosynthesis, salvage and degradation in disks of potato (*Solanum tuberosum* L.) tubers. *Planta* **215**, 821–828.
- Kilic, F. and Rudnick, G. (2000). Oligomerization of serotonin transporter and its functional consequences. *Proc. Natl. Acad. Sci. USA* **97**, 3106–3111.
- Kombrink, E. and Beevers, H. (1983). Transport of purine and pyrimidine bases and nucleosides from endosperm to cotyledons in germinating castor bean seedlings. *Plant Physiol.* **73**, 370–376.
- Koncz, C. and Schell, J. (1986). The promoter of the T-DNA gene 5 controls the tissue-specific expression of chimaeric genes carried by a novel type of *Agrobacterium* binary vector. *Mol. Gen. Genet.* **204**, 389–396.
- Kong, W., Engel, K., and Wang, J. (2004). Mammalian nucleoside transporters. *Curr. Drug Metab.* **5**, 63–84.
- Krogh, A., Larsson, B., von Heijne, G., and Sonnhammer, E.L.L. (2001). Predicting transmembrane protein topology with a hidden Markov model: Application to complete genomes. *J. Mol. Biol.* **305**, 567–580.
- Lager, I., Fehr, M., Frommer, W. B., and Lalonde S. (2003). Development of a fluorescent nanosensor for ribose. *FEBS Lett.* **553**, 85–89.
- Lazar, G., Zhang, H., and Goodman, H.M. (1993). The origin of the bifunctional dihydrofolate reductase thymidylate synthetase isogenes of *Arabidopsis thaliana*. *Plant J.* **3**, 657–668.
- Li, G., Lui, K., Baldwin, S. A., and Wang, D. (2003). Equilibrative Nucleoside Transporters of *Arabidopsis thaliana* cDNA cloning, expression pattern, and analysis of transport activities. *J. Biol. Chem.* **278**, 35732–35742.
- Looger, L.L., Dwyer, M.A., Smith, J.J., and Hellinga, H.W. (2003). Computational design of receptor and sensor proteins with novel functions. *Nature* **423**, 185–190.

- Lu, F., Brennan, R. G., and Zalkin, H.** (1998a). *Escherichia coli* Purine Repressor: Key Residues for the Allosteric Transition between Active and Inactive Conformations and for Interdomain Signaling. *Biochemistry* **37**, 15680-15690.
- Lu, F., Schumacher, M.A., Arvidson, D.N., Haldimann, A., Wanner, B. L., Zalkin, H., and Brennan, R.G.** (1998b). Structure-based Redesign of Corepressor Specificity of the *Escherichia coli* Purine Repressor by Substitution of Residue 190. *Biochemistry* **37**, 971-982.
- Ludewig, U. and Frommer, W.B.** (2003a). Genes and proteins for solute transport and sensing. In *The Arabidopsis Book*. (Somerville C.R. & Meyerowitz E.M., eds) American Society of Plant Biologist, Rockville, doi/101199/tab.0092, (www.aspb.org/publications/arabidopsis/).
- Ludewig, U., von Wiren, N., and Frommer, W.B.** (2002). Uniport of NH₄⁺ by the root hair plasma membrane ammonium transporter LeAMT1;1. *J. Biol. Chem.* **277**, 13548-13555.
- Ludewig, U., Wilken, S., Wu, B., Jost, W., Obrdlik, P., El Bakkoury, M., Marini, A.M., André, B., Hamacher, T., Boles, E., von Wirén, N., and Frommer W.B.** (2003b). Homo- and Hetero-oligomerization of Ammonium Transporter-1 Uniporters. *J. Biol. Chem.* **278**, 45603-45610.
- Lutkenhaus, J. and Sundaramoorthy, M.** (2003). MinD and role in deviant Walker A motif, dimerization and membrane binding in oscillation. *Mol. Microbiol.* **48**, 295-303.
- Martin, T., Wöhner, R. V., Hummel, S., Willmitzer, L., and Frommer, W.B.** (1992). Using the GUS Gene as a Reporter of Gene Expression. In *GUS Protocols*, S.R. Gallagher, ed (San Diego, CA: Academic Press), pp. 23-43.
- Michaelis, S.** (1993). STE6, the yeast a-factor transporter. *Semin. Cell Biol.* **4**, 17-27.
- Minet, M., Millington, W.R., and Wurtman, R.J.** (1992). Complementation of *Saccharomyces cerevisiae* auxotrophic mutants by *Arabidopsis thaliana* cDNA. *Plant J.* **2**, 417-422.
- Miyawaki, A., Griesbeck, O., Heim, R., and Tsien, R.Y.** (1999). Dynamic and quantitative Ca²⁺ measurements using improved cameleons. *Proc. Natl. Acad. Sci. USA* **96**, 2135-2140.
- Miyawaki, A., Llopis, J., Heim, R., McCaffery, J.M., Adams, J. A., Ikura, M., and Tsien, R.Y.** (1997). Fluorescent indicators for Ca²⁺ based on green fluorescent proteins and calmodulin. *Nature* **388**, 834-835.
- Moffatt, B. and Somerville, C.** (1988). Positive selection for male-sterile mutants of *Arabidopsis* lacking adenine-phyosphoribosyltransferase activity. *Plant Physiol.* **86**, 1150-1154.
- Möhlmann, T., Mezher, Z., Schwerdtfeger, H., and Neuhaus, E.** (2001). Characterisation of a concentrative type of adenosine transporter from *Arabidopsis thaliana* (*ENT1, At*). *FEBS Lett.* **509**, 370-374.
- Mowbray, S.L., and Björkman, A.J.** (1999). Conformational Changes of Ribose-binding Protein and Two Related Repressors are Tailored to fit the Functional Need. *J. Mol. Biol.* **294**, 487-499.
- Nagai, T., Ibata, K., Park, E. S., Kubota, M., Mikoshiba, K., and Miyawaki, A.** (2002). A variant of yellow fluorescent protein with fast and efficient maturation for cell biological applications. *Nat. Biotechnol.* **20**, 87-90.
- Nishimura, A., Morita, M., Nishimura, Y., and Sugino, Y.** (1990). A rapid and highly efficient method for preparation of competent *Escherichia coli* cells. *Nucleic Acids Res.* **18**, 6169.
- Obrdlik, P., El-Bakkoury, M., Hamacher, T., Cappellaro, C., Vilarino, C., Fleischer, C., Ellerbrok, H., Kamuzini, R., Ledent, V., Blaudez, D., Sanders, D., Revuelta, J.L., Boles, E., André, B., and Frommer, W.B.** (2004). K⁺ channel interactions detected by a genetic system optimized for systematic studies of membrane protein interactions. *Proc. Natl. Acad. Sci. USA* **in press**.
- Pélissier, H.C., Frerich, A., Desimone, M., Schumacher, K., and Tegeder, M.** (2004). PvUPS1, an Allantoin Transporter in Nodulated Roots of French Bean. *Plant Physiol.* **134**, 664-675.
- Preiss, J.** (1988). Biosynthesis of Starch and its regulation. In: *The Biochemistry of Plants* (CA: Academic Press), pp. 181-254.

- Rainbird, R.M., Thorne, and J.H., Hardy, R.W.F.** (1984). Role of amides, amino acids, and ureides in the nutrition of developing soybean seeds. *Plant Physiol.* **74**, 329-334.
- Reinders, A., Schulze, W., Kühn, C., Barker, L., Schulz, A., Ward, J.M., and Frommer, W. B.** (2002a). Protein-Protein Interactions between Sucrose Transporters of Different Affinities Colocalized in the Same Eucleate Sieve Element. *Plant Cell* **14**, 1567-1577.
- Reinders, A., Schulze, W., Thaminy, S., Stagljar, I., Frommer, W.B., and Ward, J.M.** (2002b). Intra- and Intermolecular Interactions in Sucrose Transporters at the Plasma Membrane Detected by the Split-Ubiquitin System and Functional Assays. *Structure* **10**, 763-772.
- Rentsch, D., Laloi, M., Rouhara, I., Schmelzer, E., Delrot, S., and Frommer, W.B.** (1995). NTR1 encodes a high affinity oligopeptide transporter in *Arabidopsis*. *FEBS Lett.* **370**, 264-268.
- Rolfes, R.J. and Zalkin, H.** (1988). *E. coli* gene *PurR* encoding a repressor protein for purine nucleotide synthesis. Cloning, nucleotide sequence and interaction with *PurF* operator. *J. Biol. Chem.* **263**, 19653-19661.
- Sambrook, J., Fritsch, E.F., and Maniatis, T.** (1989). *Molecular cloning: A laboratory manual* (2nd edition). Cold Spring Harbor Laboratory Press, N. Y.
- Sanger, F., Nicklen, S., and Coulson, A.R.** (1977). DNA sequencing with chain-terminating inhibitors. *Proc. Natl. Acad. Sci. USA* **74**, 5463-5467.
- Saraste M., Sibbald, P.R., and Wittinghofer A.** (1990). The P-loop-a common motif in ATP- and GTP-binding proteins. *Trends Biochem. Sci.* **15**, 430-434.
- Sawert, A., Backer, A.I., and Wagner, K.G.** (1988). Age-dependent decrease of nucleoside pools in cereal leaves. *Plant Cell Physiol.* **29**, 61-65.
- Sawert, A., Backer, A.I., Plank-Schumacher, K.H., and Wagner, K.G.** (1987). Determination of nucleotides and nucleosides in cereal leaves by high-performance liquid chromatography. *Plant Physiol.* **127**, 183-186.
- Schaaf, G.** (2004). *Molecular and Biochemical Characterization of Plant Transporters Involved in the Cellular Homeostasis of Mn and Fe (Hohenheim)*, pp. p. 106.
- Schmid, J.A., Just, H., and Sitte, H.H.** (2001). Impact of oligomerization on the function of the human serotonin transporter. *Biochem. Soc. Trans.* **29**, 732-736.
- Schneider, E. and Hunke, S.** (1998). ATP-binding cassette (ABC) transport systems: Functional and structural aspects of the ATP hydrolysis subunits/domains. *FEMS Microbiol. Rev.* **22**, 1-20.
- Schubert, K.R. and Boland, M.J.** (1990). The ureides. In *The Biochemistry of Plants*, B.J. Mifflin, Mifflin, L. P. J., ed (San Diego: Academic Press), pp. 197-283.
- Schulten, H.R. and Schnitzer, M.** (1998). The chemistry of soil organic nitrogen: a review. *Biol. Fertil Soils* **26**, 1-15.
- Schulze, W.X., Reinders, A., Ward, J., Lalonde, S., and Frommer, W.B.** (2003). Interactions between co-expressed *Arabidopsis* sucrose transporters in the split-ubiquitin system. *BMC Biochem.* **4**, 3.
- Seidel, C.A.M., Schulz, A., and Sauer, M.H.M.** (1996). Nucleobase-Specific Quenching of Fluorescent Dyes. 1. Nucleobase One-Electron Redox Potentials and Their Correlations with Static and Dynamic Quenching Efficiencies. *J. Phys. Chem.* **100**, 5541-5553.
- Séron, K., Blondel, M.O., Haguenaer-Tsapis, R., and Volland, C.** (1999). Uracil-Induced Down-Regulation of the Yeast Uracil Permease. *J. Bacteriol.* **181**, 1793-1800.
- Soussi-Boudekou, S., Vissers, S., Urrestarazu, A., Jauniaux, J. C., and André, B.** (1997). Gzf3p, a fourth GATA factor involved in nitrogen-regulated transcription in *Saccharomyces cerevisiae*. *Mol. Microbiol.* **23**, 1157-1168.
- Stasolla, C., Katahira, R., Thorpe, T.A., and Ashihara, H.** (2003). Purine and pyrimidine nucleotide metabolism in higher plants. *J. Plant Physiol.* **160**, 1-25.
- Stasolla, C., Loukanina, N., Ashahira, H., Yeung, E.C., and Thorpe, A.T.** (2001). Purine and pyrimidine metabolism during the partial drying treatment of white spruce (*Picea glauca*) somatic embryos. *Physiol. Plant.* **111**, 93-101.
- Stasolla, C., Loukanina, N., Ashahira, H., Yeung, E.C., and Thorpe, A.T.** (2002). Pyrimidine nucleotide and nucleic acid synthesis in embryos and megagametophytes of white spruce (*Picea glauca*) during germination. *Physiol. Plant.* **115**, 155-165.
- Stefkova, J., Poledne, R., and Hubacek, J.A.** (2004). ATP-binding cassette (ABC) transporters in human metabolism and diseases. *Physiol Res.* **53**, 235-243.

- Stougaard, J.** (1994). Substrate-dependent negative selection in plants using a bacterial cytosine deaminase. *Plant J.* **3**, 755-761.
- Swint-Kruse, L., Larson, C., Pettitt, B.M., and Matthews, K.S.** (2002). Fine-tuning function: correlation of hinge domain interactions with functional distinctions between LacI and PurR. *Protein Sci.* **11**, 778-794.
- Thran, Y.** (1999). The Effect of uracil on the Germination and Growth of some leguminous plants. *Turk. J. Bot.* **23**, 241-244.
- Torres, G.E., Carneiro, A., Seamans, K., Fiorentini, C., Sweeney, A., Yao, W.-D., and Caron, M. G.** (2003). Oligomerization and Trafficking of the Human Dopamine Transporter. *J. Biol. Chem.* **278**, 2731-2739.
- Tsukaguchi, H., Tokui, T., Mackenzie, B., Berger, U.V., Chen, X.Z., Wang, Y., Brubaker, R.F., and Hediger, M.A.** (1999). A family of mammalian Na⁺-dependent L-ascorbic acid transporters. *Nature* **399**, 70-75.
- Vadez, V. and Sinclair, T.R.** (2000). Ureide degradation pathway in intact soybean leaves. *J. Exp. Bot.* **51**, 1459-1465.
- van der Donk, J.A.V.M.** (1974). Synthesis of RNA and proteins as a function of time and type of pollen tube style interactions in *Petunia pollen hybrida* L. *Mol. Gen. Genet.* **134**, 93-98.
- Veenhoff, L.M., Heuberger, E. H. M. L., and Poolman, B.** (2001). The lactose transport protein is a cooperative dimer with two sugar translocation pathways. *EMBO J.* **20**, 3056-3062.
- von Wirén, N., Gazzarrini, S., Gojon, A., and Frommer, W. B.** (2000). The molecular physiology of ammonium uptake and retrieval. *Curr. Opin. Plant Biol.* **3**, 254-261.
- Wagner, K.G. and Backer, A.I.** (1992). Dynamics of Nucleotides in Plants Studied on a Cellular Basis. *Int. Rev. Cytol.* **134**, 1-84.
- Walker, J.E., S.M., Runswick M.J., and Gay N.J.** (1982). Distantly related sequences in the alpha- and beta-subunits of ATP synthase, myosin, kinases and other ATP-requiring enzymes and a common nucleotide binding fold. *EMBO J.* **1**, 945-951.
- Ward, J.M.** (2001). Identification of novel families of membrane proteins from the model plant *Arabidopsis thaliana*. *Bioinformatics Discovery Note* **17**, 560-563.
- Winkler, R.G., Blevis, D.G., Polacco, J.C., and Randall, D.D.** (1987). Ureide Catabolism in Soybeans. *Plant Physiol.* **83**, 585-591.
- Wormit, A., Traub, M., Flörchinger, M., Neuhaus, H.E., and Möhlmann, T.** (2004). Characterisation of three novel members of the *Arabidopsis thaliana* equilibrative nucleoside transporter (ENT) family. *Biochemical J.* **Immediate Publication**, **BJ20040386**.
- Xiang, C., Han, P., Lutziger, I., Wang, K., and Oliver, D.J.** (1999). A mini binary vector series for plant transformation. *Plant Mol. Biol.* **40**, 711-717.
- Ye, K. and Schultz, J.S.** (2003). Genetic engineering of an allosterically based glucose indicator protein for continuous glucose monitoring by fluorescence resonance energy transfer. *Anal. Chem.* **75**, 3119-31127.
- Yoo, H.S., Cunningham, T.S., and Cooper, T.G.** (1992). The allantoin and uracil permease gene sequence of *Saccharomyces cerevisiae* are nearly identical. *Yeast* **8**, 997-1006

6. Appendices

6.1. Sequences of primers

Tab. 1: Sequences of Primers

Primer	Sequence
P1	5'-ATAGGATCCATCCATTTAGAGCCCGAGAAT-3'
P2	5'-ATATCTAGATTACTTTCTATGTCCAGAAGA-3'
P3	5'- ATAGGATCCTGACGAAGAAGGTGCGATGATG-3'
P4	5'-ATATCTAGACTAAGTAAATCGCGTCTCTCT-3'
P5	5'-CTCATAGAGCTTGAGAAGCAAAGAGCTATAATAGTCTTTGGC-3'
P6	5'-GCCAAAGACTATTATAGCTCTTTGCTTCTCAAGCTCTATGAG-3'
P7	5'-GCTATAAAGGTCTTTGGCATAAGCACATAATCGGATTGG-3'
P8	5'-CCGATTATTGTGCTTATGCCAAAGACCTTTATAGC-3'
P9	5'-GCTATAAAGGTCTTTGGCAGAAGCACATAATCGGATTGG-3'
P10	5'-CCAATCCGATTATTGTGCTTCTGCCAAAGACCTTTATAGC-3'
P11	5'-GCCATAAAGGTGTTCCGAATACGAAAGATAATCGGACTAGC-3'
P12	5'-GCTAGTCCGATTATCTTTTCGTATTCCGAACACCTTTATGGC-3'
P13	5'-CCCAGCCTTGAAAATAATTAATTTATAATTTTAAAAGATAAAAAGAGAGATA GAAAGATG-3'
P14	5'-AAGCTGGATCGCTCGAGTCGACTGCAGGCCGCCGGCCGTCATTTT CTATGTCCCGAGGAAG-3'
P15	5'-ATAGGGCCCGTGGGAATACTCAGGTATCG-3'
P16	5'-ATACCATGGCTGGACGTAACTCCTCTTC-3'
P17	5'-ACAAGTTTGTACAAAAAAGCAGGCTCTCCAACCACCATGCTTTTAGCC TACTATCTC-3'
P18	5'-TCCGCCACCACCAACCACTTTGTACAAGAAAGCTGGGTACTTTCTATGTCCAG AAGAAG-3'
P19	5'-ACAAGTTTGTACAAAAAAGCAGGCTCTCCAACCACCATGATGATAGCTCAAGAA TTGGG-3'
P20	5'-TCCGCCACCACCAACCACTTTGTACAAGAAAGCTGGGTAAAGTAAATCGCGTCTCT-3'
P21	5'-GAGCTCATGTATATGATAGAGAGCAAAGG-3'
P22	5'-GGATCCATTTTCTATGTCCCGAGGAAGCC-3'
P23	5'-GAGCTCATGCTTTTAGCCTTACTATCTCTAG-3'
P24	5'-GGATCCACTTTCTATGTCCAGAAGAAGCC-3'
P25	5'-GAGCTCATGATAGCTCAAGAATTGGGA-3'
P26	5'-GGATCCAAGTAAATCGCGTCTCTTTTCC-3'
P27	5'-ATAACTAGTCTTACAAGAACAGCAAGCTTT-3'
P28	5'-ATAGGATCCCTTTCTATCTCTTTTTATAT-3'
P29	5'-ATATCTAGAATGATCTTATCATAGTTGTAT-3'
P30	5'-ATAGGATCCACAAGCTATGGCACCTCCTTT-3'
P31	5'-ATATCTAGAAATCACTGAAACTTCTTCAA-3'
P32	5'-ATAACTAGTTTTATAAAATCACCAAATCCC-3'
P33	5'-ATATCTAGAGCTTTCATTTAGTTGCAACCC-3'
P34	5'-ATAGGATCCACATCCTATAGCTCCTGCTTT-3'
P35	5'-ATAGGATCCTGACGAAGAAGGTGCGATGATG-3'
P36	5'-ATATCTAGACTAAGTAAATCGCGTCTCTCT-3'
P37	5'-ACTAGTTAAAAGAGAGATAGAAAGATG-3'
P38	5'-AAGCTTCTTTTAAAATTTTGGAGTTTG-3'
P39	5'-CTCGAGCTTTTAAAATTTTGGAGTTTG-3'
P40	5'-TCTAGATAAAAAGAGAGATAGAAAGATG-3'
P41	5'-ATAAAGCTTATCCTATCTAGGTCAGATTTCG-3'

P42 5'-TCTAGAATACTCGAGACTTTTCTTCCTCCTGTTTAT-3'
P43 5'-GGTACCGGAGGCGGCGTTAACCACACCAAGTCTATCG-3'
P44 5'-GGTACCGGCGCCTTTACGACGATAGTCGCGGAACGG-3'
P45 5'-GGTACCGGAGGCGGCACCAAGTCTATCGGTTTGCTGGC-3'
P46 5'-GGTACCGGCGCCGCGTTCAATCAATCAAGCGCGGATGC-3'
P47 5'-GAAATCGGCGTCATCCCCGGCCCGCTGGAACAGAACACCGGCGCAG-3'
P48 5'-CTGCGCCGGTGTCTGTTCCAGCGGGCCGGGATGACGCCGATTTC-3'
P49 5'-GTAGATAAGTTTTCCGTGACG-3'
P50 5'-GAACCTAGCAAAGGTAGTGTC-3'
P51 5'-CATTGCAAACATAACAGACG-3'
P52 5'-GTATCTTTACATTCTCTGGAC-3'
P53 5'-CCAAAACAAATAAATTAACGAG-3'
P54 5'-TGGAATAATCAAGATAAGTATG-3'
P55 5'-CTTTGACGTTGGAGTCCAC-3'
P56 5'-CGTACAACCGGTATTGTGCTGG-3'
P57 5'-GGACCTGCCTCATCATACTCG-3'
P58 5'-CAATTTCTGCAAGCAACGGGTTAAC-3'
P59 5'-ACAAGTGGAAGTGCCTGAACAGCG-3'
P60 5'-CATCAAAAGACCTGGAGACTAATG-3'
P61 5'-CTCACAAGTGGAAGAGCCTGAACG-3'
P62 5'-GAGTGCCAGAGACTATTTGGAG-3'
P63 5'-CGATACTAAAGGAAGTGCCTGAAC-3'

6.2. *UPS* expression in plants of *UPS1* PTGS lines

Tab. 2: Relative expression levels of 2-day-old seedlings from different *UPS1* PTGS lines (T4 generation) grown on MS agar plates without Basta™ selection in comparison to lines transformed with the empty pCB302.3 vector or wild type.

lines	UPS1	UPS2	UPS5
3(2)	0	0	0
11(4)	0	0	0
15(2)	-	-	0
15(3)	0	0	0
36(3)	-	-	0
42(1)	-	-	0

Tab. 3: Relative expression levels of 5-day-old seedlings from different *UPS1* PTGS lines (T3 generation) grown on MS agar plates with Basta™ in comparison to lines transformed with the empty pCB302.3 vector.

lines	UPS1	UPS2	UPS5
1	0	+	
2	-	+	
3	--	+	
4	--		
5	--	+	
6	0		
9	--	+	
12	0		+
15	-		
22	-		
27	--		
35	-		
37	--		+
41	0		+
42	--		
45	-		

Tab. 4: Relative expression levels of 14-day-old seedlings from different *UPS1* PTGS lines (T3 generation) grown on modified MS agar plates (20 mM N) without Basta™ in comparison to lines transformed with the empty pCB302.3 vector or wild type.

lines	UPS1	UPS2	UPS5
2	--	-	0
3	--	--	0
4	--	--	-
5	-	0	0
6	--	0	+
7	--	0	0
8	--	-	--
9	--	-	--
11	-	-	-
12	-	-	--
13	--	0	--
15	--	-	--
40	-	-	-

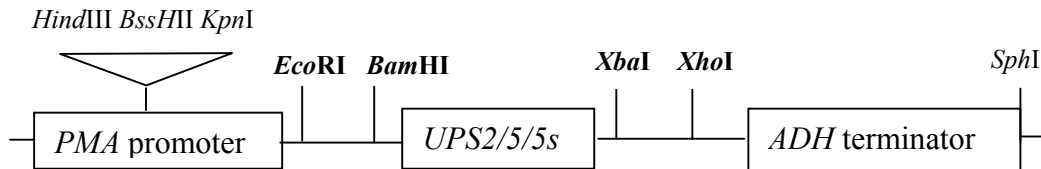
++: expression severely enhanced
 +: expression slightly enhanced
 0: no changes
 -: expression slightly reduced
 --: expression severely reduced

6.3. Maps of constructs

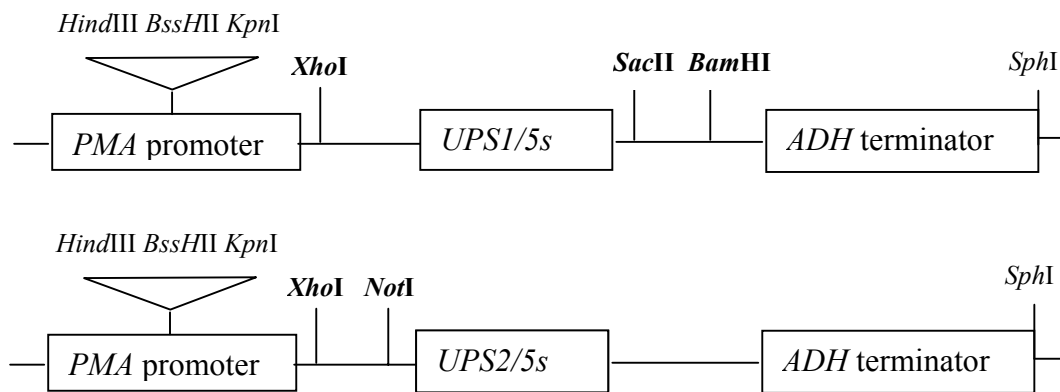
UPS2/UPS5, for example means, a similar construct was cloned using either the *UPS2* or the *UPS5* sequence.

6.3.1. Constructs for expression in yeast

pDR199

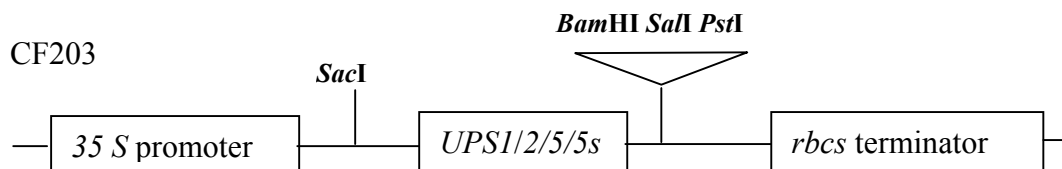


pMD200



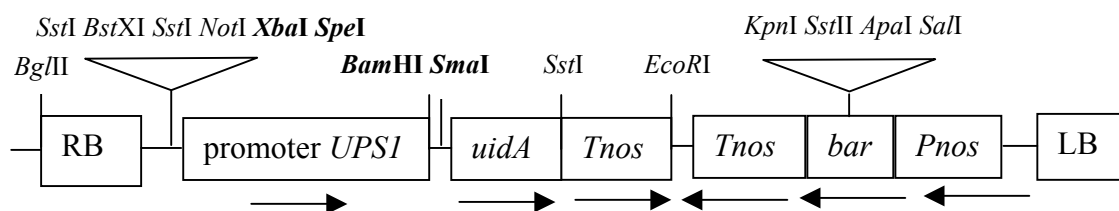
6.3.2. GFP-expression constructs

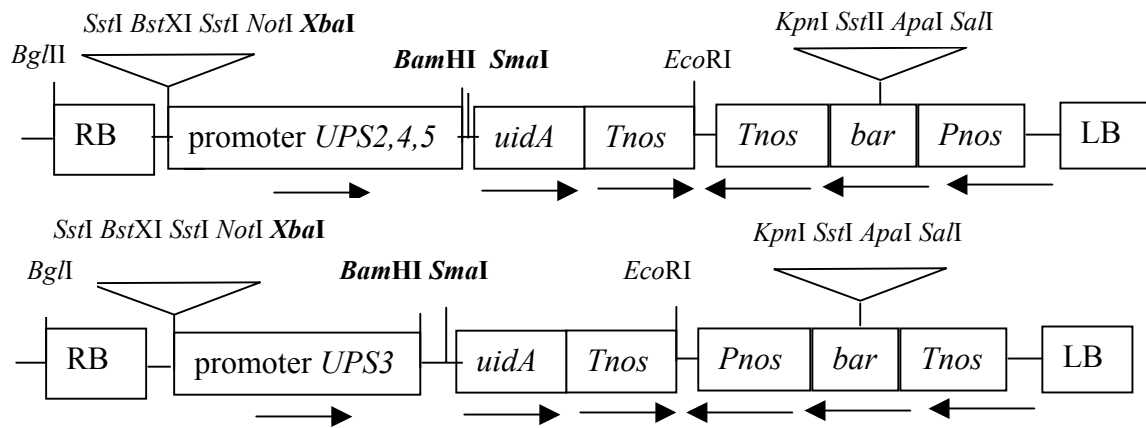
CF203



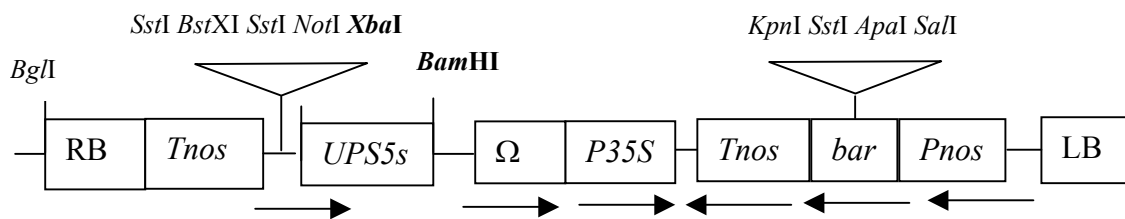
6.3.3. Promoter-GUS constructs

pCB308



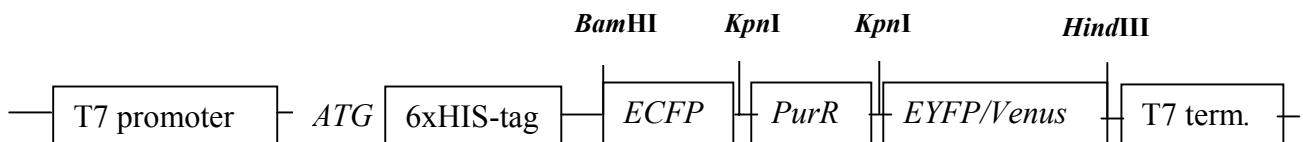


6.3.4. UPS5s over-expression construct



6.3.5. FLIP_{PurR}

pRSETB



7. Acknowledgements

First of all, I would like to thank Prof. Dr. Wolf B. Frommer for giving me the opportunity to carry out this work. I am grateful for his never-ending interest in the project, his ideas, his enthusiasm and his valuable comments. In addition, I would like to thank him for giving me the great opportunity of spending 3 months in his laboratory at the Carnegie Institution of Washington (Stanford).

I am thankful to the Reinhold und Maria Teufel Stiftung for giving me a stipend to spend these months at the Carnegie Institution.

A special thanks goes to Prof. Dr. Claudia Oecking for helping me with the application for the stipend and to Prof. Dr. Hans U. Seitz, who always had an open door to give help and advice.

I would like to thank Dr. Yan-Hua Su and Dr. Uwe Ludewig for a good and successful collaboration concerning the electrophysiological measurements.

Also I want to thank Dr. Marcelo Desimone for everything that he did for the UPS project and for me.

I am grateful to Dr. Guillaume Pilot for giving me a lot of help and advice, especially during the writing process. A special thanks also goes to Dr. Réjane Pratelli who did a great job on correcting my English.

I am very thankful to Dr. Sylvie Lalonde, Dr. Daniel Wipf, and Dr. Burkhard Schulz for a lot of help and advice with a broad array of problems. In addition, I would like to thank Dr. Petr Obrdlík for help and advice especially concerning the split ubiquitin system and Dr. Karin Schumacher for nice tips about vectors and transgenic plants.

I am also grateful to Dr. York Stierhof and his team for help with the microtome and tissue embedding.

I would like to express my thanks to Michael Fitz for great support and an enjoyable atmosphere in the lab. I also want to thank Yvonne Sauermann for her support. A special thanks also to Timo, who did a very good job as a HIWI.

A special thanks goes to Melanie Hilpert for help and advice and an enjoyable time in California. In addition, I am grateful to Sakiko, Ida, Karen, and Marcus for a good time in “The German House” and for help with so many things in California, from the airport shuttle to getting a bike for me. I would also like to express my thanks to the lab mates of the Frommer lab in Carnegie and in Tuebingen for the nice environment in which to work, especially Giorgio and Nadine.

Of course, I would like to express my thanks to the secretaries, Elke and Silvia and especially Felicity.

A special thanks to Tanja Sikler and the gardeners team for excellent care of the greenhouse *Arabidopsis* plants.

Finally, I want to thank my friends and my parents for an enjoyable time and their support.

Lebenslauf

Name: Anja Schmidt
Geburtsdatum: 05.11.1972
Geburtsort: Korbach (Deutschland)

Schule

1979-1983 Grundschule Medebach (Deutschland)
1983-1985 Gymnasium der Stadt Medebach – Sekundarstufe I
1985-1992 Alte Landesschule Korbach (Gymnasium)
6/1992 Abitur

Studium

1992-1999 Studium der Germanistik (Gymnasiallehramt) Philipps-Universität Marburg (Deutschland)
1992-1999 Studium der Biologie (Gymnasiallehramt) Philipps-Universität Marburg
1994-1999 Studium der Chemie (Gymnasiallehramt) Philipps-Universität Marburg
1999 Abschluss der Staatsexamensarbeit: „Nachweis, Isolierung und Umwandlung von Milch-Inhaltsstoffen – Ausgewählte Versuche“ unter Anleitung von Prof. Hartwig Perst, Institut für Organische Chemie, Philipps-Universität Marburg
6/1999 1. Staatsexamen (Chemie, Germanistik), Philipps-Universität Marburg
11/1999 1. Staatsexamen (Biologie), Philipps-Universität Marburg

Hilfskraft- und Mitarbeiterstellen an Universitäten

5/1996-7/1996;
10/1996-1/1997;
10/1997-2/1998;
5/1998-7/1998 studentische Hilfskraft am Fachbereich Biologie der Philipps-Universität Marburg
12/1999-7/2001 wissenschaftliche Mitarbeiterin, Albert-Ludwigs-Universität Freiburg, Biologie II, Biochemie der Pflanzen (Deutschland)

Dissertation

8/2001 – 8/2004 Dissertation am Zentrum für Molekularbiologie der Pflanzen (ZMBP), Eberhard Karls Universität Tübingen (Deutschland)
3/2004-5/2004 Carnegie Institution of Washington (USA)
unter Anleitung von Prof. Wolf B. Frommer:
“Characterization of a novel family of nucleobase transporters”

im Selbstverlag herausgegeben von:

Anja Schmidt
Steinbruchstr. 7/1
72076 Tübingen